

UNIVERSITY OF VENDA



SCHOOL OF MATHEMATICAL & NATURAL SCIENCES

Multiscale Modelling of HIV/AIDS Transmission Dynamics

Author:
MARTIN CANAAN MAFUNDA

Supervisor:
PROF. W. GARIRA
Co-Supervisor:
DR. S. MOYO

*A dissertation submitted in fulfilment of the requirements
for the degree of Master of Science*

in the

Modelling Health and Environmental Linkages Research Group (MHELRG)
Department of Mathematics & Applied Mathematics

July 23, 2018

Declaration of Authorship

I, **MARTIN CANAAN MAFUNDA**, declare that this dissertation titled, “**Multiscale Modelling of HIV/AIDS Transmission Dynamics**” and the work presented in it are my own. I confirm that:

- This work was done wholly or mainly while in candidature for a masters degree at this University.
- Where any part of this dissertation has previously been submitted for a degree or any other qualification at this University or any other institution, this has been clearly stated.
- Where I have consulted the published work of others, this is always clearly acknowledged.
- Where I have quoted from the work of others, the source is always given. With the exception of such quotations, this dissertation is entirely my own work.
- I have acknowledged all main sources of help.
- Where the dissertation is based on work done by myself jointly with others, I have made clear exactly what was done by others and what I have contributed myself.

Signed:

Date:

“Having people who are clueless about their HIV status is the worst national nightmare ever and it culminates to a waste of national resources. The simple reason being the fact that if we all knew better about our HIV status, condoms would only be used when necessary thereby cutting down on their associated costs”

Martin Canaan Mafunda

“The sciences do not try to explain, they hardly even try to interpret, they mainly make models. By a model is meant a mathematical construct which, with the addition of certain verbal interpretations, describes observed phenomena. The justification of such a mathematical construct is solely and precisely that it is expected to work—that is, correctly to describe phenomena from a reasonably wide area.”

John von Neumann

Abstract

Infectious diseases remain a major public health concern. Well-known for causing sickness and death, enormous pain and suffering, increased time spent on patient care and huge economic losses due to lost production. Infectious diseases continue to be a scourge without equal. In this work, we address the following research question: Can we use a multiscale model of HIV/AIDS transmission dynamics to assess the comparative effectiveness of health interventions that are implemented at different scale domains? To achieve the set objectives of the study, we use multiscale modelling approach, a new and emerging computational high-throughput technique for mathematically studying problems that have many characteristics across several scales. To be more specific, we perform three tasks in addressing the research question. First, we develop a within-host submodel and use it to show its associated limitations which only a multiscale model can resolve. Second, we develop a between-host submodel and use it to motivate the need for multiscale modelling of the HIV/AIDS disease system. Finally, we link the two submodels to produce a nested HIV/AIDS multiscale model that affords us the opportunity to compare effectiveness of five preventive and treatment HIV/AIDS health interventions. Analysis of the multiscale model shows that it is possible to jointly study two key aspects (immunology and epidemiology) of infectious diseases. The multiscale model provides the means for making meaningful comparative effectiveness on available preventive and treatment health interventions. Consequently, we employ the multiscale model to show that impact of HIV/AIDS packages increases as more interventions are integrated into the packages. Specifically, the study shows that combined HAART and male circumcision is more effective than an intervention involving HAART alone. Overall, our study successfully illustrates the utility of multiscale modelling methodology as a tool for assessing the comparative effectiveness of HIV/AIDS preventive and treatment interventions. For purposes of informing public health policy, we use the study results to infer that condom use, male circumcision and pre-exposure prophylaxis are more effective in controlling the transmission dynamics of HIV/AIDS at the start of the epidemic as compared to when the disease is endemic in the community while the converse is also true for HAART.

Keywords: *Infectious diseases, Mathematical Modelling, Multiscale Modelling, Within- and Between-host, HIV/AIDS, Comparative effectiveness, HAART*

Acknowledgements

All praise and honour unto the Lord, my Almighty God, who gave me the will, strength and the resources to complete this project. Without his abundance grace and blessings, this project would never been accomplished. I would like to thank my supervisor, Prof W. Garira, for the support and guidance he extended to me during the entire period of my MSc studies. I would also like to thank my co-supervisor, Dr S. Moyo, for all the wonderful contributions he made to my MSc studies. Gratitude and appreciation are also expressed to all my beloved *Mafunda* and *Canaan* families and my caring and lovely wife Susan for their continued support and encouragement throughout the entire project period. Furthermore, my special thanks goes to all members of Modelling Health and Environmental Linkages Research Group (MHELRG) for their support and unwavering commitment towards my work. Last but not least, I acknowledge the support from South Africa Centre for Epidemiological Modelling and Analysis (SACEMA) for their continued financial support throughout my entire MSc study period.

Contents

Declaration of Authorship	ii
Abstract	iv
Acknowledgements	v
1 Introduction	1
1.1 Background	1
1.1.1 HIV Infection	2
1.1.2 HIV Transmission	2
1.1.3 HIV Preventive and Treatment Interventions	3
1.2 Problem Statement	3
1.3 Aims and Objectives	4
1.4 Methodology	4
1.5 Review of Literature on Multiscale Modelling	5
1.5.1 Multiscale Modelling and Infectious diseases	5
1.5.2 Viral Infections	7
1.5.3 Multiscale Modelling and HIV/AIDS	8
1.6 Limitations of Multiscale Modelling	10
1.7 Outline of the thesis	11
2 Within-host model for HIV Infection	12
2.1 Introduction	12
2.2 Within-Host Model	12
2.3 The Infection Free Equilibrium	15
2.3.1 Computation of the within-host reproduction number (\mathfrak{R}_0)	16
2.3.2 Interpretation of \mathfrak{R}_0	17
2.4 Local Stability of the Infection Free Equilibrium	18
2.5 Global Stability of the Infection Free Equilibrium	19
2.6 The endemic equilibrium state and its stability	20
2.6.1 Local Stability of Endemic Equilibrium State	21
2.7 Sensitivity Analysis	23
2.8 Within-host model with interventions	25
2.9 Assessing the comparative effectiveness of HIV Combination Treatment regimens	26
2.9.1 Comparative effectiveness of HAART using the effective within-host reproduction number (\mathfrak{R}_E) as an indicator of effectiveness	28
2.9.2 Comparative effectiveness of HAART using the effective endemic-value of plasma viral load V_h^{*E} as an indicator of intervention effectiveness	30
2.10 Summary	31

3	Between-Host Model for HIV/AIDS transmission dynamics	33
3.1	Introduction	33
3.1.1	Model Formulation	33
3.2	Feasible region of the equilibria of the model	36
3.3	The Disease Free Equilibrium	37
3.4	Derivation of Between-Host Basic Reproduction Number (R_0)	37
3.5	Stability Analysis of Disease Free Equilibrium	38
3.5.1	Local Stability of DFE	38
3.5.2	Global stability of DFE (E^0)	39
3.6	Determination of Endemic Equilibria	40
3.6.1	The Endemic Equilibrium	40
3.6.2	Local stability of the endemic equilibrium	42
3.6.3	Global Stability of the Endemic Equilibria	47
3.7	Sensitivity Analysis	49
3.8	Controlled Between-Host Model	50
3.8.1	Analysis of the Controlled Model	51
3.9	Assessing the comparative effectiveness of HIV/AIDS Combination Preventive Interventions	52
3.9.1	Assessment of comparative effectiveness using the Effective Reproduction Number (R_E)	52
3.9.2	Assessment of comparative effectiveness using the controlled endemic value of HIV Prevalence	55
3.9.3	Assessment of comparative effectiveness using the controlled endemic value of Community Viral Load	58
3.10	Summary	61
4	Multiscale Modelling of HIV/AIDS Disease System	62
4.1	Introduction	62
4.2	Multiscale Model Development	69
4.2.1	The two Submodels of HIV/AIDS Transmission Dynamics	69
4.2.2	Integration of the two Submodels into a Single Multiscale Model	71
4.2.3	Simplifying the Complete Multiscale Model for HIV/AIDS Transmission Dynamics	77
4.3	Analysis of the Baseline Multiscale Model	80
4.3.1	The Disease-free Equilibrium and the Reproductive Number	80
4.3.2	Local stability of DFE	83
4.3.3	Global stability of DFE	84
4.3.4	The Endemic Equilibrium State	86
4.3.5	Local Stability of the Endemic Equilibrium	87
4.3.6	Sensitivity Analysis of the Transmission Metrics of Baseline Multiscale Model	90
4.3.7	The Influence of Within-host Scale on Between-host Scale HIV/AIDS Transmission Dynamics	93
4.4	The Multiscale Model for HIV/AIDS Transmission with Combination Health Interventions	97
4.4.1	Analysis of the Multiscale Model With HIV/AIDS Combination Preventive Health Interventions	100
4.4.2	Assessing the comparative effectiveness of HIV/AIDS Combination Preventive interventions	102
4.5	Summary	117

5 Discussion and Conclusions	119
Bibliography	121

List of Figures

2.1	A conceptual diagram of the within-host HIV infection dynamics. . . .	15
3.1	A conceptual diagram of the between-host model for HIV / AIDS transmission dynamics	35
4.1	A conceptual diagram of the full multiscale model of HIV / AIDS transmission dynamics. In this Figure δ_H stands for $\widehat{\delta}_H(V_h, T_s)$ and α_H stands for $\widehat{\alpha}_H(V_h, T_s)$	76
4.2	Effect of burst size of infected CD4+ T cells parameter (N_v) on (a) population of susceptible humans (S_H), (b) HIV/AIDS prevalence (I_H) and (c) community viral load (V_H) for different values of N_v : $N_v = 97.5, N_v = 227.5, N_v = 422.5, N_v = 650.0, N_v = 1,527.5, N_v = 1,722.5, N_v = 1,852.5$	94
4.3	Effect of rate of transcription of HIV-1 RNA to DNA inside CD4+ T cells parameter (α_c) on (a) population of susceptible humans (S_H), (b) HIV/AIDS prevalence (I_H) and (c) community viral load (V_H), for different values of α_c : $\alpha_c = 6e^{-5}, \alpha_c = 0.000158, \alpha_c = 0.000293, \alpha_c = 0.00045, \alpha_c = 0.0010575, \alpha_c = 0.0011925, \alpha_c = 0.0012825$	95
4.4	Effect of rate of virus entry into cytoplasm of CD4+ T cells (β_h) on (a) population of susceptible humans (S_H), (b) HIV/AIDS prevalence (I_H), (c) community viral load (V_H), for different values of β_h : $\beta_h = 0.000203, \beta_h = 0.000473, \beta_h = 0.000878, \beta_h = 0.00135, \beta_h = 0.0031725, \beta_h = 0.0035775, \beta_h = 0.0038475$	96
4.5	Histogram summarizing the results of the assessment of comparative effectiveness of HIV/AIDS interventions using the three different indicators of intervention effectiveness: (a) effective reproductive number (\mathcal{R}_E) - red colour, (b) intervention induced endemic value of community viral load (V_H) - gold colour, and (c) intervention induced HIV prevalence endemic value (I_H) - black colour, when each of the five different HIV/AIDS interventions is assumed to have a low efficacy of 0.30	114
4.6	Histogram summarizing the results of the assessment of comparative effectiveness of HIV/AIDS interventions using the three different indicators of intervention effectiveness: (a) effective reproductive number (\mathcal{R}_E) - red colour, (b) intervention induced endemic value of community viral load (V_H) - gold colour, and (c) intervention induced HIV prevalence endemic value (I_H) - black colour, when each of the five different HIV/AIDS interventions is assumed to have a medium efficacy of 0.60	115

4.7 Histogram summarizing the results of the assessment of comparative effectiveness of HIV/AIDS interventions using the three different indicators of intervention effectiveness: (a) effective reproductive number (\mathcal{R}_E) - red colour, (b) intervention induced endemic value of community viral load (V_H) - gold colour, and (c) intervention induced HIV prevalence endemic value (I_H) - black colour, when each of the five different HIV/AIDS interventions is assumed to have a high efficacy of 0.90 116

List of Tables

2.1	Table of parameter descriptions and initial parameter values for the within-host model given by system (2.1)	14
2.2	Sensitivity indices of the two metrics of baseline within-host HIV infection dynamics.	24
2.3	Parameter structural transformations of the post -control model	26
2.4	Results of the assessment of comparative effectiveness of HIV treatment regimens using the effective within-host reproduction number (\mathcal{R}_E) as an indicator of treatment effectiveness when each of the three HAART components is assumed to have: (a) low efficacy of 0.30, (b) medium efficacy of 0.60, and (c) high efficacy of 0.90.	28
2.5	Results of the assessment of comparative effectiveness of HIV treatment regimens using the effective within-host viral load (V_h^{*E}) as an indicator of treatment effectiveness when each of the three HAART components is assumed to have: (a) low efficacy of 0.30, (b) medium efficacy of 0.60, and (c) high efficacy of 0.90.	30
3.1	Table of parameter description and initial parameter values for the between-host model given by (3.3)	35
3.2	Sensitivity indices of the two metrics of baseline between-host HIV transmission dynamics.	50
3.3	Results of the assessment of comparative effectiveness of HIV/AIDS preventive interventions using the basic reproduction number (R_0) as an indicator of treatment effectiveness when each of the six preventive interventions is assumed to have: (a) low efficacy of 0.30, (b) medium efficacy of 0.60, and (c) high efficacy of 0.90.	54
3.4	Results of the assessment of comparative effectiveness of six HIV/AIDS interventions using the HIV Prevalence (I_H) as an indicator of intervention effectiveness when each of the six preventive interventions is assumed to have: (a) low efficacy of 0.30, (b) medium efficacy of 0.60, and (c) high efficacy of 0.90.	57
3.5	Results of the assessment of comparative effectiveness of HIV/AIDS preventive interventions using the CVL (V_H) as an indicator of treatment effectiveness when each of the six preventive interventions is assumed to have: (a) low efficacy of 0.30, (b) medium efficacy of 0.60, and (c) high efficacy of 0.90.	60
4.1	Results of the assessment of the sensitivity of the four HIV/AIDS transmission metrics (\mathcal{R}_0 , V_H , \mathcal{R}_0 and V_h) to the baseline HIV multilevel model parameters.	91
4.2	Summary of the action of health interventions on HIV/AIDS transmission dynamics.	100

4.3	Key for interpretation of the symbols used in the the description of results of the assessment of comparative effectiveness of HIV/AIDS interventions in Tables (4.4), (4.5) and (4.6) as well as the numerical values/ranges of values used in the calculations	104
4.4	Results of the assessment of comparative effectiveness of HIV/AIDS interventions using the effective reproductive number (\mathcal{R}_E) as the indicator of intervention effectiveness when each of the five interventions is assumed to have: (a) low efficacy of 0.30, (b) medium efficacy of 0.60, and (c) high efficacy of 0.90.	105
4.5	Results of the assessment of comparative effectiveness of HIV/AIDS interventions using the intervention induced endemic value of community viral load (V_H) as the indicator intervention effectiveness when each of the five interventions is assumed to have: (a) low efficacy of 0.30, (b) medium efficacy of 0.60, and (c) high efficacy of 0.90.	108
4.6	Results of the assessment of comparative effectiveness of HIV/AIDS interventions using the intervention induced endemic value of HIV/AIDS prevalence (I_H) as the population level indicator of intervention effectiveness when each of the five interventions is assumed to have: (a) low efficacy of 0.30, (b) medium efficacy of 0.60, and (c) high efficacy of 0.90.	112

List of Abbreviations

HIV	Human Immunodeficiency Virus
AIDS	Acquired Immunodeficiency Syndrome
TasP	Treatment as Prevention
CVL	Community Viral Load
CPL	Community Pathogen Load
CEL	Comparative effectiveness at low efficacy
CEM	Comparative effectiveness at medium efficacy
CEH	Comparative effectiveness at high efficacy
HAART	Highly Active Antiretroviral Therapy

I dedicate this work to my beloved wife Susan and my beautiful baby Tawananyasha Treasure for the love and support that sustained me throughout the entire research period.

Chapter 1

Introduction

1.1 Background

Infectious diseases are clinically evident illnesses that result from the presence of microbial pathogenic agents such as parasites, helminth, protozoa, bacteria, fungi, virus, toxic proteins (for example prions) or higher order organisms (for example, worms) (Martcheva et al., 2015b). Well-known for causing sickness and death, enormous pain and suffering, increased time spent on patient care and huge economic losses due to lost production, infectious diseases remain a major public health concern both globally and locally (CDC, 2014 (accessed October 26, 2016); Gutierrez et al., 2015). However, despite recording successes in terms of disease management and control (such as diagnostics, therapeutics, vaccines e.t.c), infectious diseases continue to be a scourge without equal. In the face of these challenges, it is important to proactively study the immunology and epidemiology of infectious disease systems so that the signs, symptoms and consequences of such diseases could be reduced or even eliminated.

Meanwhile, we define explicitly the two important terms in the study of infectious diseases: Immunology and Epidemiology. Immunology is the study of the immune system in all its biological, chemical and physical aspects. This key aspect of infectious diseases is important as it's understanding has served as a foundation upon which within-host model describing host-pathogen interactions have been developed (Ikeda et al., 2014; De Boer et al., 2010; Culshaw and Ruan, 2000; Conway and Perelson, 2015; Magombedze et al., 2008; Zhang et al., 2015). Moreover, we define the immune system as a complex and highly regulated system whose function is to protect the human body from invading pathogens. Epidemiology, on the other hand, is defined as the study of distribution and determinants of health-related states or events and the application of such knowledge to control health-related problems (John M. Last, 2014). The definitions of immunology and epidemiology have two important implications in mathematical modelling of infectious diseases. However, before we delve into the implications, we need to first provide clarity on how infectious agents (well known as pathogens) invade the immune system. At their initial inoculum, the pathogen launches an attack on the immune system which is also met with counter-attacks by the immune system. Once the pathogens have withstood the attacks of the immune system and overcome it, they successfully accomplish transmission and infection. The first implication is that the distribution and determination of health-related states/events are attributable, in part, to the extent in which the immune system overcomes/succumbs to infectious agents. Therefore, epidemiological processes can be referred to as the emergent properties of processes that occur at the immunological level of human beings. An emergent phenomena is defined as complex patterns that emerge at higher scale through the

interaction of individuals at a lower scale (Garira, 2017). The second implication is that epidemiological processes, in turn, play a vital role in determining the extent to which the immune system responds to invading pathogens (Martcheva et al., 2015b). For instance, it is well-known that predominant risk factors of infectious diseases such as low socio-economic status, poor nutrition and poor housing are all operative at the epidemiological scale but their role in terms of fuelling the spread of infectious diseases can be traced back to the immune system (Roberts et al., 2015). Moreover, several researches have shown how these risk factors have been promoting the spread of infectious diseases by making the immune system vulnerable to invading pathogens. Thus, the non-separable nature of scales that characterises infectious diseases implies that mathematical modelling of such complex problems should encompass the multi-level nature of such diseases. Consequently, researchers have been lobbying for the launch of high-throughput computational techniques such as multiscale modelling that allows the study of huge and complex disease problems that are multiscale in nature (Garira et al., 2014; Martcheva et al., 2015b; Sloot and Hoekstra, 2009). In this study, we investigated the problem of HIV/AIDS using a multiscale modelling framework and we developed a multiscale model that linked within- and between-host scales and use the model to make inferences about the properties of the complex HIV/AIDS disease system.

1.1.1 HIV Infection

The Human Immunodeficiency Virus (HIV) is the etiological agent of the Acquired Immunodeficiency Syndrome (AIDS). HIV infection is characterised by three stages namely the acute (primary) infection, clinically asymptomatic stage (chronic infection) and the AIDS (drug therapy) stage. The acute stage (which can last for 2-10 weeks post-infection) is also known as the initial inoculum stage, is associated with a decreasing population of CD4+ T-helper lymphocytes and a large spike in the level of circulating HIV. The Asymptomatic stage, also known as the chronic stage of HIV infection is associated with a gradual decrease in the HIV RNA levels to a level called the set point viral load. During this stage, the T-helper lymphocytes densities are characterised by a sharp rise due to the immune response to the virus. The AIDS stage is characterised by low CD4+ levels and an overgrowing HIV RNA viral load. HIV patients who are in this stage become vulnerable to opportunistic infections as their weakened immune system becomes opportune to several diseases.

1.1.2 HIV Transmission

Transmission is a defining characteristic of infectious diseases and it is the most important point of contact between within- and between-host models. HIV is transmitted either sexually (via contact with body fluids such as vaginal fluids, semen, rectal fluids), vertically (when an HIV infected pregnant mother passes it onto their unborn child), sharing of needles (especially among injection drug users (IDUs)), breast milk during breastfeeding or through blood transfusion in health settings (Simpson and Gumel, 2017). However, in the Sub-Saharan Africa region, the majority of HIV cases are as a result of heterosexual transmission. With regard to transmission, it has been recently shown that it results from complex and dynamic relationships that take place at varying spatial and temporal scales but yet still represents an understudied aspect of infectious disease systems (Garira, 2017). Consequently, HIV preventive and treatment should be designed to address social, economic and structural factors that place specific individuals at risk of contracting the deadly chronic viral

infection. However, effective design of such interventions requires that we integrate across several temporal and spatial scales associated with the entire HIV disease system's organization. In this study, we developed a multiscale model of HIV/AIDS transmission and used it to compare the effectiveness of various HIV/AIDS interventions with the goal of identifying high-impact interventions.

1.1.3 HIV Preventive and Treatment Interventions

The birth of antivirals has been recorded as a major advance in the prevention and treatment of HIV/AIDS. These technological advances have played a significant role in transforming HIV/AIDS disease from being an acute and deadly infection to a chronic one. Several preventive and therapeutic strategies have been applied to control the spread of HIV/AIDS in the population. These include voluntary medical male circumcision (VMMC), condom use, voluntary HIV testing, public health education and counselling, access to sterile needles, the use traditional medicines and the use of antiretroviral treatment (ART). In most Sub-Saharan Africa, for instance, the following are implemented; HIV testing and linkage to care, access to condoms and sterile syringes, prevention programs for people living with HIV and their partners, prevention programs for people at high-risk of HIV infection (for example, sex workers), substance abuse treatment, screening and treatment for other sexually transmitted diseases, the use of traditional medicines and ART. In developed countries such as the United States of America, some of these control strategies have been proven to be effective in reducing the risk of HIV infection. This has been shown to be the case especially when they are designed to address the social, economic, and structural factors that place specific individuals or groups at risk of contracting HIV. For instance, it was highlighted in Simpson and Gumel, 2017 that the implementation of these aforementioned control strategies in the US resulted in a stable HIV incidence. In the context of Africa, in particular, the Sub-Saharan Africa, HIV has remained a major public health concern despite having witnessed several successes in reducing the outcomes of HIV infection (for instance improved life expectancy due to reduced disease-induced death rate brought about by antiretroviral therapy). Therefore, there is an urgent need to formulate effective strategies if sustainable development goals (SDGs) on HIV/AIDS are to be achieved. In this study, medical and public health interventions are combined and their population-level impact compared based on three epidemiological quantities (basic reproduction number, HIV prevalence and community viral load).

1.2 Problem Statement

A gap has been created in our attempt to gain an in-depth understanding of the transmission processes of infectious diseases including HIV/AIDS disease, as such endeavours require knowledge of processes at various scales of infectious diseases and how these scales are intertwined (Garira, 2017). Mathematical models have advanced the understanding of the transmission of many infectious diseases (including HIV, Malaria, Cholera, and Tuberculosis). However, most disease modellers have until recently studied the progression of these infections separately. But linking the immunology and epidemiology progression of these infectious diseases mathematically, which is sometimes called host-level immuno-epidemiological model (Garira, 2017), will allow us to examine how inter-individual differences in immune responses affect the population dynamics of pathogenic agents (in this case, HIV) to produce

the epidemiological patterns of infection observed in heterogeneous host populations; to provide answers to questions relating to the distribution and frequency of infection and disease as well as facilitating the proper investigation of how the types and levels of immunity vary over time subject to the exposure to pathogenic infection. With regards to HIV/AIDS disease, several mathematical studies have been carried out and the majority of them considered within-host and between-host processes separately. In this study, we will fill this gap by developing a multiscale modelling framework that will link the within-host infection progression with the between-host disease progression of HIV/AIDS. To be more specific, this work will attempt to address the following research question:

- Can we use a multiscale model of HIV/AIDS transmission dynamics to assess the comparative effectiveness of health interventions that are implemented at different scale domains?

1.3 Aims and Objectives

The overall aim of the study is to develop a multiscale model for HIV/AIDS transmission dynamics and to use it to assess the comparative effectiveness of HIV/AIDS intervention strategies. Specifically, the study aims at achieving the following objectives:

- To develop a multiscale model of HIV/AIDS transmission that incorporates the role of within-host scale processes in determining the outcome of the disease progression at the between-host scale (population-level).
- To use the model to assess the comparative effectiveness of 5 HIV/AIDS preventive and treatment methods (TasP (fusion inhibitors, reverse transcriptase inhibitors and protease inhibitors), condom use and male circumcision).

1.4 Methodology

In this work, we use multiscale modelling framework to link the two most commonly studied scales in the transmission of HIV/AIDS disease system which are: the within-host scale (associated with infection dynamics within a single-host where immunological processes take place) and the between-host scale (associated with disease transmission within the host population where epidemiological processes take place). Since a multiscale model represents another form of a mathematical modelling process, it is of utmost importance to first of all give the precise definition of the term "mathematical modelling" before we delve into multiscale modelling. We define mathematical modelling *as a scientific process that use mathematical concepts, formulas and theories for setting up mathematical problems representing real-world phenomena*. Similarly, a multiscale model is a mathematical model that integrate multiple scales of biological organisation, ranging from molecular, cellular and tissue models to organ, whole-organism and population scale models (Schleicher et al., 2016). Multiscale modelling is applied to systems that have important features across many orders of magnitude in time and space such as the HIV/AIDS disease system among other complex systems. These models are common in the natural sciences and engineering disciplines such as chemistry, meteorology, product development, decision support systems, optimization among many other disciplines. The usefulness of multiscale models lies in its ability to facilitate the description and understanding

of problems that span across several orders of spatial and temporal scales. Furthermore, in the context of infectious diseases, the advent of multiscale models have opened up many opportunities for researchers to apply computational approaches in solving problems arising from the field of infectious diseases. In addition, multiscale models are useful in that they allow for deeper understanding of the progression of a disease across scales. For instance, at the within-host scale, we can use multiscale modelling framework to study "how factors such as frequency of infection or genetic variation affect levels of immunity" while at the between-host scale, we can also employ the methodology to examine "how immune responses influence the prevalence of infection and the burden of disease" (Garira, 2017). Lastly, the ever-growing importance of multiscale modelling can easily be traced from its application and its wide use in engineering, mathematics, physics, meteorology, computer science, product development among other fields and more recently in its application in the study of infectious diseases.

In this work we investigate the problem of HIV/AIDS intervention research strategies. The implementation of the multiscale modelling includes the use of ordinary differential equations which represent processes at two scales (within-host and between-host). The detailed description of the methodology is presented in Chapter (4).

1.5 Review of Literature on Multiscale Modelling

Here, we present a brief review of the literature on multi-scale modelling. The development of multiscale models began in the 1970s in fields such as physics, meteorology and chemistry (Gutierrez et al., 2015). Like any other mathematical modelling process, the choice to use multiscale modelling approach as a tool for addressing real world problems is in itself a decision-making process which depends entirely on the goal behind the formulation of a model as well as the specific research questions to be answered. In other words, the decision to apply multiscale models rest upon the structure of the underlying problem. For instance, there are situations in which the underlying problem may require the launch of complex models such as multiscale models. In this study, we propose the use of multiscale modelling because our research question dictates that we carry out a comparative effectiveness of HIV/AIDS interventions (both medical and public health), a task far beyond the reach of well-known traditional single-scale modelling approaches. Specific examples in which multiscale modelling was applied relates to its application, in the early 1980s, in solving a meteorological problem by combining the interactions of soil and vegetation with the atmosphere. The results obtained from combining the effects of those three determinants brought another deeper insight in computational weather forecasts as the results were considered "**more realistic**". Other applications of multiscale modelling where it has made an impact include the pharmaceutical research industry, chemical engineering, physics, product engineering, medicine among many other fields.

1.5.1 Multiscale Modelling and Infectious diseases

In the context of infectious diseases, we have to date witnessed major theoretical advances in the field of multiscale modelling as the field continue to gradually draw the attention of researchers. Multiscale models have been developed to address several infectious diseases modelling problems chief among them include tuberculosis

(Fallahi-Sichani et al., 2011), malaria (Fedosov et al., 2011; Ademiloye et al., 2017; Martin, 2017), influenza (Heldt et al., 2013), HIV (Hosseini and Gabhann, 2012) and so on. For the purpose of this work, a categorization framework presented recently in (Garira, 2017) will be summarised. In his work, Garira presented a categorization framework for categorizing multiscale models for infectious diseases. The categorization framework is based on five integration frameworks and five criteria. The integration framework which we summarize here as S^2MEP integration framework include the serial, simultaneous, multi-domain, embedded and parallel integration frameworks. On the other hand, the five criteria consists of (I) the nature of between-scales information flow (that is, whether uni-directional or bi-directional), (II) the relationship among scales involved, (III) the order of scale incorporation into the multiscale model (top-down, bottom-up or concurrent), (IV) transmission biodiversity level and (V) the structure or formalisms of various sub-models that constitute the multiscale models. Consequently, five categories of multiscale models that integrate the within-host scale and between-host scale of infectious disease systems have been identified. The five categories of multiscale models are (I) individual-based multiscale models (IMSMs), (II) nested multiscale models (NMSMs), (III) embedded multiscale models (EMSMs), (IV) hybrid multiscale models (HMSMs) and (V) coupled multiscale models (CMSMs). Below are brief explanations for each of the named multiscale model type as adopted from (Garira, 2017):

- **IMSMs:** these are multiscale models formed when the within-host sub-model is used to describe the entire infectious disease system across both the within-host scale and between-host scale. As result, no explicit between-host scale submodel is used in this approach.
- **NMSMs:** these are multiscale models that are formed by integrating within-host scale and between-host scale while allowing the between-host scale to be dependent on the within-host processes, they assume that the within-host scale dynamics is independent of the between-host scale.
- **EMSMs:** formed based on the embedded integration framework, EMSMs are developed when both submodels (the within-host scale sub-model and the between-host-scale submodel) feature in the multiscale model.
- **HMSMs:** formed based on multi-domain integration framework, HMSMs results when within-host and between-host submodels with different structure/formalisms are integrated, that is, when the within-host scale and the between-host scale belong to different domains
- **CMSMs:** formed based on parallel integration framework, CMSMs takes an ecosystem view to multiscale modelling of the host level immuno-epidemiology of infectious disease systems and considers the overlap of biodiversity and drivers of infectious disease systems.

It is important to note that the choice of the multiscale model applied in addressing a particular problem depends on the characteristics of the problem to be investigated and the main purpose of modelling (Garira, 2017). For the purpose of this study, we use a nested multiscale model as it allows us to assume uni-directional

flow of information in which the within-host scale feeds information into the between-host processes of HIV/AIDS. To link the dynamics, we use the serial integration framework. In linking the submodels using this integration framework, we first solve the within-host submodel and then use its results to build the between-host submodel, which in turn describes the entire multiscale infectious disease system. Further details regarding this integration technique are well articulated in Garira, 2017.

In infectious diseases modelling, multiscale modelling framework has been applied to address a variety of questions. One common question is *"What is the impact of within-host dynamics on population-scale quantities such as the basic reproduction number and prevalence?"*. For example, Feng et al., 2012 used multiscale modelling to study the transmission of *Toxoplasma gondii*, an obligate intracellular, parasitic alveolate that causes the disease toxoplasmosis. For modelling, they coupled within-host dynamics with between-host dynamics to produce a multiscale model which they further used to show the existence of backward bifurcations. Moreover, their model results showed that multiscale modelling had the potential to provide outcomes that could not have been obtained if they had independently considered the role of epidemiological and immunological processes on the dynamics of *T. gondii*. In terms of implications of this study's results, infection was shown to persist at population-level even when the isolated between-host reproduction number was less than one; a result which elucidated the importance of within-host dynamics on between-host threshold quantities such as the basic reproductive number. In this present study, we extend the investigation to include the effects of within-host dynamics on HIV prevalence and the community viral load.

In another study, Garira et al., 2014 developed a framework for linking within-host and between-host for infections with free-living pathogens in the environment. This study investigated and confirmed the influence of within-host processes on between-host dynamics through numerical simulation of the multiscale model. Despite using an embedded framework to integrating the within- and between-host submodels, their results provide a good basis for this current study. This is especially true in that their study provided a useful guide on how public health and medical interventions could best be integrated for improved infectious disease control management, a development which is very similar to the main aim of this study, which seeks to carry out an assessment on the comparative effectiveness of HIV/AIDS health (both medical and public) interventions to identify high-impact interventions. It is also important to highlight that the work by Garira and his collaborators was without its own limitations. For instance, their study only investigated the influence of within-host on between-host. In addition, they deducted and inferred from the sensitivity analysis results the parameters that could be best targeted for effective control of the disease. In this study, we extend the same idea by performing a rigorous analysis on the model as well as evaluating different health intervention strategies with the goal to identify effective high-impact HIV/AIDS package services.

1.5.2 Viral Infections

A viral infection is a proliferation of a harmful virus inside the body, for example, cold, influenza, chickenpox, human immunodeficiency virus (HIV) among others. These viruses can affect many areas of the body, including the reproductive, respiratory, and gastrointestinal systems. By definition, viruses are small particles of genetic

material (either DNA or RNA) that are surrounded by a protein coat. Some viruses also have a fatty "envelope" covering. Because viruses are incapable of reproducing on their own but rather depend on the organisms they infect (hosts) for their very survival, a deeper understanding of viral infections requires a clear understanding of various levels (host and pathogen levels) and scales (cellular, tissue and organ scales) across which viruses experience during their invasion and growth processes. A detailed description of levels and scales are found in Garira, 2017. For the purpose of this study, we describe the scales that form the main basis of multiscale modelling. At the cellular level, we consider activities and behaviour of the different immune cells (e.g. T-cells) and different pathogen processes (e.g. HIV). Processes at cellular scale may be within-cell or between-cell scales. The within-cell scale represents viral infection events that occur inside infected cells while between-cell scale represents the transmission of the pathogen among cell populations. The other two important scales that this study considers include within-host and between-host scales. The within-host scale is associated with disease dynamics within a single-host where immunological processes take place and the between-host scale is concerned with disease transmission within the host population where epidemiological processes take place.

1.5.3 Multiscale Modelling and HIV/AIDS

In the context of HIV / AIDS, multiscale models have also been developed at various scales of the entire complex disease system. Specifically, a recent review of multiscale HIV immunoepidemiological modelling of within-host and between-host (Dorratoltaj et al., 2017) discloses that a multiscale framework turned out to be insightful for understanding the mechanisms and identifying potential therapeutic targets for human infection with HIV. Furthermore, the review also presented some of the topics that have been successfully addressed using the multiscale modelling framework such as intervention research (Yeghiazarian et al., 2013; Magombedze et al., 2008; Shen et al., 2015; Sun et al., 2016; Metzger et al., 2011) , super-infection (Martcheva and Li, 2013), drug resistance ((Saenz and Bonhoeffer, 2013)), evolution Lythgoe et al., 2013; Doekes et al., 2017 and co-infection ((Cuadros et al., 2011)). Consequently, in this section we shall describe several multiscale models of HIV that were previously developed and have played the key role in providing a deeper understanding of the processes involved with HIV infection/transmission dynamics. The disease scales considered in this study are within- and between-host scales. The within-host scale describes infection dynamics within an infected host and it encompasses the molecular, cellular and tissue scales. The between-host, on the other hand, describes the transmission of the disease from one infected host to the other.

Hosseini and Gabhann, 2012 developed a multi-scale model to address an intervention research problem in which they specifically sought to investigate the impact of A3G-Vif interactions on HIV replication. The study investigated the potential power of mainly three apolipoprotein B mRNA editing enzyme 3G (APOBEC3G) or (A3G)-based therapies which are: antibody to viral infectivity factor (Vif), up-regulation of A3G and mutated forms of A3G (an enzyme which is a member of the APOBEC family which is a potent inhibitor of HIV infection). In contrast, viral infectivity factor (Vif) - a viral protein, is known to have an antagonistic effect on APOBEC3G through protecting the virus by binding to A3G and causing the degradation of this enzyme. For multiscale modelling, the dynamics at the within-cell scale were described by ordinary differential equations (ODEs) submodel whilst

the dynamics at between-cell scale were described by delay differential equations (DDEs) submodel. The within-host submodel was unidirectionally coupled to the between-cell scale submodel. Although this study laid a firm theoretical foundation for our work, it mainly focused on intra-cellular, inter-cellular and extra-cellular events which are all within-host processes thereby overlooking the role of between-host processes in influencing the course of HIV/AIDS disease system. Therefore, our study aims to address this limitation through explicitly acknowledging the role of between-host processes in shaping the course of whole HIV/AIDS disease system.

In another intervention research study, (Magombedze et al., 2008) used a multiscale model to study the immunopathogenesis of HIV-1 infection. The multiscale model, recently classified in Garira, 2017 as cytoimmuno-epidemiological, was used to assess virological responses at both within-cell scale and between-cell scale antiretroviral drugs. In developing the multiscale model, Magombedze and his collaborators first developed a basic mathematical model of the immunopathogenesis of HIV-1 infection that incorporates three distinct stages in the infection cycle of HIV-1: entry of HIV-1 into the cytoplasm of CD4+ T cells, transcription of HIV-1 RNA to DNA within CD4+ T cells, and production of HIV-1 viral particles within CD4+ T cells. The multiscale model was then extended to incorporate the effect of three major categories of anti-HIV-1 drugs: fusion/entry inhibitors (FIs), reverse transcriptase inhibitors (RTIs) and protease inhibitors (PIs). The results established that the actual drug efficacy of FIs and PIs was the same as their effective efficacies while the effective drug efficacy for the RTIs was found to depend on the rate of transcription of the HIV-1 RNA to DNA and the longevity of infected CD4+T cells where virions have only entered the cytoplasm and that this effective efficacy was less than the actual efficacy. This study suggested that, of the three anti-HIV drug categories (FIs, RTIs and PIs), any drug combination of two drugs that includes RTIs is the weakest in the control of HIV-1 infection. Despite having unearthed hidden information about the immunopathogenesis of HIV-1 infection and the role of HAART drug regimens, this study failed to incorporate the effect of public health interventions such as condom use and male circumcision. Therefore, our study is designed in a manner that addresses this limitation in Magombedze's work. For instance, in this current study, we develop a multiscale model that make it possible to carry out a comparative assessment of both medical (HAART components) and public health (condom use and male circumcision) interventions.

Yeghiazarian et al., 2013 developed a stochastic multi-scale model of HIV-1 transmission to study the impact of medical interventions at the level of individuals on the spread of infection across the whole population. For modelling, they integrated within-host cellular dynamics and their outcomes, patient health states, and sexual contact networks. The multiscale model captured disease states and progression within individuals, and similar to our study, the model allowed for simulation of therapeutic strategies. The results demonstrated the potential of early ART initiation in substantially changing a new course of HIV/AIDS disease progression at the population level. It is vital to note that in carrying an evaluation on the possible HIV interventions, this study considered only medical interventions. The limitation of this approach emanates from the fact that meaningful identification of high-impact interventions requires that all HIV/AIDS interventions (both medical and public health) be assessed while taking into account the entire HIV/AIDS disease system. When HIV/AIDS disease system is considered in its entirety, meaningful comparative effectiveness can be carried out which then leads to the reasonable identification

of essential (high-impact) HIV package services. Hence, this study develops a multi-scale model of HIV/AIDS transmission dynamics (deterministic, not stochastic) and extend the model to incorporate the effect of both medical and public health interventions. Furthermore, we also use the controlled multiscale model to derive model metrics which we use to carry out an assessment of the comparative effectiveness of HIV/AIDS interventions.

Martcheva and Li, 2013 studied a case of superinfection by developing a two-strain based multiscale model that coupled immunological and epidemiological dynamics across scales. For mathematical modelling, within-host and between-host submodels based on partial differential equations (PDEs) were first developed separately. They then coupled the two submodels through the age-since-infection structure of the epidemiological variables, that is, transmission rate between-hosts and death rate of individuals was assumed to depend on viral load within-host over time. Numerical simulations were performed on the multiscale model and the results were used to suggest that epidemiological reproduction number and HIV population prevalence are monotone functions of the within-host parameters with reciprocal trends. In this current study, we use the multiscale model to show that HIV prevalence is not a reliable metric for evaluating interventions as results obtained through its use falls short of the consistency we would expect when the number interventions applied to the model are increased. Moreover, in our current study, we incorporate another metric for the community viral load and use it to prove its suitability as a metric for evaluating HIV/AIDS interventions due to its level of consistency with conventional laws of mathematics.

1.6 Limitations of Multiscale Modelling

While multiscale models plays an important role in providing deeper biological insights into the complex interactions between diseases processes such as the disease triad (host, agent and the environment) through improved diagnosis facilitated by biomarker discovery, improved predictions on clinical outcomes of infections and provision of a multi-scale, systems-based approach for evaluating the wider implications of therapeutic strategies (Schleicher et al., 2016; Yeghiazarian et al., 2013), the approach is not without its own drawbacks.

Consequently, one common drawback of multiscale modelling is tied to the increased model complexity associated with the computational approach, that is, very few population-level quantities can be computed analytically in a closed form. This means that little can be learned from studying the effect of within-host processes on the between-host processes outside of extensive computer-based systems. Another drawback of multiscale modelling arise from the fact that it is characterised by a large number of parameters such that the modelling framework itself is always associated with problems that must be overcome to make the model results credible and reliable. Thus, a high degree of parameter values is negative in the sense that it is hard to ensure that all parameters have realistic values. This constitutes one of the limitations for our study as the parameter values that were used in simulating the multiscale model were not from a single epidemic setting. Consequently, this has negatively compromised the reliability and credibility of the study's results as they cannot be taken as characterizing a specific HIV/AIDS epidemic system. In addition, from a mathematical modelling perspective, multiscale models are also faced with the challenge of parameter unidentifiability as pointed out in Schleicher et al.,

2016. This is a scenario which arises from the known fact in mathematics that many model parameters have to be inferred from system-wide dynamic data. Because the determination process is non-unique, the problem of parameter unidentifiability arises and may potentially cause model predictions to come with an arbitrarily large uncertainty range. As a result, model predictions will be reduced to merely suggestions as opposed to unique consequences of model and data.

However, despite all the drawbacks raised here pertaining to the deployment of multiscale modelling computational approaches as aids to ensuring the deeper understanding of HIV/AIDS research topics, it is an invaluable and indispensable computational tool as it is capable of presenting opportunities to infer the synergistic dynamics of HIV at the individual and population level. Besides previous results obtained through application of multiscale models have by far exposed the weaknesses of single-scale models to the extent that it has presented the methodology as an important mathematical tool whose associated complexities are worthy the biological insights derived from their implementation (Sun et al., 2016; Feng et al., 2013).

1.7 Outline of the thesis

- **Chapter 2** discusses weaknesses of single-scale models as opposed to multiscale models. Specifically, this chapter shows that the within-host HIV infection model could not be extended to assess the effectiveness of preventive strategies for purposes of informing HIV/AIDS health policy.
- **Chapter 3** develops the mathematical model that describes the transmission dynamics of HIV/AIDS at population-level. In this chapter, we described and analysed the population-scale dynamics of the HIV/AIDS disease system. The main results showed the inability of the between-host model in successfully assessing the effectiveness medical interventions (drug regimens). Specifically, using the between-host models, the comparativeness of HIV/AIDS drugs were the same, a result contradictory to the results which were previously shown in Chapter 2. To resolve the anomaly, we presented a multiscale model in Chapter 4.
- **Chapter 4** provides the development of multiscale model that combine the immunological (within-host) and epidemiological (between-host) models. We use the resulting multiscale model to identify the most effective intervention combinations that could best work to control the transmission of HIV/AIDS.
- **Chapter 5** provides results, discussion, conclusion and the recommendations.

Chapter 2

Within-host model for HIV Infection

2.1 Introduction

This chapter describes within-host dynamics of HIV infection. We consider a simple model for depicting the reproduction processes of HIV pathogen within an infected individual host. The model is developed for the purpose of showing how the study of within-host processes in isolation of between-host processes can be a futile endeavour for realising meaningful benefits of mathematical epidemic models at the population level. Henriegel defined multi-scale modelling as an area that links data, models and knowledge to create new perspectives. Thus, the purpose of this chapter is to develop a simple within-host model for HIV pathogenic reproduction processes and qualitatively investigate its analytic properties with the view to further motivate the study of HIV/AIDS using multi-scale models. Furthermore, the chapter intends to show the shortfalls associated with within-host modelling of HIV/AIDS as opposed to the multiscale modelling of the HIV/AIDS disease system as a whole. To achieve the objectives of this chapter, we develop a within-host model of HIV-1 infection in section (2.2) and then use the resulting model to motivate the need for developing multiscale models through evaluating the effectiveness of different drug combinations (medical intervention scale) while emphasizing on how the model fails to capture the effects of public health interventions (that is, condom use and voluntary medical male circumcision).

2.2 Within-Host Model

We develop a mathematical model that describes HIV infection dynamics within an individual host. The model consists of 4 state variables, namely, the susceptible CD4+ T-cells (T_s), exposed CD4+ T-cells (T_c), infected CD4+ T-cells (T_v) and within-host viral load (V_h). We use ordinary differential equations to describe the

movement of T-helper cells from one state to the other using the law of mass action:

$$\left\{ \begin{array}{l} \frac{dT_s}{dt} = \Lambda_s - \beta_h V_h T_s - \mu_s T_s, \\ \frac{dT_c}{dt} = \beta_h V_h T_s - (\alpha_c + \mu_c) T_c, \\ \frac{dT_v}{dt} = \alpha_c T_c - (\alpha_v + \mu_v) T_v, \\ \frac{dV_h}{dt} = N_v \alpha_v T_v - (\alpha_h + \mu_h) V_h. \end{array} \right. \quad (2.1)$$

The first equation (1) of model system (2.1) describes the dynamics of healthy (susceptible) CD4+ T cells in which parameter Λ_s represents the source of CD4+ T cells from the thymus or bone marrow. The second term represents the collision, fusion and entry of HIV virions into the cytoplasm of CD4+ T cells at rate β_h . The last term of the equation represents the natural death of susceptible CD4+ T cells at rate μ_s .

The second equation of the model system describes the dynamics of exposed CD4+ T cells (that is, healthy CD4+ T cells that have allowed viral entry into their cytoplasm). The first term of equation (2) is generated from the collision process as depicted by the second term of the first equation (that is, the first term represents the transfer term from equation (1) of the model system) Thus, $\beta_h V_h T_s$ is the source of exposed CD4+ T cells that are waiting for transcription of HIV RNA to DNA to occur. Moreover, this equation describes the transformation phase that the successful infection process of CD4+ T cells passes through before transcription occurs. The last term of this equation represents (1) the death of exposed CD4+ T cells at rate μ_c during this exposure stage and (2) the proportion of infected CD4+ cells that successfully shed to produce HIV virions at rate α_c .

Similarly, equation (3) models the dynamics of HIV infected CD4+ T cells (that is, exposed CD4+ T cells that have successfully changed to become infected after the RNA to DNA transcription process has occurred. The first term of the equation represent the transfer term from equation (2). The second term of the equation jointly represents the natural death of infected CD4+ T cells at rate μ_v and the loss of infected CD4+ T cells as they shed to produce new HIV virions at rate α_v .

Finally, the fourth equation of the model system describes the dynamics of viral load. The first term represent the source of new virions resulting from the bursting of infected CD4+ T cells. The last term represents the natural death of viral particles at rate α_h as well as the proportion of virions that are excreted into the blood system at rate μ_h . The table below shows parameters of the model, their description and their initial values:

SL. No.	Parameter	Meaning	Initial Value	Range Explored	Units	Source/Rational
1.	N_v	HIV Viral burst size	650	(160 - 1150)	virions day^{-1}	Martcheva and Li, 2013 Martcheva et al., 2015b
2.	α_v	lytic death rate of T_v cells	0.09	static	per cell day^{-1}	De Boer et al., 2010; Culshaw and Ruan, 2000
3.	α_c	Transition rate from T_c to T_v	0.00045	$(1.125 \times 10^{-4} - 7.875 \times 10^{-4})$	- day^{-1}	Magombedze et al., 2008
4.	Λ_s	Production rate of T_s cells	50000	(12500 - 87500)	$\mu L day^{-1}$	Martcheva and Li, 2013
5.	β_h	fusion /collision rate	0.00135	$(7 \times 10^{-8} - 1)$	per sexual contact day^{-1}	Zhang et al., 2015
6.	μ_s	Natural death of T_s cells	0.02	constant	per cell day^{-1}	Magombedze et al., 2008; Martcheva and Li, 2013 Culshaw and Ruan, 2000
7.	α_h	shedding rate of V_h	0.09	(0.0225-0.1575)	virions day^{-1}	Conway and Perelson, 2015; Culshaw and Ruan, 2000 Martcheva et al., 2015b
8.	μ_h	Virus clearance rate	1.5	static	virions day^{-1}	Ikeda et al., 2014; De Boer et al., 2010
9.	μ_c	Natural death of T_c cells	0.02	static	cells day^{-1}	Ikeda et al., 2014
10.	μ_v	Natural death of T_v cells	0.15	(0.0375-0.2625)	$\mu L day^{-1}$	Ikeda et al., 2014

Table 2.1: Table of parameter descriptions and initial parameter values for the within-host model given by system (2.1)

The state transition system below depicts the transfer processes that are involved as targeted CD4+ cells change their states and how the model variables are linked

with the HIV-RNA plasma viral load within an infected human host.

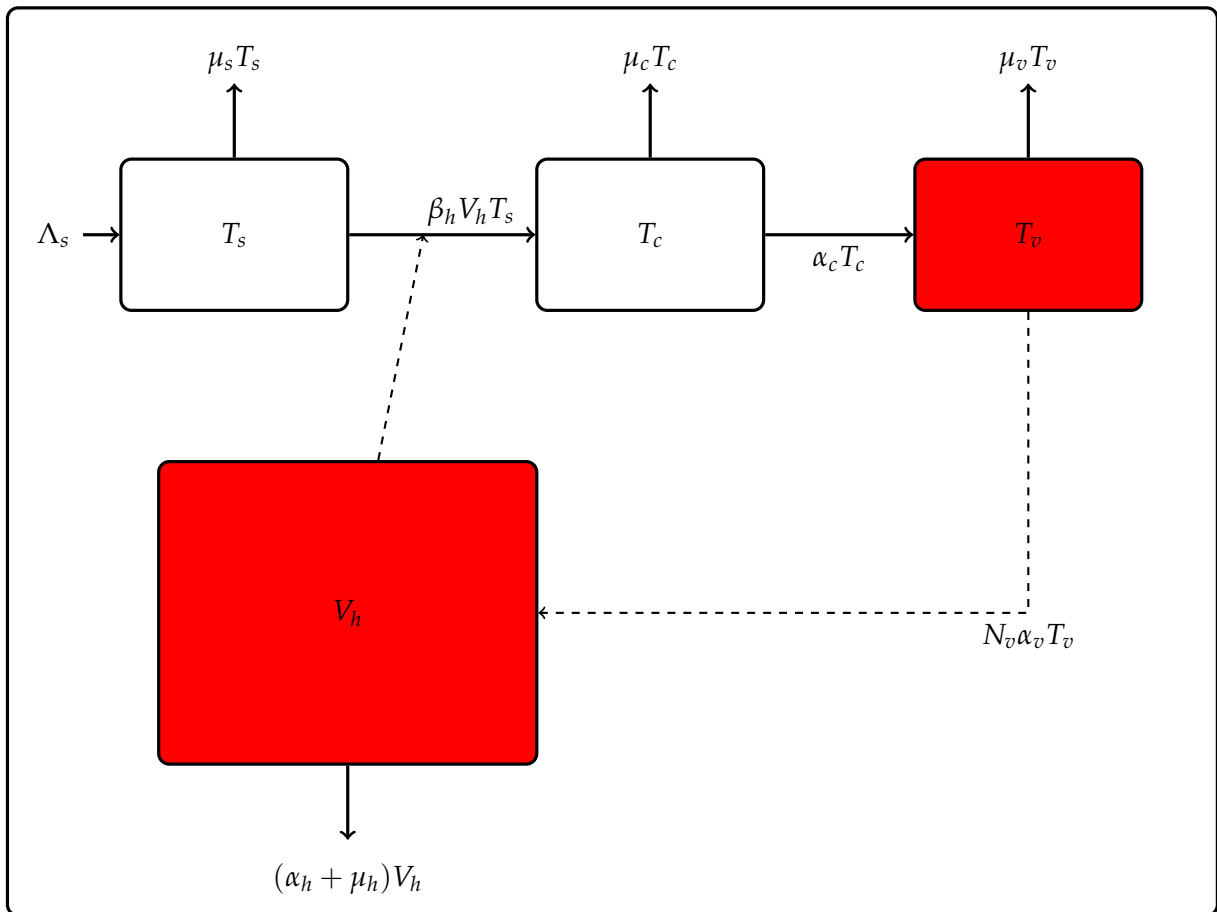


Figure 2.1: A conceptual diagram of the within-host HIV infection dynamics.

2.3 The Infection Free Equilibrium

The infection free equilibrium (E^0) of system (2.1) denotes the point at which all the sub-populations of the within-host model are free of HIV and it is instructive for the infection free equilibrium to be computed and its stability established as the persistence or the eventual elimination of HIV infection wholly depends on whether or not the IFE is stable or unstable. For our model system (2.1), the IFE is given as

$$E^0 = \left(\frac{\Lambda_s}{\mu_s}, 0, 0, 0 \right) \quad (2.2)$$

Now, to explore the stability nature of the IFE, we must derive the basic reproduction number (\mathfrak{R}_0). In the next subsection, we will derive the within-host reproductive number for model system (2.1). The determination of the stability nature of the IFE is usually derived at using the within-host reproduction number. In general, the IFE is stable if $\mathfrak{R}_0 < 1$ and unstable otherwise. We reserve the next section for the derivation of the within-host reproduction number (\mathfrak{R}_0).

2.3.1 Computation of the within-host reproduction number (\mathfrak{R}_0)

The basic reproduction number is the basic unit for measuring the extent to which the infection will persist or die out when one infected CD4-T cell is introduced into a population of totally susceptible healthy CD4-T cells. It is defined as the number of secondary infection cases produced by one typical infective CD4+ T-cell when introduced in a totally susceptible population of healthy cells. Generally, when the basic reproduction number is less than a unit, it simply means that the infection will not persist in a population whilst a basic reproduction number of more than a unit implies that the infection will continue to invade the entire population unless some preventative and control measures are put in place to contain the invasion.

We use the next generation approach to compute the basic reproduction number of the model. Using the approach, we assume that the model system (2.1) can be written in the form:

$$\begin{cases} \frac{dX}{dt} = f(X, Y, Z), \\ \frac{dY}{dt} = g(X, Y, Z), \\ \frac{dZ}{dt} = h(X, Y, Z). \end{cases} \quad (2.3)$$

where $X \in R^r, Y \in R^s, Z \in R^n, r, s, n \geq 0$. The components X, Y, Z are represented as follows:

$$\begin{cases} X = (T_s) - \text{non-infected}, \\ Y = (T_c, T_v) - \text{infected but not infectious}, \\ Z = (V_h) - \text{infectious}. \end{cases} \quad (2.4)$$

Now let $U_0 = (X^*, 0, 0) \in R^{r+s+n}$ (where $r = 1, s = 2$ and $n = 1$) denote the infection-free equilibrium (IFE), that is, $U_0 = (X^*, 0, 0)$ such that $f(X^*, 0, 0) = g(X^*, 0, 0) = h(X^*, 0, 0)$. Also, we assume that the equation $g(X^*, Y, Z) = 0$ implicitly determines the function $Y = \tilde{g}(X^*, Z)$. Now expressing T_c and T_v in terms of T_s and V_h , we have:

$$\begin{cases} \tilde{g}_1(X^*, Z) = \frac{\beta_h \Lambda_s Z}{\mu_s(\alpha_c + \mu_c)}, \\ \tilde{g}_2(X^*, Z) = \frac{\beta_h \alpha_c \Lambda_s Z}{\mu_s(\alpha_c + \mu_c)(\alpha_v + \mu_v)}. \end{cases} \quad (2.5)$$

Now we let $A = D_Z h(X^*, \tilde{g}(X^*, 0), 0)$ and also assume that A can be written in the form $A = M - D$ with $M \geq 0$ and $D > 0$, a diagonal matrix. Since $\frac{dZ}{dt} = h(X, Y, Z)$, it follows that:

$$h(X, Y, Z) = N_v \alpha_v Y_2 - (\alpha_h + \mu_h) Z \quad (2.6)$$

The expressions (2.5) and (2.6) imply that

$$h(X^*, \tilde{g}(X^*, Z), Z) = \frac{N_v \alpha_v \beta_h \alpha_c \Lambda_s Z}{\mu_s(\alpha_c + \mu_c)(\alpha_v + \mu_v)} - (\alpha_h + \mu_h) Z \quad (2.7)$$

Now differentiating $h(X^*, \tilde{g}(X^*, Z), Z)$ with respect to Z , we get:

$$D_Z h(X^*, \tilde{g}(X^*, Z), Z) = \frac{N_v \alpha_v \alpha_c \Lambda_s \beta_h}{\mu_s (\alpha_c + \mu_c) (\alpha_v + \mu_v)} - (\alpha_h + \mu_h) \quad (2.8)$$

At infection free equilibrium (IFE), $(T_s^0, T_c^0, T_v^0, V_h^0) = (\frac{\Lambda_s}{\mu_s}, 0, 0, 0)$ such that

$$D_Z h(X^*, \tilde{g}(X^*, \mathbf{0}), \mathbf{0}) = \frac{N_v \alpha_v \alpha_c \Lambda_s \beta_h}{\mu_s (\alpha_c + \mu_c) (\alpha_v + \mu_v)} - (\alpha_h + \mu_h) \quad (2.9)$$

But $A = D_Z h(X^*, \tilde{g}(X^*, \mathbf{0}), \mathbf{0}) = M - D$ which implies that:

$$\begin{cases} M &= \frac{N_v \alpha_v \alpha_c \Lambda_s \beta_h}{\mu_s (\alpha_c + \mu_c) (\alpha_v + \mu_v)} \\ D &= (\alpha_h + \mu_h), \end{cases} \quad (2.10)$$

Since the within-host reproduction number (\mathfrak{R}_0) is given by $\rho(MD^{-1})$, we proceed to find D^{-1} which is represented as follows:

$$D^{-1} = \frac{1}{\alpha_h + \mu_h} \quad (2.11)$$

This implies that the within-host reproduction number is given by

$$\mathfrak{R}_0 = \frac{\Lambda_s}{\mu_s} \cdot \frac{N_v \alpha_v}{(\alpha_v + \mu_v)} \cdot \frac{\alpha_c}{(\alpha_c + \mu_c)} \cdot \frac{\beta_h}{(\alpha_h + \mu_h)} \quad (2.12)$$

Therefore, the result (2.12) represents the number of secondary infectious cells resulting from one typical infectious CD4+ T-cell when introduced to a completely susceptible population of healthy CD4+ T-cells during the infected cell's period of infectiousness. If \mathfrak{R}_0 is greater than unit then HIV infection is going to invade and persist in the population of CD4+ T-cells, thereby marking the continued attack by HIV of healthy CD4+ T-cells. In mathematical terms, the expression for (\mathfrak{R}_0) implies that infection by HIV will only cease to infect other healthy CD4+ T-cells if and only if $N_v \alpha_v \alpha_c \Lambda_s \beta_h$ is less than $\mu_s (\alpha_v + \mu_v) (\alpha_c + \mu_c) (\alpha_h + \mu_h)$.

2.3.2 Interpretation of \mathfrak{R}_0

For the purpose of interpreting the within-host reproduction threshold quantity (\mathfrak{R}_0), we re-write the threshold parameter as follows:

$$\mathfrak{R}_0 = \frac{\Lambda_s}{\mu_s} \cdot \frac{\alpha_c}{(\alpha_c + \mu_c)} \cdot \frac{N_v \alpha_v}{(\alpha_v + \mu_v)} \cdot \frac{\beta_h}{(\alpha_h + \mu_h)} \quad (2.13)$$

- $\frac{\Lambda_s}{\mu_s}$ — Total population of healthy CD4+ T-cells
- $\frac{\alpha_c}{\alpha_c + \mu_c}$ — Total number of latently infected CD4+ T-cells.
- $\frac{N_v \alpha_v}{\alpha_v + \mu_v}$ — Total number of productively infected CD4+ T-cells.
- $\frac{\beta_h}{\alpha_h + \mu_h}$ — Total number of effectively infectious virions.

Therefore, it follows from the above description that the within-host reproduction number is the product of healthy cells, the number of healthy cells that successfully goes to latent stage, the number of latent cells that successfully become productively infected and the number of effectively infectious virions.

2.4 Local Stability of the Infection Free Equilibrium

Using the theorem in Driessche and Watmough, 2002, the infection-free equilibrium is locally asymptotically stable (LAS) if $\mathfrak{R}_0 < 1$ and unstable otherwise. The preceding statement can be summarized by the following theorem:

Theorem 2.4.1. *The infection-free equilibrium (E^0) of model system (2.1) is locally asymptotically stable whenever $\mathfrak{R}_0 < 1$ and unstable otherwise.*

Proof. Since $E^0 = \left(\frac{\Lambda_s}{\mu_s}, 0, 0, 0 \right)$ is the infection free equilibrium of the model system (2.1), we need to show that $\forall \lambda_i \in \mathfrak{R}^4, \mathfrak{R}(\lambda_i) < 0$. It follows that the Jacobian matrix evaluated at E^0 is given by

$$J(E^0) = \begin{pmatrix} -\mu_s & 0 & 0 & -\frac{\beta_h \Lambda_s}{\mu_s} \\ 0 & -(\alpha_c + \mu_c) & 0 & \frac{\beta_h \Lambda_s}{\mu_s} \\ 0 & \alpha_c & -(\alpha_v + \mu_v) & 0 \\ 0 & 0 & N_v \alpha_v & -(\alpha_h + \mu_h) \end{pmatrix} \quad (2.14)$$

Finding the eigenvalues of the Jacobian matrix implies solving the following characteristic polynomial

$$|J(E^0) - \lambda \mathbb{I}| = 0 \quad (2.15)$$

After simplifying, we get the following equation

$$(\lambda + \mu_s) [a_0 \lambda^3 + a_1 \lambda^2 + a_2 \lambda + a_3] = 0 \quad (2.16)$$

$$\begin{cases} a_0 = 1, \\ a_1 = [(\alpha_c + \mu_c) + (\alpha_v + \mu_v) + (\alpha_h + \mu_h)], \\ a_2 = [(\alpha_c + \mu_c) [(\alpha_h + \mu_h) + (\alpha_v + \mu_v)] + (\alpha_h + \mu_h)(\alpha_v + \mu_v)], \\ a_3 = (\alpha_c + \mu_c)(\alpha_v + \mu_v)(\alpha_h + \mu_h) [1 + \mathfrak{R}_0]. \end{cases} \quad (2.17)$$

From equation (2.16), it is clear that one of the 4 eigenvalues has a real part less than 0. Now we proceed to determine the nature of the remaining eigenvalues for the second part of the polynomial equation. Applying the Routh Array criteria, we define the Routh array table whose elements are the coefficients (a_i 's) of the characteristic polynomial $P(\lambda)$ in Eq. (2.16):

$$\begin{array}{c|ccc}
 \lambda^3 & a_0 & a_2 & 0 & + \\
 \lambda^2 & a_1 & a_3 & 0 & + \\
 \lambda^1 & \frac{a_2 a_1 - a_3}{a_1} & & & \text{known + if } \mathfrak{R}_0 < 1 \\
 \lambda^0 & a_1 & & & +
 \end{array}$$

Since we have shown that there is no sign change whenever $\mathfrak{R}_0 < 1$ it confirms the stability of the infection-free equilibrium. Conversely, $\mathfrak{R}_0 > 1$ would mean a sign change, first, from positive to negative and then from negative to positive thereby making the infection-free equilibrium unstable. Therefore, this completes the proof of Theorem (2.4.1). \square

2.5 Global Stability of the Infection Free Equilibrium

In the previous section we used the theorem in (Castillo-Chavez et al., 2002) to show that the infection-free equilibrium is locally asymptotically stable (LAS) whenever $\mathfrak{R}_0 < 1$ and unstable otherwise. In this section, we state the two conditions that, if met, will guarantee the global asymptotic stability of the infection-free equilibrium point. To do that, we first assume that model system (2.1) can be re-written in the form:

$$\begin{cases} \frac{d\mathbf{X}}{dt} = F(\mathbf{X}, \mathbf{Z}), \\ \frac{d\mathbf{Z}}{dt} = G(\mathbf{X}, \mathbf{Z}), G(\mathbf{X}, \mathbf{0}) = 0. \end{cases} \quad (2.18)$$

where $x \in R^m$ denotes the number of uninfected individual CD4+ T- cells and $I \in R^n$ denotes the number of infected individual CD4+ T- cells including latent, infectious etc. If E^0 denotes the infection-free equilibrium of the system (2.1). In this case, the new two classes for the model system are represented as follows

$$\begin{cases} X = T_s, \\ Z = (T_c, T_v, V_h). \end{cases} \quad (2.19)$$

The conditions (H1) and (H2) below must be met for our model to be globally asymptotically stable (GAS).

- (H1). For $\frac{d\mathbf{X}}{dt} = F(\mathbf{X}, \mathbf{0})$, \mathbf{X}^* is globally asymptotically stable (g.a.s)
- (H2). $G(\mathbf{X}, \mathbf{Z}) = AZ = \widehat{G}(\mathbf{X}, \mathbf{Z})$, $\widehat{G}(\mathbf{X}, \mathbf{Z}) \geq 0$ for $(\mathbf{X}, \mathbf{Z}) \in \mathcal{R}$, where $A = D_{\mathbf{Z}}G(\mathbf{X}, \mathbf{0})$ is an M-Matrix (that is, the off-diagonal elements of the A are non-negative) and \mathcal{R} is the region where the model makes biological sense.

In relation to our model system (2.1), the new classification of the model equations is as follows

$$\begin{cases} F(\mathbf{X}, \mathbf{Z}) = (\Lambda_s - \beta_s V_h T_s - \mu_s T_s), \\ \widehat{G}(\mathbf{X}, \mathbf{Z}) = \begin{pmatrix} \beta_s V_h T_s - (\alpha_c + \mu_c) T_c \\ \alpha_c T_c - (\alpha_v + \mu_v) T_v \\ N_v \alpha_v T_v - (\alpha_h + \mu_h) V_h \end{pmatrix}. \end{cases} \quad (2.20)$$

$$F(\mathbf{X}, \mathbf{0}) = (\Lambda_s - \mu_s T_s) \quad (2.21)$$

and

$$A = \begin{pmatrix} -(\alpha_c + \mu_c) & 0 & \frac{\beta_h \Lambda_s}{\mu_s} \\ \alpha_c & -(\alpha_v + \mu_v) & 0 \\ 0 & N_v \alpha_v & -(\alpha_h + \mu_h) \end{pmatrix} \quad (2.22)$$

Using A and $G(X, Z)$, we deduce $\widehat{G}(X, Z)$ as follows

$$\widehat{G}(X, Z) = \begin{pmatrix} 0 \\ 0 \\ 0 \end{pmatrix} \quad (2.23)$$

It is clear that $\widehat{G}(X, Z) \geq 0$ and also that $x^* = \frac{\Lambda_s}{\mu_s}$ is a global asymptotic stable (g.a.s) equilibrium for $\frac{dx}{dt} = F(X, 0)$. Hence, by the theorem above E^0 is globally asymptotically stable (GAS). The results obtained above are summarised by the following theorem.

Theorem 2.5.1. *The fixed point E^0 is a globally asymptotically stable (GAS) equilibrium of the model system (2.1) provided that $\mathfrak{R}_0 < 1$ (LAS) and that assumptions (H1) and (H2) are satisfied.*

2.6 The endemic equilibrium state and its stability

At the endemic equilibrium state, all compartments are infected with HIV and the endemic equilibrium state is denoted by:

$$E^* = (T_s^*, T_c^*, T_v^*, V_h^*). \quad (2.24)$$

In this section, we derive the expressions for the endemic equilibrium. Besides showing the uniqueness of its existence, we will also some interpretations of the endemic equilibrium expressions. The endemic equilibrium points of the system are computed by setting the system's equations to 0 and then solve simultaneously for the

state variables. Thus

$$\begin{cases} \Lambda_s - \beta_h V_h T_s - \mu_s T_s & = 0, \\ \beta_h V_h T_s - (\alpha_c + \mu_c) T_c & = 0, \\ \alpha_c T_c - (\alpha_v + \mu_v) T_v & = 0, \\ N_v \alpha_v T_v - (\alpha_h + \mu_h) V_h & = 0. \end{cases} \quad (2.25)$$

Solving the system for T_s , T_c , T_v and V_h , we obtained the following expressions for the endemic states:

$$\begin{cases} T_s^* & = \frac{\Lambda_s}{\mu_s \mathfrak{R}_0}, \\ T_c^* & = \frac{\mu_s (\alpha_v + \mu_v) (\alpha_h + \mu_h) (\mathfrak{R}_0 - 1)}{N_v \alpha_v \alpha_c \beta_h}, \\ T_v^* & = \frac{\mu_s (\alpha_h + \mu_h) (\mathfrak{R}_0 - 1)}{N_v \alpha_v \beta_h}, \\ V_h^* & = \frac{\mu_s}{\beta_h} (\mathfrak{R}_0 - 1) \end{cases} \quad (2.26)$$

where \mathfrak{R}_0 is as defined by equation (2.12). From result (2.26), it can be shown that the infection equilibrium exists if and only if $\mathfrak{R}_0 > 1$.

2.6.1 Local Stability of Endemic Equilibrium State

To determine the local stability of infection equilibrium for the model system (2.1), we linearise equations of our model system in order to obtain the Jacobian matrix. We then evaluate the Jacobian matrix of the model system (2.1) at the infection equilibrium (E^*),

$$E^* = \left(\frac{\Lambda_s}{\mu_s \mathfrak{R}_0}, \frac{\mu_s (\alpha_v + \mu_v) (\alpha_h + \mu_h) (\mathfrak{R}_0 - 1)}{N_v \alpha_v \alpha_c \beta_h}, \frac{\mu_s (\alpha_h + \mu_h) (\mathfrak{R}_0 - 1)}{N_v \alpha_v \beta_h}, \frac{\mu_s}{\beta_h} (\mathfrak{R}_0 - 1) \right) \quad (2.27)$$

The Jacobian matrix of the model system (2.1) evaluated at the infection equilibrium is given by

$$J(E^*) = \begin{pmatrix} -\mu_s \mathfrak{R}_0 & 0 & 0 & \frac{-\Lambda_s \beta_h}{\mu_s \mathfrak{R}_0} \\ \mu_s (\mathfrak{R}_0 - 1) & -(\alpha_c + \mu_c) & 0 & \frac{\Lambda_s \beta_h}{\mu_s \mathfrak{R}_0} \\ 0 & \alpha_c & -(\alpha_v + \mu_v) & 0 \\ 0 & 0 & N_v \alpha_v & -(\alpha_h + \mu_h) \end{pmatrix} \quad (2.28)$$

We test for stability of the infection equilibrium (E^*) by calculating the eigenvalues (λ_s) of the above Jacobian matrix. The characteristic equation for the Jacobian matrix

is given by

$$P(\lambda) = m_0\lambda^4 + m_1\lambda^3 + m_2\lambda^2 + m_3\lambda + m_4. \quad (2.29)$$

where,

$$\begin{cases} m_0 = 1, \\ m_1 = y_1 + y_2 + y_3 + y_4, \\ m_2 = y_1y_2 + (y_1 + y_2)(y_3 + y_4) + y_3y_4, \\ m_3 = y_1y_2y_3 + y_1y_2y_4 + y_1y_3y_4, \\ m_4 = \frac{y_1y_2y_3y_4(\mathfrak{R}_0 - 1)}{\mathfrak{R}_0}. \end{cases} \quad (2.30)$$

for $(y_1, y_2, y_3, y_4) = (\mu_s\mathfrak{R}_0, (\alpha_c + \mu_c), (\alpha_v + \mu_v), (\alpha_h + \mu_h))$. In order to determine the stability of the infection equilibrium (E^*), we use the Routh-Hurwitz Stability Criteria to determine the sign of the eigenvalues of the characteristic polynomial (2.29). According to Routh-Hurwitz Criteria, given a polynomial

$$P(\lambda) = m_0\lambda^n + m_1\lambda^{n-1} + m_2\lambda^{n-2} + m_3\lambda^{n-3} + \dots + m_{n-1}\lambda + m_n. \quad (2.31)$$

with a real constant coefficients m_i where $i = 1, 2, \dots, n$ is considered. Now, from the equation (2.31), we will form Routh Array as shown below:

$$\begin{array}{c|cccccccc} \lambda^n & m_0 & m_2 & m_4 & m_6 & - & - & - \\ \lambda^{n-1} & m_1 & m_3 & m_5 & m_7 & - & - & - \\ \lambda^{n-2} & a_1 & a_2 & a_3 & - & - & - & - \\ \lambda^{n-3} & b_1 & b_2 & - & - & - & - & - \\ \lambda^{n-4} & c_1 & - & - & - & - & - & - \\ \lambda^{n-5} & \cdot & & & & & & \\ \cdot & \cdot & & & & & & \\ \cdot & \cdot & & & & & & \\ \lambda^2 & \cdot & & & & & & \\ \lambda^1 & \cdot & & & & & & \\ \lambda^0 & \cdot & & & & & & \end{array}$$

m_i (for $i = 1, 2, 3, 4 \dots, n$) coefficients are taken from the characteristic equation $P(\lambda)$ and are arranged as shown in the routh array above. Other elements are calculated from these element. Coefficients a_i (for $i = 1, 2, 3, 4 \dots, n$) are calculated as

$$\begin{cases} a_1 = \frac{m_1m_2 - m_3m_0}{m_1}, \\ a_2 = \frac{m_1m_4 - m_5m_0}{m_1}, \\ a_3 = \frac{m_1m_6 - m_7m_0}{m_1}. \end{cases} \quad (2.32)$$

Using the Routh Hulwitz Criteria, the process is continued until we get a zero in the row with a_i coefficients. Similarly, b_i coefficients and c_i coefficients are calculated as

follows:

$$\left\{ \begin{array}{l} b_1 = \frac{m_3 a_1 - m_1 a_2}{a_1}, \\ b_2 = \frac{m_5 a_1 - m_1 a_3}{a_1}, \\ c_1 = \frac{b_1 a_2 - b_2 a_1}{b_1}. \end{array} \right. \quad (2.33)$$

In our case, we define the routh array table whose elements are the coefficients (m_i 's) of the characteristic polynomial $P(\lambda)$ in Eq. (2.31):

$$\begin{array}{c|ccc} \lambda^4 & m_0 & m_2 & m_4 \\ \lambda^3 & m_1 & m_3 & 0 \\ \lambda^2 & a_1 & a_2 & \\ \lambda^1 & b_1 & & \\ \lambda^0 & c_1 & & \end{array}$$

where,

$$\left\{ \begin{array}{l} a_1 = \frac{m_1 m_2 - m_3 m_0}{m_1}, \\ = \frac{(y_2 + y_3 + y_4)(y_1^2 + y_1 y_2 + y_1 y_3 + y_1 y_4 + y_2 y_3 + y_2 y_4 + y_3 y_4)}{y_1 + y_2 + y_3 + y_4} > 0, \\ a_2 = m_4, \\ = \frac{y_1 y_2 y_3 y_4 (\mathfrak{R}_0 - 1)}{\mathfrak{R}_0} > 0, \text{ if and only if } \mathfrak{R}_0 > 1, \\ b_1 = \frac{a_1 m_3 - m_1 a_2}{a_1}, \\ = \frac{m_3(m_1 m_2 - m_3) - m_1^2 m_4}{m_2 m_1 - m_3} > 0, \\ c_1 = a_2 = m_4 \\ = \frac{y_1 y_2 y_3 y_4 (\mathfrak{R}_0 - 1)}{\mathfrak{R}_0} > 0, \text{ if and only if } \mathfrak{R}_0 > 1. \end{array} \right. \quad (2.34)$$

Since $m_0, m_1, a_1, b_1, c_1 > 0$, we have shown that the signs in the first column of Routh Array are all the same and this confirms stability of the infection equilibrium. Consequently, this completes our test for stability and subsequently conclude that the infection equilibrium for the model system is stable.

2.7 Sensitivity Analysis

In this section, we carry out the sensitivity analysis on the model with respect to its model parameters. To perform the analysis, we use the two quantities that were derived from analytically solving the model system: (I) the within-host reproduction

quantity (\mathfrak{R}_0) and (II) the within-host virus (V_h^*). Furthermore, we used parameter values that are relevant to HIV infection dynamics within an infected individual (within-host) to determine the effect of any changes in the parameter values on the outcome (response) variables (the associated within-host reproduction number and the within-host viral load) and to identify the parameters that have the most effect on the within-host infection dynamics. The two metrics were chosen for further analysis because of the following reasons: (I) \mathfrak{R}_0 is a used metric for characterising HIV dynamics at the beginning of an infection, hence it is important to investigate this quantity as it is strategic for policymakers and health decision makers alike to know the best possible ways (strategies/alternatives) for managing HIV when individuals have just acquired the virus. (II) V_h^* , the endemic value of HIV-RNA plasma viral load, is a quantity that characterises HIV infection dynamics when it has reached endemic levels. This quantity requires further investigation because when HIV infection has fully established it may require completely different strategies to effectively and efficiently manage and control it. To perform the sensitivity analysis on \mathfrak{R}_0 and V_h^* , we must, first of all, let both \mathfrak{R}_0 and V_h^* be differentiable on the parameter u so that the normalized forward sensitivity index at u is given by:

$$\begin{cases} \mathbf{Y}_u^{\mathfrak{R}_0} = \frac{\partial \mathfrak{R}_0}{\partial \mathbf{u}} \cdot \frac{\mathbf{u}}{\mathfrak{R}_0}, \\ \mathbf{Y}_u^{V_h^*} = \frac{\partial V_h^*}{\partial \mathbf{u}} \cdot \frac{\mathbf{u}}{V_h^*} \end{cases} \quad (2.35)$$

The sensitivity results of the outcome variables subject to the model parameters are summarised in table (2.2) below.

Table 2.2: Sensitivity indices of the two metrics of baseline within-host HIV infection dynamics.

SL. No.	Parameter	Sensitivity index of \mathfrak{R}_0	Sensitivity index of V_h^*
1.	α_h	-0.375	-0.424
2.	β_h	+1	+0.132
3.	μ_s	-1	-0.132
4.	μ_h	-0.625	-0.707
5.	Λ_s	+1	+1.132
6.	α_c	+0.978	+1.107
7.	μ_c	-0.978	-1.107
8.	α_v	+0.625	+0.707
9.	μ_v	-0.625	-0.707
10.	N_v	+1	+1.132

The sensitivity results presented in table (2.2) shows the importance of various model parameters at two different stages of HIV infection as measured by the outcome variables From the table we deduce the following:

- Parameters β_h and μ_s are shown to be of much importance depending on the stage of HIV infection. For instance, they are shown to have a great impact on HIV infection at the start of infection relative to their importance when the

dynamics have reached endemic levels. Consequently, these two parameters presents great potential drug targets as targeting them will have notable effects on \mathfrak{R}_0 . This result confirms the importance of early HIV counselling and testing as we have shown that HIV can be controlled successfully when its treated whilst the patients are still at their early stages of infection. Furthermore, interventions aimed at reducing the overall effect of β_h should be promoted, for instance, the use of pre-exposure prophylaxis (PrEP).

- Parameters $\Lambda_s, \mu_h, \alpha_c, \alpha_v, \mu_v$ and N_v are important at both levels of HIV infection. However, the results show that their importance is more pronounced when the infection has reached endemic levels relative to their importance at the start of the HIV infection. This result is affirmed by the fact that \mathfrak{R}_0 -Sensitivity $< V_h^*$ -Sensitivity for all the parameters in question.

Overall, our sensitivity results suggest that β_h, α_c and N_v can be potentially targeted for effective control of HIV. Consequently, in the next section, we will introduce the interventions to the model directed at reducing the overall effect of these parameters in the infection dynamics of HIV.

2.8 Within-host model with interventions

The main purpose of mathematical modelling of infectious diseases is to understand the dynamics of the disease so that effective control measures can be taken to ensure that the problem is eradicated or in some cases eventually eliminated. In this section, we apply interventions to the model and present both its qualitative and numerical properties with the goal to show the limitation of mathematical models that consider a select single scale of a multiscale HIV / AIDS disease system, especially, when the overall aim is to understand the entire HIV / AIDS disease as a complex system. Consequently, we controlled the model by introducing three medical interventions as dictated by the sensitivity analysis results. The controlled model is given as:

$$\left\{ \begin{array}{l} \frac{dT_s}{dt} = \Lambda_s - (1 - \gamma)\beta_h V_h T_s - \mu_s T_s, \\ \frac{dT_c}{dt} = (1 - \gamma)\beta_h V_h T_s - [(1 - \epsilon)\alpha_c + \mu_c] T_v, \\ \frac{dT_v}{dt} = (1 - \epsilon)\alpha_c T_c - (\alpha_v + \mu_v) T_v, \\ \frac{dV_h}{dt} = (1 - \kappa)N_v \alpha_v T_v - (\alpha_h + \mu_h) V_h. \end{array} \right. \quad (2.36)$$

All variables and parameters of the controlled within-host model are as defined previously in table (2.1) whereas γ, ϵ and κ represents the overall efficacies of possible interventions at the within-host level. The intervention, (γ) , represents the role of fusion inhibitors (FIs) in interfering with the binding and fusion stage of HIV life cycle. In particular, fusion inhibitors disrupts the HIV life cycle by stopping the binding of HIV to the CD4 receptor and one of the two co-receptors on the surface of the CD4+ T-lymphocyte. The intervention, (ϵ) , represents the role of reverse transcriptase inhibitors (RTIs) in preventing the HIV enzyme called reverse transcriptase from converting the single-stranded HIV-RNA to double-stranded HIV DNA.

Lastly, the intervention, (κ) , represents the role of protease inhibitors (PIs) in successfully interfering with the assembly stage of HIV life cycle which result in the assembly of new virions. The assembly stage of the HIV life cycle is associated with an HIV enzyme called protease which is responsible for cutting long chains of HIV proteins produced during the transcription stage into smaller individual proteins. Consequently, as smaller HIV proteins come together with copies of HIV's RNA genetic material, a new virus particle is assembled. The analysis of the controlled model is the same as the uncontrolled within-host model except that the parameters β_h , α_c and N_v have been modified according to the following transformations:

Table 2.3: Parameter structural transformations of the post-control model

Parameter	Transformation
β_h	$(1 - \gamma)\beta_h$
α_c	$(1 - \epsilon)\alpha_c$
N_v	$(1 - \kappa)N_v$

Based on the interventions applied to the model, the new effective within-host reproduction number denoted by \mathfrak{R}_E becomes:

$$\mathfrak{R}_E = \frac{\Lambda_s (1 - \kappa) N_v \alpha_v}{\mu_s} \cdot \frac{(1 - \epsilon) \alpha_c}{(1 - \epsilon) \alpha_c + \mu_c} \cdot \frac{(1 - \gamma) \beta_h}{\alpha_h + \mu_h} \quad (2.37)$$

Similarly, the effective endemic equilibrium point for the controlled model denoted by

$$E^{*E} = (T_s^{*E}, T_c^{*E}, T_v^{*E}, V_h^{*E}) \quad (2.38)$$

is given by:

$$\left\{ \begin{array}{l} T_s^* = \frac{\Lambda_s}{\mu_s \mathfrak{R}_E}, \\ T_c^{*E} = \frac{\mu_s (\alpha_v + \mu_v) (\alpha_h + \mu_h) (\mathfrak{R}_E - 1)}{(1 - \kappa) (1 - \epsilon) (1 - \gamma) N_v \alpha_v \alpha_c \beta_h}, \\ T_v^{*E} = \frac{\mu_s (\alpha_h + \mu_h) (\mathfrak{R}_E - 1)}{(1 - \kappa) (1 - \gamma) N_v \alpha_v \beta_h}, \\ V_h^{*E} = \frac{\mu_s}{(1 - \gamma) \beta_h} (\mathfrak{R}_E - 1) \end{array} \right. \quad (2.39)$$

Using similar methods and techniques, we can also show that the endemic equilibria of the controlled model uniquely exists whenever $\mathfrak{R}_E > 1$.

2.9 Assessing the comparative effectiveness of HIV Combination Treatment regimens

In this section, we present results of assessing the comparative effectiveness of TasP components (FIs, RTIs and PIs) using indicators derived from the within-host model

with combination drug interventions given in (2.36). The two indicators of effectiveness of the three HAART's drug components are: (1) within-host reproduction number (\mathfrak{R}_E) and (2) the within-host plasma viral load (V_h^{*E}). The indicators of effectiveness of the HIV treatment interventions are given below:

$$\begin{cases} \mathfrak{R}_E &= \frac{\Lambda_s (1 - \kappa) N_v \alpha_v}{\mu_s (\alpha_v + \mu_v)} \cdot \frac{(1 - \epsilon) \alpha_c}{(1 - \epsilon) \alpha_c + \mu_c} \cdot \frac{(1 - \gamma) \beta_h}{\alpha_h + \mu_h}, \\ V_h^{*E} &= \frac{\mu_s}{(1 - \gamma) \beta_h} (\mathfrak{R}_E - 1). \end{cases} \quad (2.40)$$

We use these quantities in carrying out the analysis because they characterise the dynamics of HIV at the beginning of the infection (for instance, \mathfrak{R}_E) and when the infection has reached endemic levels (in this case, V_h^{*E}). The purpose of this investigation is that besides the need to assess the impact of introducing treatment at the beginning of HIV infection as well as the impact of introducing treatment when infection has reached endemic levels, we also need to show the need for employing multiscale modelling framework in our mathematical modelling efforts to address the problem of HIV/AIDS as a complex system. In particular, we need to demonstrate that HIV/AIDS disease system cannot be effectively controlled while isolating our efforts to either one of the two important scales of the entire HIV/AIDS complex disease system but rather through making concerted efforts to simultaneously study the dynamics across its entire spectrum. Moreover, we wish to identify the most appropriate drug regimen of combination of drugs for each of the two crucial stages of HIV infection cycle. Tables (2.4) and (2.5) show results of the assessment on comparative effectiveness HAART components (FIs, RTIs and PIs) corresponding to efficacy values of 0.3, 0.6 and 0.9 for each of the two indicators of comparative effectiveness (\mathfrak{R}_E and V_h^{*E}). Since we considered 8 different combinations of HAART's components, the comparative effectiveness of these interventions is measured on a scale ranging from 1 to 8 with 1 denoting the lowest comparativeness (i.e. the baseline measure when no intervention is considered) while 8 denotes the highest comparative effectiveness. In subsections to follow, we discuss the results of the assessment of the comparative effectiveness of three HAART components when each of the two indicators of intervention effectiveness are used.

2.9.1 Comparative effectiveness of HAART using the effective within-host reproduction number (\mathcal{R}_E) as an indicator of effectiveness

No.	Indicator of Intervention effectiveness	Calculated $\mathcal{R}_{E-L-eff}$	CEL	Calculated $\mathcal{R}_{E-M-eff}$	CEM	Calculated $\mathcal{R}_{E-H-eff}$	CEH
1	Baseline Within-host Reproduction Number (\mathcal{R}_E)	11,385.20	1	11,385.20	1	11,385.20	1
2	FIs induced Within-host Reproduction Number (\mathcal{R}_{E_γ})	7,969.64	3	4,554.08	3	1,138.52	3
3	RTIs induced Within-host Reproduction Number (\mathcal{R}_{E_c})	8,022.60	2	4,615.01	2	1,161.52	2
4	PIs induced Within-host Reproduction Number (\mathcal{R}_{E_κ})	7,969.64	3	4,554.08	3	1,138.52	3
5	FIs and RTIs induced Within-host Reproduction Number ($\mathcal{R}_{E_{\gamma c}}$)	5,615.82	5	1,846.00	5	116.15	5
6	FIs and PIs induced Within-host Reproduction Number ($\mathcal{R}_{E_{\gamma\kappa}}$)	5,578.75	7	1,821.63	7	113.85	7
7	RTIs and PIs induced Within-host Reproduction Number ($\mathcal{R}_{E_{c\kappa}}$)	5,615.82	5	1,846.00	5	116.15	5
8	HAART induced Within-host Reproduction Number ($\mathcal{R}_{E_{\gamma c\kappa}}$)	3,931.07	8	738.40	8	11.62	8

Table 2.4: Results of the assessment of comparative effectiveness of HIV treatment regimens using the effective within-host reproduction number (\mathcal{R}_E) as an indicator of treatment effectiveness when each of the three HAART components is assumed to have: (a) low efficacy of 0.30, (b) medium efficacy of 0.60, and (c) high efficacy of 0.90.

Table (2.4) shows the results of the assessment of the comparative effectiveness of 7 different (individual and combinations) HAART components obtained using (\mathcal{R}_E) as an indicator of intervention effectiveness. From table (2.4), we deduce the following results regarding the comparative effectiveness of the 7 interventions for controlling the within-host replication of HIV:

- Among the three HAART component interventions implemented at within-host scale as mono-therapy, FIs and PIs have highest and equal comparative effectiveness while RTIs have the least comparative effectiveness since ($\mathcal{R}_{E_\gamma} = \mathcal{R}_{E_\kappa} > \mathcal{R}_{E_c}$). This result agree well with previous results on sensitivity analysis where it was shown that the within-host reproduction number (\mathcal{R}_0) is highly and equally sensitive to parameters β_h and N_v . This result has an important implication in terms of providing new ways of using existing therapeutic agents. For instance, having two drugs with the same overall effect (such

as FIs and PIs) means that either of the two drugs can be applied for a same desired result, hence the two drugs can be administered on alternative basis. This entails a cost-effectiveness way of fighting against HIV infection, thereby promoting the sustainability of such health programs.

- When HAART component interventions are considered as double therapy, the results show, as expected, that the combination of FIs and PIs, denoted by $\mathfrak{R}_{E_{\gamma\kappa}}$, has the highest comparative effectiveness while $(\mathfrak{R}_{E_{\gamma\epsilon}})$ and $(\mathfrak{R}_{E_{\epsilon\kappa}})$ are tied and having the least comparative effectiveness.
- Finally, we note from the results that treatment presents the highest comparative effectiveness with an increase in efficacy as demonstrated by $\mathfrak{R}_{E-L} > \mathfrak{R}_{E-M} > \mathfrak{R}_{E-H}$ for all 7 individual, double and triple therapy combinations compared.

Overall, we note that when interventions are implemented the goal should be to achieve higher levels of efficacy as we have observed that overall drug effectiveness increases with an increased level of drug efficacy. This is demonstrated by the fact that Calculated $\mathfrak{R}_{E-H-eff} < \text{Calculated } \mathfrak{R}_{E-M-eff} < \text{Calculated } \mathfrak{R}_{E-L-eff}$. Hence, the need to address or to be fully aware of the many psychological, social and behavioural factors that may influence the efficacy of medication and the overall therapeutic outcome for HIV-infected individuals.

2.9.2 Comparative effectiveness of HAART using the effective endemic-value of plasma viral load V_h^{*E} as an indicator of intervention effectiveness

No.	Indicator of Intervention effectiveness	Calculated (V_h^{*E}) -L-eff	CEL	Calculated (V_h^{*E}) -M-eff	CEM	Calculated (V_h^{*E}) -H-eff	CEH
1	Baseline Endemic of Within-Host Virus (V_h^{*E})	168,654.74	1	168,654.74	1	168,654.74	1
2	FIs induced Within-host Endemic Value ($V_{h_\gamma}^{*E}$)	168,648.39	2	168,632.52	2	168,521.41	2
3	RTIs induced Within-host Endemic Value ($V_{h_\epsilon}^{*E}$)	118,838.48	3	68,355.70	3	17,192.93	3
4	PIs induced Within-host Endemic Value ($V_{h_\kappa}^{*E}$)	118,053.88	5	67,453.01	5	16,852.14	5
5	FIs and RTIs induced Within-host Endemic Value ($V_{h_{\gamma\epsilon}}^{*E}$)	118,832.13	4	68,333.48	4	17,059.60	4
6	FIs and PIs induced Within-host Endemic Value ($V_{h_{\gamma\kappa}}^{*E}$)	118,047.53	6	67,430.79	6	16,718.81	6
7	RTIs and PIs induced Within-host Endemic Value ($V_{h_{\epsilon\kappa}}^{*E}$)	83,182.49	7	27,333.39	7	1,705.96	7
8	HAART induced Within-host Endemic Value ($V_{h_{\gamma\epsilon\kappa}}^{*E}$)	83,176.14	8	27,311.17	8	1,572.63	8

Table 2.5: Results of the assessment of comparative effectiveness of HIV treatment regimens using the effective within-host viral load (V_h^{*E}) as an indicator of treatment effectiveness when each of the three HAART components is assumed to have: (a) low efficacy of 0.30, (b) medium efficacy of 0.60, and (c) high efficacy of 0.90.

Table (2.5) show the results of the assessment of comparative effectiveness of 7 different individual and combinations of HAART components obtained using V_h^{*E} as an indicator of intervention effectiveness. From table (2.5), we deduce the following results regarding the comparative effectiveness of the 7 interventions when plasma viral load has reached endemic levels:

- We note from the results that for mono-therapy, PIs have the highest comparative effectiveness followed by RTIs while FIs have the least comparative effectiveness. The results are in agreement with sensitivity analysis results which showed that N_v is highly sensitive to V_h^* followed by α_c and β_h in the same order as presented above. Also, of notable importance is the result that the comparative effectiveness of combined FIs and RTIs is less than that for PIs alone. This may be attributable to the PIs's mechanism of control as they function by blocking the integration process which leads to the production of many copies of HIV RNA. This result is important to public health decision makers since the quantitative results are suggesting a drop of polytherapy (involving

FIs and RTIs) in favour of PIs. However, this result presents the challenge of overrelying on quantitative decision making as a basis for selecting the alternative as some options may require further qualitative analysis before they are chosen for implementation. For instance, before selecting monotherapy option as the best option, cost benefit analysis must be carried out on all competing alternatives. Comparing the advantages of monotherapy and polytherapy, one would end up selecting the combination of FIs and RTIs instead of PIs alone because the benefits of two or more drugs (such as lower treatment failure, lower case-fatality ratios, fewer side effects, slower development to resistance) may be far more exceeding than the benefits associated with taking monotherapy (such as possible avoidance of unwanted side effects and dangerous drug interactions).

- When treatment is considered as double therapy, the combination of RTIs and PIs have the highest comparative effectiveness followed by FIs and PIs while the combination FIs and RTIs has the least comparative effectiveness. This also demonstrates the importance of N_v in determining the dynamics of plasma viral load (V_h). For decision making regarding the effective design and implementation of health interventions, these results show that to effectively reduce further infection of CD4+ T-cells, the double therapy including FIs and PIs outperforms therapy involving FIs combined with either RTIs or PIs.
- Finally, we note from the results that treatment presents highest comparative effectiveness with an increase in efficacy as demonstrated by $V_h\text{-L-eff} > V_h\text{-M-eff} > V_h\text{-H-eff}$ for all the 7 individual, double and triple therapy combinations investigated.

In the previous section, we deduced the importance of targeting certain stages of HIV infection depending on whether the infection is still in its initial stage or has reached levels of endemicity. Moreover, we showed the importance of recognizing the existence of clear molecular targets that pertains to HIV life cycle and host-virus interactions, we also show how increased understanding of the forces that drive infection at different stages can be important in developing several interruption schedules for effectively controlling the HIV pathogen from causing further damage to the adaptive immune system in HIV infected people. Overall, our results reveal that HAART components are better-off when they are implemented together. However, it is important to highlight that making an assessment on the comparative effectiveness of drug interventions has got its own drawbacks which are tied to the nature of modelling employed. For instance, in this section, we used a metric attached to the within-host model thereby limiting the utility of the model as it cannot allow interventions that are implemented at other scales to be evaluated. Hence, our basis for suggesting the launch of high throughput computational multiscale model that allows us to link all scales that characterises the entire HIV/AIDS disease system for easy comparison of all interventions linked to the disease's management and control efforts.

2.10 Summary

In this chapter we developed a simple within-host model for HIV infection. An analysis of the model was made to investigate its key mathematical properties. We derived the basic reproduction number of the model which we then used to show the stability of the infection free equilibrium. We also derived the explicit expressions

for the model's endemic equilibria and proved the uniqueness of the endemic equilibrium point. We carried out sensitivity analysis on the model to investigate how sensitive were the model parameters in relation to the basic reproduction number and the endemic value of the within-host viral load. The sensitivity results established model parameters that are worth targeting for effective treatment and control at different stages of the HIV life cycle. In particular, the two metrics: (1) within-host reproduction number (\mathcal{R}_0) and endemic value of plasma viral load (V_h) were used because they respectively describe the course of HIV infection at the start of its cycle and the course of HIV infection when it has reached endemic levels. These two metrics were then used to carry out a comparative assessment on HAART components such as fusion inhibitors (FIs), reverse transcriptase inhibitors (RTIs) and protease inhibitors (PIs). We calculated and ranked the values associated with each indicator for every individual and combination HAART components. Despite demonstrating important results regarding effective treatment and control of HIV infection, our analysis were limited to the assessment of interventions which operate at the within-host scale such as the medical intervention scale. This created a gap which we will be filled later in Chapter (4) when we develop a multiscale model that offers us with the room to carry out a comparative assessment of both medical (e.g. HAART) and public health (e.g. condoms, male circumcision e.t.c) interventions as facilitated by multiscale modelling framework's capability to bridge within-host and between-host scales. In a nutshell, the mathematical model for investigating within-host HIV infection dynamics is associated with a weakness which relates to its failure to capture the emergent properties, that is, benefits realised at a scale above resulting from decisions made at a lower scale. In the next chapter, we will develop a mathematical model for studying HIV/AIDS transmission dynamics at between-host (population) scale with the goal to motivate further the development of multiscale models in Chapter (4). For instance, we know that between-host models will only allow us to make a meaningful comparison of public health interventions but at the same time will fail to provide us with an opportunity for incorporating meaningful comparison on the effectiveness of medical interventions, thereby pushing further our agenda for developing a multiscale model for HIV/AIDS as stated earlier in this chapter.

Chapter 3

Between-Host Model for HIV/AIDS transmission dynamics

3.1 Introduction

In this chapter, we develop a mathematical model for describing HIV/AIDS transmission dynamics at the population level (between-host scale). The model consists of three state variables: Susceptible hosts (S_H), Infected hosts (I_H) and Community Viral Load (V_H). The mathematical model is an extension of the well-known traditional SI model and is unique in that it incorporates the role of community pathogen load, a concept that owes its foundation to disease modelling studies pertaining to mathematical modelling of environmentally-driven diseases (Garira et al., 2014), studies with which the environment is seen as a direct reservoir for infectious agents. The purpose of this chapter is to use the model to show that it has some limitations associated with it, which can only be removed by adopting a multiscale modelling framework when studying complex HIV/AIDS disease systems. Further, we will attempt to link this model with the within-host model with a view of developing a multiscale model.

3.1.1 Model Formulation

The model to be developed is based on the transmission dynamics of HIV/AIDS in a community of heterosexually-active adults. One of the key assumptions to be made in the model formulation process is that individual's viral loads are traceable such that they can be aggregated to form a pool of community pathogen load (CPL) (Garira, 2017). The total population of the heterosexually-active adult population at time t , denoted by $N(t)$, is divided into two sub-populations of individuals who are wholly susceptible to HIV infection ($S_H(t)$) and individuals infected with HIV infection ($I_H(t)$) so that

$$N_H(t) = S_H(t) + I_H(t) \quad (3.1)$$

At any time t , new recruits enter the heterosexual human population through the development of young heterosexual individuals to become sexually-active at a constant rate Λ_H . There is a constant natural death rate μ_H in the population. However, infected individuals have an additional mortality of δ_H . Susceptible individuals acquire human immunodeficiency virus (HIV) through having unprotected heterosexual sex with infected individuals, whose aggregate viral loads constitute the community viral load (V_H), at a rate $\lambda_H(t)$ where

$$\lambda_H(t) = \frac{\beta_H V_H}{V_0 + V_H} \quad (3.2)$$

with β_H being the maximum rate of exposure, V_0 is the half saturation constant and V_H is as per the description given above. In hypothesizing the functional form of the force of infection, we assumed that huge values of the variable (V_H) have the same effect on the acquisition of HIV, hence the saturating functional form of $\lambda_H(t)$. Furthermore, to demonstrate the role of community viral load in the transmission dynamics of HIV/AIDS, we model the community viral load by assuming the phenomenological relationship in which we consider that as infected individuals pass through various stages of HIV pathogenesis, each individual contributes to the community viral pool at a rate $N_h\alpha_h$. Consequently, to find the total contribution of the HIV pathogen by an infected individual to the total community viral load pool, we multiply the rate of individual contribution to the community virus by the total number of people who are infected. Thus, $N_h\alpha_h I_H(t)$ describes the total HIV pathogen load contributed by all infected individuals to the community viral load pool. We make the assumption that community viral load becomes reduced as infected individuals cease their contribution due to natural viral clearance (for instance, due to death). Thus, the model for the transmission of HIV/AIDS in a sexually-active community of adults is given by the following deterministic system of non-linear differential equations:

$$\left\{ \begin{array}{l} \frac{dS_H}{dt} = \Lambda_H - (\lambda_H + \mu_H)S_H, \\ \frac{dI_H}{dt} = \lambda_H S_H - (\mu_H + \delta_H)I_H, \\ \frac{dV_H}{dt} = N_h\alpha_h I_H - \alpha_H V_H. \end{array} \right. \quad (3.3)$$

where:

$$\lambda_H = \frac{\beta_H V_H}{V_0 + V_H} \quad (3.4)$$

and represents the force of infection (that is, the rate at which susceptible individuals acquire HIV). The description of all parameters used in developing the model is presented in the table below.

SL. No.	Parameter	Meaning	Initial Value	Range Explored	Units	Source/Rational
1.	β_H	Transmission rate	0.03	constant	day^{-1}	Fraser et al., 2007; Quinn et al., 2000
2.	Λ_H	Recruitment rate	0.034	constant	people day^{-1}	Assumed
3.	α_H	Natural viral clearance rate	0.24	constant	viral copies day^{-1}	Assumed
4.	μ_H	Natural death rate	0.000002	constant	day^{-1}	Estimated
5.	δ_H	AIDS induced death rate	0.000006	constant	per day	Estimated
6.	V_0	Half saturation constant	2×10^8	constant	virions day^{-1}	Estimated

Table 3.1: Table of parameter description and initial parameter values for the between-host model given by (3.3)

The state transition system below depicts the transfer processes that are involved as the people change their states and how model variables are linked with the community viral load.

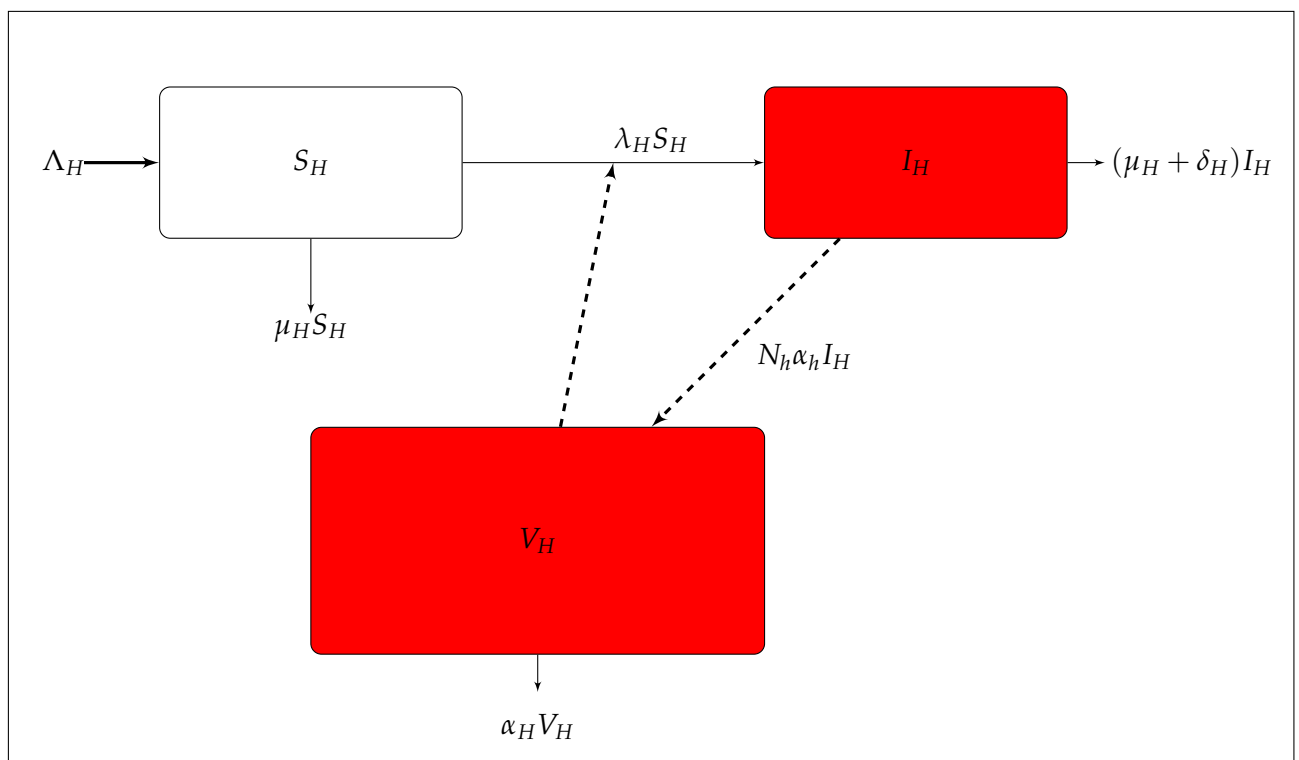


Figure 3.1: A conceptual diagram of the between-host model for HIV/AIDS transmission dynamics

3.2 Feasible region of the equilibria of the model

All parameters and state variables of the model (3.3) are assumed to be non-negative, to be consistent with human population. Furthermore, it can also be verified that for model system (3.3), all solutions with non-negative initial conditions remain bounded and non-negative. Since $N_H(t) = S_H(t) + I_H(t)$ it follows that

$$\frac{dN_H(t)}{dt} = \frac{dS_H(t)}{dt} + \frac{dI_H(t)}{dt} \quad (3.5)$$

Substituting for $\frac{dS_H(t)}{dt}$ and $\frac{dI_H(t)}{dt}$ into equation (3.5) yields the following result

$$\left\{ \begin{array}{l} \frac{dN_H(t)}{dt} = \Lambda_H - \mu_H S_H(t) - (\mu_H + \delta_H) I_H(t) \\ \phantom{\frac{dN_H(t)}{dt}} = \Lambda_H - \mu_H (S_H(t) + I_H(t)) - \delta_H I_H(t) \\ \phantom{\frac{dN_H(t)}{dt}} \leq \Lambda_H - \mu_H N_H(t) \end{array} \right. \quad (3.6)$$

This implies that

$$\limsup_{t \rightarrow \infty} (N_H(t)) \leq \frac{\Lambda_H}{\mu_H} \quad (3.7)$$

Since $S_H(t)$ and $I_H(t)$ are subsets of $N_H(t)$ and $N_H(t)$ is also bounded above following the result obtained in (3.7), we can conclude using the Bolzano Weierstrass Theorem that $S_H(t)$ and $I_H(t)$ are bounded above. That is,

$$S_H(t) \leq \frac{\Lambda_H}{\mu_H} \text{ and } I_H(t) \leq \frac{\Lambda_H}{\mu_H} \quad (3.8)$$

Similarly, the boundedness of $V(t)$ can be shown as follows:

Since $I_H \leq \frac{\Lambda_H}{\mu_H}$ by (3.9), it follows that

$$\frac{dV_H}{dt} \leq \frac{N_h \alpha_h \Lambda_H}{\mu_H} - \alpha_H V_H. \quad (3.9)$$

Solving the first order differential equation, we obtain the following result

$$V_H(t) \leq \frac{N_h \alpha_h \Lambda_H}{\mu_H \alpha_H} + A e^{-\alpha_H t}. \quad (3.10)$$

Equation (3.10) implies that

$$\limsup_{t \rightarrow \infty} (V_H(t)) \leq \frac{N_h \alpha_h \Lambda_H}{\mu_H \alpha_H}. \quad (3.11)$$

To sum up the results obtained above, we conclude this section by stating the following theorem

Theorem 3.2.1. *System (3.3) is a dynamical system on the compact set*

$$\mathbb{K} = \left\{ S_H(t), I_H(t), V_H(t) \in \mathbb{R}_+^3; N_H(t) \leq \frac{\Lambda_H}{\mu_H}, V_H(t) \leq \frac{N_h \alpha_h \Lambda_H}{\mu_H \alpha_H} \right\} \quad (3.12)$$

3.3 The Disease Free Equilibrium

The disease free equilibrium (E^0) of system (3.3) denotes the point at which all the sub-populations of the model are free of HIV and it is instructive for the DFE equilibrium to be computed and its stability nature be analysed as the persistence or the eventual elimination of diseases wholly depend on whether or not the DFE is stable or unstable. For our model system (3.3), the DFE is given as

$$E^0 = \left(\frac{\Lambda_H}{\mu_H}, 0, 0 \right) \quad (3.13)$$

In order to explore the local stability of the DFE, we must derive the basic reproduction number. In this chapter, we define the basic reproduction number as the number of secondary infectives produced by one typical infective individual when introduced into a wholly susceptible population during his/her period of infectiousness. The next section is aimed at deriving the basic reproductive number for model (3.3).

3.4 Derivation of Between-Host Basic Reproduction Number (R_0)

We use the next generation approach to compute the basic reproduction number of the model. Using this approach, we first assume that the model system (3.3) can be written in the form:

$$\begin{cases} \frac{dX}{dt} = f(X, Y, Z), \\ \frac{dY}{dt} = g(X, Y, Z), \\ \frac{dZ}{dt} = h(X, Y, Z). \end{cases} \quad (3.14)$$

where $X \in R^r, Y \in R^s, Z \in R^n, r, s, n \geq 0$. The components X, Y, Z are represented as follows:

$$\begin{cases} X = S_H - \text{non-infected}, \\ Y = I_H - \text{infected but not infectious}, \\ Z = V_H - \text{infectious}. \end{cases} \quad (3.15)$$

Now let $U_0 = (X^*, 0, 0) \in R^{r+s+n}$ (where $r = s = n = 1$) denote the DFE, that is, $U_0 = (X^*, 0, 0), f(X^*, 0, 0) = g(X^*, 0, 0) = h(X^*, 0, 0)$. Assume that the equation $g(X^*, Y, Z) = 0$ implicitly determines the function $Y = \tilde{g}(X^*, Z)$. Now expressing I_H in terms of S_H and V_H , we have:

$$\tilde{g}(X^*, Z) = \frac{\beta_H V_H S_H}{(V_0 + V_H)(\mu_H + \delta_H)} \quad (3.16)$$

Now we let $A = D_Z h(X^*, \tilde{g}(X^*, 0), 0)$ and also assume that A can be written in the form $A = M - D$ with $M \geq 0$ and $D > 0$, a diagonal matrix. Since $\frac{dZ}{dt} = h(X, Y, Z)$, it follows that:

$$h(X, Y, Z) = N_h \alpha_h I_H - \alpha_H V_H \quad (3.17)$$

which also implies that:

$$h(X^*, \tilde{g}(X^*, Z), Z) = \frac{N_h \alpha_h \beta_H \Lambda_H Z}{\mu_H (V_0 + Z) (\mu_H + \delta_H)} - \alpha_H Z \quad (3.18)$$

Now differentiating $h(X^*, \tilde{g}(X^*, Z), Z)$ with respect to Z , we get:

$$D_Z h(X^*, \tilde{g}(X^*, Z), Z) = \frac{N_h \alpha_h \beta_H V_0 \Lambda_H}{\mu_H (\mu_H + \delta_H) (V_0 + Z)^2} - \alpha_H \quad (3.19)$$

At disease-free equilibrium (DFE), $(S_H^0, I_H^0, V_H^0) = (\frac{\Lambda_H}{\mu_H}, 0, 0)$:

$$D_Z h(X^*, \tilde{g}(X^*, 0), 0) = \frac{N_h \alpha_h \beta_H \Lambda_H}{\mu_H V_0 (\mu_H + \delta_H)} - \alpha_H \quad (3.20)$$

But $A = D_Z h(X^*, \tilde{g}(X^*, 0), 0) = M - D$ which implies that:

$$\begin{cases} M = \frac{N_h \alpha_h \beta_H \Lambda_H}{\mu_H V_0 (\mu_H + \delta_H)} \\ D = \alpha_H \end{cases} \quad (3.21)$$

Since the basic reproduction number is given by $\rho(MD^{-1})$, it follows that:

$$R_0 = \frac{N_h \alpha_h \beta_H \Lambda_H}{\alpha_H \mu_H V_0 (\mu_H + \delta_H)} \quad (3.22)$$

Since all parameters of the are assumed to be non-negative, it is clear from the above result that $R_0 > 0$.

3.5 Stability Analysis of Disease Free Equilibrium

3.5.1 Local Stability of DFE

To prove that the DFE is locally asymptotically stable, we need to show that all real parts of the eigen-values of the Jacobian matrix evaluated at E^0 are negative whenever $R_0 < 1$. The Jacobian matrix is given by

$$J(E^0) = \begin{pmatrix} -\mu_H & 0 & -\frac{\beta_H \Lambda_H}{\mu_H V_0} \\ 0 & -(\mu_H + \delta_H) & \frac{\beta_H \Lambda_H}{\mu_H V_0} \\ 0 & N_h \alpha_h & -\alpha_H \end{pmatrix} \quad (3.23)$$

The characteristic polynomial $P(\lambda)$ is given by

$$P(\lambda) = (\lambda + \mu_H) (\lambda^2 + \lambda(\mu_H + \delta_H + \alpha_H) + \alpha_H(\mu_H + \delta_H)(1 + R_0)) \quad (3.24)$$

Equating $P(\lambda)$ to 0 and solving for possible values of λ . It is evident that $\lambda = -\mu_H$ and we proceed to determine the stability nature of the remaining part of the polynomial. We employ the Routh table to make the determination

				Sign
λ^2	m_0	m_2	1	+
λ	m_1	0	$(\mu_H + \delta_H + \alpha_H)$	+
λ^0	m_2		$\alpha_H(\mu_H + \delta_H)(1 + R_0)$	+ve if and only if $R_0 < 1$.

The results presented above are be summarised by Theorem 2 in Driessche and Watmough, 2002.

Theorem 3.5.1. *The disease free equilibrium E^0 of the between-host HIV/AIDS transmission model is locally asymptotically stable when $R_0 < 1$ and unstable otherwise.*

3.5.2 Global stability of DFE (E^0)

To prove that the disease free equilibrium is globally asymptotically stable, we state the following theorem

Theorem 3.5.2. *The disease-free equilibrium (E^0) = $\left(\frac{\Lambda_H}{\mu_H}, 0, 0\right)$ is globally asymptotically stable (GAS) if $R_0 \leq 1$.*

Proof. Let $S_{H0} = \frac{\Lambda_H}{\mu_H}$ and consider the following combination of linear functions and Volterra-type Lyapunov function:

$$L_0 = L_0(S_H, I_H, V_H) = S_H - S_H^0 \ln(S_H) + I_H + c_1 V_H$$

Using the fact that $\Lambda_H = \mu_H S_H^0$, the Lie derivative of L_0 in the direction of the vector field given by the right hand side of the model system (3.3) is

$$\begin{aligned} \dot{L}_0 &= \frac{dS_H}{dt} - \frac{S_H^0}{S_H} \cdot \frac{dS_H}{dt} + \frac{dI_H}{dt} + c_1 \frac{dV_H}{dt}, \\ &= \frac{dS_H}{dt} \left(1 - \frac{S_H^0}{S_H}\right) + \frac{dI_H}{dt} + c_1 \frac{dV_H}{dt}, \\ &= \frac{1}{S_H} (S_H - S_H^0) \left(\Lambda_H - \frac{\beta_H V_H S_H}{V_0 + V_H} - \mu_H S_H\right) + \\ &\quad \frac{\beta_H V_H S_H}{V_0 + V_H} - (\mu_H + \delta_H) S_H + c_1 (N_h \alpha_h I_H - \alpha_H V_H), \\ &= \frac{-\mu_H}{S_H} (S_H - S_H^0)^2 + [c_1 N_h \alpha_h - (\mu_H + \delta_H)] I_H + \left[\frac{\beta_H S_H^0}{V_0 + V_H} - c_1 \alpha_H\right] V_H. \end{aligned}$$

Choose c_1 such that

$$\frac{\beta_H S_H^0}{V_0 + V_H} - c_1 \alpha_H = 0$$

Since $V_H = 0$ at disease-free equilibrium, it follows that

$$c_1 = \frac{\beta_H S_H^0}{\alpha_H V_0}$$

Substituting the value of c_1 into the right hand side of the Lie derivative yields

$$\begin{aligned} \dot{L}_0 &= \frac{-\mu_H}{S_H} (S_H - S_H^0)^2 + \left[\frac{\beta_H S_H^0 N_h \alpha_h}{\alpha_H V_0} - (\mu_H + \delta_H) \right] I_H, \\ &= \frac{-\mu_H}{S_H} (S_H - S_H^0)^2 + (\mu_H + \delta_H) [R_{H0} - 1] I_H \leq 0 \end{aligned}$$

Since it is easy to see that the largest invariant subset contained in the set

$$\mathbb{K} = \{(S_H, I_H, V_H) \in \mathbb{K} / \dot{L}_0 = 0\}$$

is the disease-free equilibrium E^0 , we conclude by LaSalle's Invariance Principle that the DFE point is globally asymptotically stable (GAS). \square

3.6 Determination of Endemic Equilibria

Similar to disease-free equilibrium state, the endemic equilibrium state is obtained by setting the left-hand side of the model system (3.3) equal to zero. But S_H , I_H and V_H are non-zero, which means that all model compartments are infected by the HIV pathogen. Consequently, at the endemic equilibrium all the compartments are infectious and the endemic equilibrium is given by $E^* = (S_H^*, I_H^*, V_H^*)$. This section is intended to derive the explicit expressions for the endemic equilibrium and determine its uniqueness.

3.6.1 The Endemic Equilibrium

From equation (1) of system (3.3) we deduce that:

$$S_H^* = \frac{\Lambda_H}{\lambda_H^* + \mu_H} \quad (3.25)$$

Substituting (3.4) for λ_H in (3.25), we deduce the following expression for S_H^*

$$\begin{cases} S_H^* = \frac{\Lambda_H(V_0 + V_H^*)}{\beta_H V_H^* + \mu_H(V_0 + V_H^*)} \\ = \frac{\Lambda_H(V_0 + V_H^*)}{(\beta_H + \mu_H)V_H^* + \mu_H V_0} \end{cases} \quad (3.26)$$

From equation (2) of system (3.3), we deduce that:

$$I_H^* = \frac{\Lambda_H S_H^*}{\mu_H + \delta_H} \quad (3.27)$$

Now substituting the expressions (3.3) and (3.26) for λ_H^* and S_H^* respectively into equation (3.27), we derive the following expression for I_H^* .

$$\left\{ \begin{aligned} I_H^* &= \frac{\beta_H V_H^* \left[\frac{\Lambda_H (V_0 + V_H^*)}{V_H^* (\beta_H + \mu_H) + \mu_H V_0} \right]}{V_0 + V_H^*} \\ &= \frac{\Lambda_H \beta_H V_H^*}{(\mu_H + \delta_H) [V_H^* (\beta_H + \mu_H) + \mu_H V_0]} \end{aligned} \right. \quad (3.28)$$

Similarly, from equation (3) of system (3.3) we also deduce that

$$I_H^* = \frac{\alpha_H V_H^*}{N_h \alpha_h} \quad (3.29)$$

Now equating the two expressions (3.28) and (3.29) for I_H^* , we deduce the explicit expression for V_H^* as follows:

$$\frac{\alpha_H V_H^*}{N_h \alpha_h} = \frac{\Lambda_H \beta_H V_H^*}{(\mu_H + \delta_H) \{V_H^* (\beta_H + \mu_H) + \mu_H V_0\}} \quad (3.30)$$

Now cross-multiplying both sides of the equation (3.30), we obtain the following equation

$$\alpha_H (\mu_H + \delta_H) V_H^* \{(\beta_H + \mu_H) V_H^* + \mu_H V_0\} = N_h \alpha_h \Lambda_H \beta_H V_H^* \quad (3.31)$$

The equation above can be re-written as follows

$$\alpha_H (\mu_H + \delta_H) V_H^* [(\beta_H + \mu_H) V_H^* + \mu_H V_0] - N_h \alpha_h \Lambda_H \beta_H V_H^* = 0 \quad (3.32)$$

Solving the equation (3.32), we get the values of V_H^* as follows

$$\left\{ \begin{aligned} V_H^* &= 0 \text{ or} \\ \alpha_H (\mu_H + \delta_H) [(\beta_H + \mu_H) V_H^* + \mu_H V_0] - N_h \alpha_h \Lambda_H \beta_H &= 0 \end{aligned} \right. \quad (3.33)$$

The first solution for V_H^* represents its value at disease-free equilibrium and as such we consider the second value of V_H^* which is as follows

$$V_H^* = \frac{N_h \alpha_h \Lambda_H \beta_H - \alpha_H \mu_H V_0 (\mu_H + \delta_H)}{\alpha_H (\mu_H + \delta_H) (\beta_H + \mu_H)} \quad (3.34)$$

The right-hand side of the equation (3.34) can also be re-written as follows

$$V_H^* = \frac{N_h \alpha_h \Lambda_H \beta_H}{\alpha_H (\mu_H + \delta_H) (\beta_H + \mu_H)} - \frac{\mu_H V_0}{(\beta_H + \mu_H)} \quad (3.35)$$

The equation above can be re-written as follows

$$V_H^* = \frac{\mu_H V_0}{(\beta_H + \mu_H)} \left(\frac{N_h \alpha_h \Lambda_H \beta_H}{\alpha_H \mu_H V_0 (\mu_H + \delta_H)} - 1 \right) \quad (3.36)$$

Since the first term of the expression in parenthesis is the expression for the basic reproduction number, we can replace the term by R_0 to obtain the endemic value for

V_H^* as

$$V_H^* = \frac{\mu_H V_0}{\beta_H + \mu_H} (R_0 - 1) \quad (3.37)$$

Substituting the endemic value of V_H^* into equation (3.29), we obtain the endemic value of I_H^* as follows

$$I_H^* = \frac{\alpha_H \left(\frac{\mu_H V_0}{\beta_H + \mu_H} (R_0 - 1) \right)}{N_h \alpha_h} \quad (3.38)$$

Simplifying the right-hand side of the equation (3.38), we obtain the endemic value of I_H^* as

$$I_H^* = \frac{\alpha_H \mu_H V_0}{N_h \alpha_h (\beta_H + \mu_H)} (R_0 - 1) \quad (3.39)$$

Since S_H^* is given by the expression $\frac{\Lambda_H (V_0 + V_H)}{(\beta_H + \mu_H) V_H + \mu_H V_0}$, it follows from substituting the endemic value of V_H^* that the endemic value for S_H^* is given as follows

$$S_H^* = \frac{\Lambda_H (\beta_H + \mu_H R_0)}{\mu_H (\beta_H + \mu_H) R_0} \quad (3.40)$$

From the computations performed above, we can summarise the endemic equilibrium expressions as follows

$$\left\{ \begin{array}{l} S_H^* = \frac{\Lambda_H (\beta_H + \mu_H R_0)}{\mu_H (\beta_H + \mu_H) R_0}, \\ I_H^* = \frac{\alpha_H \mu_H V_0}{N_h \alpha_h (\beta_H + \mu_H)} [R_0 - 1], \\ V_H^* = \frac{\mu_H V_0}{\beta_H + \mu_H} [R_0 - 1] \end{array} \right. \quad (3.41)$$

It is clear from the expressions of I_H^* and V_H^* that the endemic equilibrium for model system (3.1) exists for $R_0 > 1$. The results obtained above can be summarised by stating the following theorem.

Theorem 3.6.1. *The model system (3.3) has a unique positive equilibrium point whenever $R_0 > 1$ and no positive equilibrium point otherwise.*

3.6.2 Local stability of the endemic equilibrium

The previous section allowed us to show that a unique positive endemic equilibrium point (EEP) exists for system (3.3) without giving any details concerning the stability of the endemic state. In this section, we will explore and establish the nature of stability of the EEP using the bifurcation approach as was previously used in Castillo-Chavez et al., 2002; Garira et al., 2014. Consequently, to determine local stability of the endemic steady state of system (3.3), we employ the Center Manifold Theory described in Garira et al., 2014. The Center Manifold Theory has been used

to determine the local stability of a non-hyperbolic equilibrium point. For convenience of interpretation of the stability we state the theorem. In order to apply the Center Manifold Theorem, we make some simplifications to our model (3.3). We let $S_H = x_1$, $I_H = x_2$, $V_H = x_3$ and by using the vector notation $\mathbf{x} = (x_1, x_2, x_3)^T$, the model system (3.3) can be written in the form $\frac{d\mathbf{x}}{dt} = F(\mathbf{x})$ with

$$F(\mathbf{x}) = (f_1, f_2, f_3) \quad (3.42)$$

such that

$$\begin{cases} \frac{dx_1}{dt} = \Lambda_H - (\lambda_H + \mu_H)x_1, \\ \frac{dx_2}{dt} = \lambda_H x_1 - (\mu_H + \delta_H)x_2, \\ \frac{dx_3}{dt} = N_h \alpha_h x_2 - \alpha_H x_3. \end{cases} \quad (3.43)$$

where:

$$\lambda_H = \frac{\beta_H x_3}{V_0 + x_3} \quad (3.44)$$

The Center Manifold Method involves evaluating the Jacobian matrix of model system (3.43) at the disease-free equilibrium E^0 denoted by $J(E^0)$. The Jacobian matrix associated with the equation system (3.43) is given by

$$J(E^0) = \begin{pmatrix} -\mu_H & 0 & -\frac{\beta_H \Lambda_H}{\mu_H V_0} \\ 0 & -(\mu_H + \delta_H) & \frac{\beta_H \Lambda_H}{\mu_H V_0} \\ 0 & N_h \alpha_h & -\alpha_H \end{pmatrix} \quad (3.45)$$

From the expression (3.22) of the basic reproductive number of system (3.43) is

$$R_0 = \frac{N_h \alpha_h \beta_H \Lambda_H}{\alpha_H \mu_H V_0 (\mu_H + \delta_H)} \quad (3.46)$$

We let $\beta_H = \beta^*$ and taking β^* as the bifurcation parameter and if we consider $R_{0H} = 1$ and solve for β^* , we obtain

$$\beta^* = \frac{\alpha_H \mu_H V_0 (\mu_H + \delta_H)}{N_h \alpha_h \Lambda_H} \quad (3.47)$$

Now substituting for β^* in the Jacobian matrix $J(E^0)$ described by (3.45), we obtain

$$J(E^0) = \begin{pmatrix} -\mu_H & 0 & -\frac{\alpha_H (\mu_H + \delta_H)}{N_h \alpha_h} \\ 0 & -(\mu_H + \delta_H) & \frac{\alpha_H (\mu_H + \delta_H)}{N_h \alpha_h} \\ 0 & N_h \alpha_h & -\alpha_H \end{pmatrix} \quad (3.48)$$

Solving for the eigenvalues for this new Jacobian matrix with β_H replaced by the expression for β^* and solving for the eigenvalues yields the following values of λ

$$\begin{cases} \lambda_1 = 0, \\ \lambda_2 = -\mu_H, \\ \lambda_3 = -(\alpha_H + \mu_H + \delta_H). \end{cases} \quad (3.49)$$

It is evident from the result obtained above that the linearised system of the transformed equation (3.43) with bifurcation point β^* has a simple zero eigenvalue. Hence the Center Manifold Theory as described in (Garira et al., 2014) can be used to analyse the dynamics of system (3.43) near $\beta_H = \beta^*$. We use the following theorem for convenient interpretation of the stability of endemic equilibrium point based on the bifurcation parameter β^* .

Theorem 3.6.2. Consider the following general system of differential equations with parameter ϕ :

$$\dot{x} = f(x, \phi), f_1 : \mathbb{R}^n \times \mathbb{R} \rightarrow \mathbb{R}, f_2 : \mathbb{C}^2(\mathbb{R}^2 \times \mathbb{R}) \quad (3.50)$$

where 0 is an equilibrium of the system, that is, $f(0, \phi) = 0 \forall \phi$ and assume that

A1. $A = D_x f(0, 0) = (\partial f_i / \partial x_j)(0, 0)$ is a linearisation of system (3.3) around the equilibrium 0 with ϕ evaluated at 0. Zero is a simple eigenvalue of A , and other eigenvalues of A have negative real values.

A2. Matrix A has a right eigenvector u and a left eigenvector v corresponding to the zero eigenvalue.

Let f_k be the k^{th} component of f and

$$\begin{aligned} a &= \sum_{i,j,k=1}^n u_k v_i v_j \frac{\partial^2 f_k}{\partial x_i \partial x_j}(0, 0), \\ b &= \sum_{i,k=1}^n u_k v_i \frac{\partial^2 f_k}{\partial x_i \partial \phi}(0, 0). \end{aligned} \quad (3.51)$$

The local dynamics of (3.3) around 0 are totally governed by a and b .

- (i) $a > 0, b > 0$. When $\phi < 0$ with $|\phi| \ll 1$, 0 is locally asymptotically stable and there exists a positive unstable equilibrium; when $0 < \phi \ll 1$, 0 is unstable and there exists a negative and locally asymptotically stable equilibrium.
- (ii) $a < 0, b < 0$. When $\phi < 0$ with $|\phi| \ll 1$, 0 is unstable; when $0 < \phi \ll 1$, is locally asymptotically stable, and there exists a positive unstable equilibrium
- (iii) $a > 0, b < 0$. When $\phi < 0$ with $|\phi| \ll 1$, 0 is unstable, and there exists a locally asymptotically stable negative equilibrium; when $0 < \phi \ll 1$, 0 is stable and a positive unstable equilibrium appears.
- (iv) $a < 0, b > 0$. When $\phi < 0$ changes from negative to positive, 0 changes its stability from stable to unstable. Correspondingly, a negative unstable equilibrium becomes positive and locally asymptotically stable

The Jacobian matrix of the model system (3.43) has a left eigenvector $u = (u_1, u_2, u_3)^T$, where

$$\begin{cases} u_1 = -\frac{\Lambda_H}{\mu_H} \cdot \frac{\beta^*}{\mu_H V_0}, \\ u_2 = \frac{\alpha_H}{N_h \alpha_h}, \\ u_3 = 1. \end{cases} \quad (3.52)$$

and the right eigenvector given by $v = (v_1, v_2, v_3)$, where

$$\begin{cases} v_1 = 0, \\ v_2 = \frac{N_h \alpha_h}{(\mu_H + \delta_H)}, \\ v_3 = 1. \end{cases} \quad (3.53)$$

Evaluating the non-zero second order derivative of F with respect to each variable, in order to determine the sign of a , we obtain

$$\begin{cases} \frac{\partial^2 f_1}{\partial x_1 \partial x_3} = -\frac{\beta_H V_0}{(V_0 + x_3)^2}, \\ \frac{\partial^2 f_1}{\partial x_3 \partial x_1} = -\frac{\beta_H V_0}{(V_0 + x_3)^2}, \\ \frac{\partial^2 f_1}{\partial x_3^2} = \frac{2\beta_H V_0 x_1}{(V_0 + x_3)^3}, \\ \frac{\partial^2 f_2}{\partial x_1 \partial x_3} = \frac{\beta_H V_0}{(V_0 + x_3)^2}, \\ \frac{\partial^2 f_2}{\partial x_3 \partial x_1} = \frac{\beta_H V_0}{(V_0 + x_3)^2}, \\ \frac{\partial^2 f_2}{\partial x_3^2} = \frac{-2\beta_H V_0 x_1}{(V_0 + x_3)^3}. \end{cases} \quad (3.54)$$

Therefore, the sign of the bifurcation constant a is determined as follows

$$\begin{aligned} a = & u_1 v_1 v_3 \frac{\partial^2 f_1}{\partial x_1 \partial x_3}(0,0) + u_1 v_3 v_1 \frac{\partial^2 f_1}{\partial x_3 \partial x_1}(0,0) + u_1 v_3^2 \frac{\partial^2 f_1}{\partial x_3^2}(0,0) \\ & + u_2 v_1 v_3 \frac{\partial^2 f_2}{\partial x_1 \partial x_3}(0,0) + u_2 v_3 v_1 \frac{\partial^2 f_2}{\partial x_3 \partial x_1}(0,0) + u_2 v_3^2 \frac{\partial^2 f_2}{\partial x_3^2}(0,0) \end{aligned} \quad (3.55)$$

Evaluating the non-zero second order derivatives at $(0,0)$, we obtain

$$\left\{ \begin{array}{l} \frac{\partial^2 f_1}{\partial x_1 \partial x_3}(0,0) = -\frac{\beta^*}{V_0}, \\ \frac{\partial^2 f_1}{\partial x_3 \partial x_1}(0,0) = -\frac{\beta^*}{V_0}, \\ \frac{\partial^2 f_1}{\partial x_3^2}(0,0) = \frac{2\Lambda_H \beta^*}{\mu_H V_0^2}, \\ \frac{\partial^2 f_2}{\partial x_1 \partial x_3}(0,0) = \frac{\beta^*}{V_0}, \\ \frac{\partial^2 f_2}{\partial x_3 \partial x_1}(0,0) = \frac{\beta^*}{V_0}, \\ \frac{\partial^2 f_2}{\partial x_3^2} = -\frac{2\Lambda_H \beta^*}{\mu_H V_0^2}. \end{array} \right. \quad (3.56)$$

Now substituting for all u'_k 's, v'_i 's, v'_j 's and $\frac{\partial^2 f_k}{\partial x_i \partial x_j}(0,0)$'s as described above. Therefore, the sign of the bifurcation constant a is determined as follows

$$\left\{ \begin{array}{l} a = u_1 v_3^2 \frac{\partial^2 f_1}{\partial x_3^2}(0,0) + u_2 v_3^2 \frac{\partial^2 f_2}{\partial x_3^2}(0,0) \\ = \left[-\frac{\Lambda_H}{\mu_H} \cdot \frac{\beta^*}{\mu_H V_0} \cdot 1^2 \cdot \frac{2\Lambda_H \beta^*}{\mu_H V_0^2} \right] + \left[\frac{\alpha_H}{N_h \alpha_h} \cdot 1^2 \cdot -\frac{2\Lambda_H \beta^*}{\mu_H V_0^2} \right], \\ = \frac{-2\Lambda_H \beta^*}{\mu_H V_0^2} \left[\frac{\Lambda_H \beta^*}{\mu_H^2 V_0} + \frac{\alpha_H}{N_h \alpha_h} \right] < 0 \end{array} \right. \quad (3.57)$$

For determining the sign of b , we compute the following non-vanishing second order derivatives of the transformed model system (3.43). After computing the second order partial derivatives, we obtain

$$\left\{ \begin{array}{l} \frac{\partial^2 f_1}{\partial x_1 \partial \beta^*} = -\frac{x_3}{V_0 + x_3}, \\ \frac{\partial^2 f_1}{\partial x_3 \partial \beta^*} = \frac{x_1 V_0}{(V_0 + x_3)^2}, \\ \frac{\partial^2 f_2}{\partial x_1 \partial \beta^*} = \frac{x_3}{V_0 + x_3}, \\ \frac{\partial^2 f_2}{\partial x_3 \partial \beta^*} = \frac{x_1 V_0}{(V_0 + x_3)^2}. \end{array} \right. \quad (3.58)$$

Therefore, the sign of the bifurcation constant b is determined as follows

$$b = u_1 v_1 \frac{\partial^2 f_1}{\partial x_1 \partial \beta^*}(0,0) + u_1 v_3 \frac{\partial^2 f_1}{\partial x_3 \partial \beta^*}(0,0) + u_2 v_1 \frac{\partial^2 f_2}{\partial x_1 \partial \beta^*}(0,0) + u_2 v_3 \frac{\partial^2 f_2}{\partial x_3 \partial \beta^*}(0,0) \quad (3.59)$$

Evaluating the non-zero second order derivatives at $(0,0)$, we obtain

$$\left\{ \begin{array}{l} \frac{\partial^2 f_1}{\partial x_1 \partial \beta^*}(0,0) = 0, \\ \frac{\partial^2 f_1}{\partial x_3 \partial \beta^*}(0,0) = \frac{\Lambda_H}{\mu_H V_0}, \\ \frac{\partial^2 f_2}{\partial x_1 \partial \beta^*} = 0, \\ \frac{\partial^2 f_2}{\partial x_3 \partial \beta^*} = \frac{\Lambda_H}{\mu_H V_0}. \end{array} \right. \quad (3.60)$$

Now substituting for all u'_k 's, v'_i 's and $\frac{\partial^2 f_k}{\partial x_i \partial \beta^*}(0,0)$'s as described above. Therefore, the sign of the bifurcation constant b is determined as follows

$$\left\{ \begin{array}{l} b = \left[\frac{-\Lambda_H \beta^*}{\mu_H^2 V_0} \cdot 1 \cdot \frac{\Lambda_H}{\mu_H V_0} \right] + \left[\frac{-\Lambda_H \beta^*}{\mu_H^2 V_0} \cdot 1 \cdot \frac{\Lambda_H}{\mu_H V_0} \right], \\ = \frac{-2\Lambda_H^2 \beta^*}{\mu_H^3 V_0^2} < 0. \end{array} \right. \quad (3.61)$$

Thus $a < 0$ and $b < 0$. Using Theorem (3.6.2), item (ii), the following result has been established which only holds for $R_0 > 1$ but close to 1. We conclude this test for the stability of the endemic equilibrium by reciting the theorem (5.3) cited in Garira et al., 2014.

Theorem 3.6.3. *The unique endemic equilibrium guaranteed by Theorem (3.6.2) is locally asymptotically stable for $R_0 > 1$ but very close to 1.*

3.6.3 Global Stability of the Endemic Equilibria

Theorem 3.6.4. *The Endemic Equilibrium E^* of model system (3.3) is globally asymptotically whenever $R_0 > 1$.*

Proof. Let's consider a Volterra-type Lyapunov function

$$\begin{aligned}
 L_1 &= L(S_H, I_H, V_H), \\
 &= (S_H - S_H^* \ln(S_H)) + (I_H - I_H^* \ln(I_H)) + a_1(V_H - V_H^* \ln(V_H)), \\
 &= \frac{dS_H}{dt} \left(1 - \frac{S_H^*}{S_H}\right) + \frac{dI_H}{dt} \left(1 - \frac{I_H^*}{I_H}\right) + a_1 \frac{dV_H}{dt} \left(1 - \frac{V_H^*}{V_H}\right), \\
 &= \left(1 - \frac{S_H^*}{S_H}\right) \left(\Lambda_H - \frac{\beta_H V_H S_H}{V_0 + V_H} - \mu_H S_H\right) + \left(1 - \frac{I_H^*}{I_H}\right) \left(\frac{\beta_H V_H S_H}{V_0 + V_H} - (\mu_H + \delta_H) I_H\right) \\
 &\quad + a_1 \left(1 - \frac{V_H^*}{V_H}\right) (N_h \alpha_h I_H - \alpha_H V_H)
 \end{aligned}$$

Since E^* is an equilibrium point, the following relations holds

$$\begin{cases}
 \Lambda_H &= \frac{\beta_H V_H^* S_H^*}{V_0 + V_H^*} + \mu_H S_H^*, \\
 (\mu_H + \delta_H) I_H^* &= \frac{\beta_H V_H^* S_H^*}{V_0 + V_H^*}, \\
 \alpha_H &= \frac{N_h \alpha_h I_H^*}{V_H^*}
 \end{cases} \quad (3.62)$$

Using the relations in (3.62), \dot{L}_1 becomes

$$\begin{aligned}
 \dot{L}_1 &= \left(1 - \frac{S_H^*}{S_H}\right) \left(\frac{\beta_H V_H^* S_H^*}{V_0 + V_H^*} + \mu_H S_H^* - \frac{\beta_H V_H S_H}{V_0 + V_H} - \mu_H S_H\right) \\
 &\quad + \left(1 - \frac{I_H^*}{I_H}\right) \left(\frac{\beta_H V_H S_H}{V_0 + V_H} - \frac{\beta_H V_H^* S_H^* I_H}{I_H^* (V_0 + V_H^*)}\right) \\
 &\quad + a_1 \left(1 - \frac{V_H^*}{V_H}\right) \left(N_h \alpha_h I_H - \frac{N_h \alpha_h I_H^* V_H}{V_H^*}\right) \quad (3.63)
 \end{aligned}$$

$$\begin{aligned}
 \dot{L}_1 &= -\frac{\mu_H}{S_H} (S_H - S_H^*)^2 + \frac{2\beta_H V_H^* S_H^*}{V_0 + V_H^*} + \left[a_1 N_h \alpha_h - \frac{\beta_H V_H^* S_H^*}{(V_0 + V_H^*) I_H^*} \right] I_H \\
 &\quad - \frac{\beta_H V_H^* S_H^{*2}}{V_0 + V_H^*} - \frac{\beta_H V_H S_H I_H^*}{(V_0 + V_H) I_H} - a_1 N_h \alpha_h I_H^* \frac{V_H}{V_H^*} - a_1 N_h \alpha_h I_H \frac{V_H^*}{V_H} \\
 &\quad + \frac{\beta_H V_H S_H^*}{V_0 + V_H} + a_1 N_h \alpha_h I_H^* \quad (3.64)
 \end{aligned}$$

Choose a_1 such that

$$a_1 N_h \alpha_h - \frac{\beta_H V_H^* S_H^*}{(V_0 + V_H^*) I_H^*} = 0 \quad (3.65)$$

Solving equation (3.65), we obtain a_1 as follows:

$$a_1 = \frac{\beta_H V_H^* S_H^*}{N_h \alpha_h (V_0 + V_H^*) I_H^*}$$

Substituting the value of a_1 into equation (3.64)

$$\begin{aligned} \dot{L}_1 = & -\frac{\mu_H}{S_H} (S_H - S_H^*)^2 + \frac{2\beta_H V_H^* S_H^*}{V_0 + V_H^*} - \frac{\beta_H V_H^* S_H^{*2}}{(V_0 + V_H^*) S_H} - \frac{\beta_H V_H S_H I_H^*}{(V_0 + V_H) I_H} \\ & - \frac{\beta_H V_H^* S_H^* V_H}{(V_0 + V_H^*) V_H^*} - \frac{\beta_H V_H^* S_H^* I_H V_H^*}{(V_0 + V_H^*) I_H^* V_H} + \frac{\beta_H V_H S_H^*}{V_0 + V_H} + \frac{\beta_H V_H^* S_H^*}{V_0 + V_H^*} \end{aligned} \quad (3.66)$$

$$\dot{L}_1 = \frac{\beta_H V_H^* S_H^*}{V_0 + V_H^*} \left[3 - \frac{S_H^*}{S_H} - \frac{V_H}{V_H^*} - \frac{I_H V_H^*}{I_H^* V_H} \right] + \frac{\beta_H V_H S_H^*}{V_0 + V_H} \left[1 - \frac{S_H I_H^*}{S_H^* I_H} \right] - \frac{\mu_H}{S_H} (S_H - S_H^*)^2 \quad (3.67)$$

It is clear from equation (3.67) that $1 - \frac{S_H I_H^*}{S_H^* I_H} \leq 0$ since $\frac{S_H}{S_H^*} \geq 1$ and $\frac{I_H^*}{I_H} \geq 1$. Furthermore, using the arithmetic-geometric mean inequality, we have $\dot{L}_1 \leq 0$, which means that L_1 is indeed a Lyapunov function. Therefore, we conclude from the LaSalle's Invariance Principle that E^* is globally asymptotically stable (GAS). \square

3.7 Sensitivity Analysis

In this section, we carry out the sensitivity analysis on R_0 and V_H^* relative to model parameters to identify parameters that have the most effect on the between-host model system. In order to perform sensitivity analysis on R_0 and V_H^* , we must let on R_0 and V_H^* be differentiable on the parameter u so that the normalized forward sensitivity index at u is given by:

$$\begin{cases} Y_u^{R_0} &= \frac{\partial R_0}{\partial u} \cdot \frac{u}{R_0}, \\ Y_u^{V_H^*} &= \frac{\partial V_H^*}{\partial u} \cdot \frac{u}{V_H^*}. \end{cases} \quad (3.68)$$

where R_0 and V_H^* are explicitly represented as follows

$$\begin{cases} R_0 &= \frac{N_h \alpha_h \Lambda_H \beta_H}{\alpha_H \mu_H V_0 (\mu_H + \delta_H)}, \\ V_H^* &= \frac{\mu_H V_0}{\beta_H + \mu_H} (R_0 - 1) \end{cases} \quad (3.69)$$

The sensitivity results for model system (3.3) are summarized in table (3.2) below.

Table 3.2: Sensitivity indices of the two metrics of baseline between-host HIV transmission dynamics.

SL. No.	Parameter	Sensitivity index of R_0	Sensitivity index of V_H^*
1.	Λ_H	1	1.000073
2.	β_H	1	0.000139
3.	μ_H	-1.25	-0.250158
4.	α_H	-1	-1.000073
5.	δ_H	-0.75	-0.750055
6.	N_h	1	1.000073
7.	α_h	1	1.000073
8.	V_0	-1	-0.000073

Based on the results shown above in Table (3.2), we observe that the between-host reproduction number R_0 is sensitive to the changes of almost all model parameters and more sensitive to changes in parameter μ_H . On the other hand, the endemic-value of the community viral load (V_H) is sensitive to the changes of parameter Λ_H , α_H , N_h , δ_H and α_h . In regard to R_0 , the sensitivity results shows that increasing Λ_H , β_H , N_h and α_h by 10% will increase the basic reproduction number by 10%. On the contrast, increasing the parameter values of V_0 , α_H , μ_H and δ_H by 10% will decrease the value of R_0 by 10%, 10%, 12.5% and 7.5 % respectively. For instance, $Y_{\mu_H}^{R_0} = -1.25$ means that increasing the parameter value of μ_H by 10% decreases the basic reproduction number by 10%. However, it is important to note that regardless of the fact that μ_H can be an important parameter for controlling HIV/AIDS based on the sensitivity results, they cannot be used as they contradict with the major goal of public health which is to provide health care for improved better lives. Consequently, sensitivity analysis results are important as they provide the basis for directing disease control efforts by allowing us to target parameters that have the most effect on the threshold quantities in the most sensible manner. Thus, we can effectively control the spread of HIV/AIDS by targeting the transmission rate and by targeting the total virus produced by each infected individual. This section has allowed to identify the key parameters of the model which can be targeted for the effective control of the disease. In the next section, we will introduce the interventions to the model and explore further on the comparative effectiveness of different individual medical and public health interventions as well as their possible combinations.

3.8 Controlled Between-Host Model

The most important aspect of modelling relates to the wise reduction of the complexity of the simulated system by ignoring unimportant parameters. In particular, the main objective of any mathematical modelling effort in the study of infectious diseases is possibly to provide some of the forays into an in-depth understanding of the interactions between the pathogen (in this case HIV) and its host (in this case, human beings) and the consequences of their complex dynamics for the spread and treatment of such diseases. In this section, we extend our modelling effort to incorporate prevention and treatment of HIV/AIDS. Consequently, four interventions that target specific parameters of the model as dictated by the sensitivity analysis results are introduced. The interventions are HAART (which target the parameter N_h , encompass the combined effectiveness of all the ARV drug regimens - fusion inhibitors,

reverse transcriptase inhibitors and protease inhibitors), condom use (which target the transmission rate (β_H) of HIV infection to new hosts), pre-exposure prophylaxis (PrEP) and voluntary medical male circumcision (VMMC). PrEP and VMMC control HIV/AIDS through the same mechanism in that they both work to reduce the transmission of HIV/AIDS by reducing the susceptibility of individuals to the HIV pathogen. The controlled model is represented as follows

$$\begin{cases} \frac{dS_H}{dt} = \Lambda_H - (\lambda_{HE} + \mu_H)S_H, \\ \frac{dI_H}{dt} = \lambda_{HE}S_H - (\mu_H + \delta_H)I_H, \\ \frac{dV_H}{dt} = (1 - \gamma)(1 - \epsilon)(1 - \kappa)N_h\alpha_h I_H - \alpha_H V_H. \end{cases} \quad (3.70)$$

where:

$$\lambda_{HE} = \frac{(1 - \sigma)\beta_H V_H}{(1 + \nu)(1 + \phi)V_0 + V_H} \quad (3.71)$$

and represents the intervention-induced force of infection (rate at which susceptible individuals acquire HIV assuming that interventions are being implemented). All model variables and parameters are as previously described. γ , ϵ and κ represents the effectiveness of fusion, reverse transcriptase and protease inhibitors respectively, σ represents the effectiveness of condoms in controlling the spread of HIV/AIDS, ϕ represents the effectiveness of pre-exposure prophylaxis (PrEP) and ν represents the effectiveness of voluntary medical male circumcision in reducing the spread of HIV/AIDS.

3.8.1 Analysis of the Controlled Model

The disease free equilibrium (E_0^c) for the model (3.70) is given by

$$\begin{cases} E_0^c = (S_{H0}^c, I_{H0}^c, V_{H0}^c) \\ = \left(\frac{\Lambda_H}{\mu_H}, 0, 0 \right) \end{cases} \quad (3.72)$$

Using the same method which was used to determine the basic reproductive number of the original model (3.3), without any intervention, it can be shown that the effective reproductive number of the modified between-host model (3.70) is

$$\begin{cases} R_E = \frac{(1 - \gamma)(1 - \epsilon)(1 - \kappa)N_h\alpha_h(1 - \sigma)\beta_H\Lambda_H}{\alpha_H\mu_H(1 + \nu)(1 + \phi)V_0(\mu_H + \delta_H)} \\ = \frac{(1 - \gamma)(1 - \epsilon)(1 - \kappa)(1 - \sigma)}{(1 + \nu)(1 + \phi)} \cdot \frac{N_h\alpha_h\beta_H\Lambda_H}{\alpha_H\mu_H V_0(\mu_H + \delta_H)} = aR_0. \end{cases} \quad (3.73)$$

where a is the combined effect of all the interventions and R_0 is the basic reproduction number of the basic model (3.3) when no intervention are applied to the model.

Theorem 3.8.1. *The DFE of the controlled model system (3.70) is locally asymptotically stable (LAS) when $R_E < 1$ and unstable otherwise.*

It also follows that R_E is positive since all parameters are positive and all intervention effectiveness are bounded in a closed interval $[0,1]$. The endemic equilibrium points for the controlled model are given as follows

$$\left\{ \begin{array}{l} \widehat{S}_{Hc}^* = \frac{\Lambda_H((1-\sigma)\beta_H + \mu_H R_E)}{\mu_H((1-\sigma)\beta_H + \mu_H)R_E} \\ \widehat{I}_{Hc}^* = \frac{\alpha_H \mu_H (1+\nu) V_0}{(1-\gamma)(1-\epsilon)(1-\kappa)N_h \alpha_h ((1-\sigma)\beta_H + \mu_H)} [R_E - 1], \\ \widehat{V}_{Hc}^* = \frac{\mu_H (1+\nu)(1+\phi) V_0}{(1-\sigma)\beta_H + \mu_H} [R_E - 1] \end{array} \right. \quad (3.74)$$

Also similar methods (such as those used previously) can be used to show that the controlled endemic equilibria is locally asymptotically stable whenever $R_E > 1$. Furthermore, it can be easily shown that the controlled endemic equilibria is GAS whenever $R_E > 1$.

3.9 Assessing the comparative effectiveness of HIV/AIDS Combination Preventive Interventions

In this section, we present the results obtained from carrying out an assessment of the comparative effectiveness of six interventions: (1) condom use, (2) voluntary medical male circumcision (VMMC), (3) pre-exposure prophylaxis (PrEP) and HAART components ((4) FIs, (5) RTIs and (6) PIs). The three indicators of the effectiveness considered in carrying the assessment are (a) the effective between-host reproduction number (R_E), (b) the controlled endemic value of the community viral load \widehat{V}_H^* and (c) the controlled endemic value of HIV/AIDS Prevalence \widehat{I}_H^* . The indicators of effectiveness are described as previously given in equations (3.73) and (3.74).

3.9.1 Assessment of comparative effectiveness using the Effective Reproduction Number (R_E)

No.	Indicator of Intervention effectiveness	Calculated $R_{E-L-eff}$	CEL	Calculated $R_{E-M-eff}$	CEM	Calculated $R_{E-H-eff}$	CEH
1	Baseline Reproduction Number (R_0)	13,746.09	1	13,746.09	1	13,746.09	1
2	FIs induced basic reproduction number (R_{E_γ})	9,622.27	4	5,498.44	4	1,374.61	5
3	RTIs induced basic reproduction number (R_{E_ϵ})	9,622.27	4	5,498.44	4	1,374.61	5
4	PIs induced basic reproduction number (R_{E_κ})	9,622.27	4	5,498.44	4	1,374.61	5

5	PrEP induced basic reproduction number (R_{E_ϕ})	10,573.92	2	8,591.31	2	7,234.79	2
6	Condom use induced basic reproduction number (R_{E_σ})	9,622.27	4	5,498.44	4	1,374.61	5
7	Male circumcision induced basic reproduction number (R_{E_ν})	10,573.92	2	8,591.31	2	7,234.79	2
8	FIs and RTIs induced basic reproduction number ($R_{E_{\gamma\epsilon}}$)	6,735.59	11	2,199.38	11	137.46	11
9	FIs and PIs induced basic reproduction number ($R_{E_{\gamma\kappa}}$)	6,735.59	11	2,199.38	11	137.46	11
10	RTIS and PIs induced basic reproduction number ($R_{E_{\epsilon\kappa}}$)	6,735.59	11	2,199.38	11	137.46	11
11	PrEP and Condom use induced basic reproduction number ($R_{E_{\phi\sigma}}$)	7,401.74	9	3,436.52	9	723.48	9
12	PrEP and Male circumcision induced basic reproduction number ($R_{0H_{\phi\nu}}^c$)	8,133.78	8	5,369.57	8	3,807.78	4
13	Condom use and male circumcision induced basic reproduction number ($R_{E_{\sigma\nu}}$)	7,401.74	9	3,436.52	9	723.48	9
14	HAART induced basic reproduction number ($R_{E_{\gamma\epsilon\kappa}}$)	4,714.91	14	879.75	14	13.75	14

15	HAART and PrEP induced basic reproduction number ($R_{E_{\gamma\epsilon\kappa\phi}}$)	3,626.85	15	549.84	15	7.23	15
16	HAART and condom use induced basic reproduction number ($R_{E_{\gamma\epsilon\kappa\sigma}}$)	3,300.44	17	351.90	17	1.37	18
17	HAART and male circumcision induced basic reproduction number ($R_{E_{\gamma\epsilon\kappa\nu}}$)	3,626.85	15	549.84	15	7.23	15
18	HAART- PrEP and Condom use induced basic reproduction number ($R_{E_{\gamma\epsilon\kappa\phi\sigma}}$)	2,538.80	19	219.94	19	0.72	19
19	HAART- PrEP and male circumcision induced basic reproduction number ($R_{E_{\gamma\epsilon\kappa\phi\nu}}$)	2,789.89	18	343.65	18	3.81	17
20	HAART- condom use and male circumcision induced basic reproduction number ($R_{E_{\gamma\epsilon\kappa\sigma\nu}}$)	2,538.80	19	219.94	19	0.72	19
21	HAART- PrEP- condom use and male circumcision induced basic reproduction number ($R_{E_{\gamma\epsilon\kappa\phi\sigma\nu}}$)	1,952.92	21	137.46	21	0.38	21

Table 3.3: Results of the assessment of comparative effectiveness of HIV/AIDS preventive interventions using the basic reproduction number (R_0) as an indicator of treatment effectiveness when each of the six preventive interventions is assumed to have: (a) low efficacy of 0.30, (b) medium efficacy of 0.60, and (c) high efficacy of 0.90.

Table (3.3) shows the results of the assessment of comparative effectiveness of medical and public health interventions for HIV/AIDS using the controlled basic reproduction number R_E as the indicator of effectiveness when each of the interventions'

efficacy are set at (a) 30% efficacy level, (b) 60% efficacy level and (c) 90% efficacy level. The results show that:

- For single interventions, FIs, RTIs, PIs and Condom use have equal and highest comparative effectiveness while male circumcision and pre-exposure prophylaxis have also equal and the least comparativeness. This is because $(R_{E_\gamma} = R_{E_c} = R_{E_\kappa} = R_{E_\sigma}) > (R_{E_\phi} = R_{E_\nu})$.
- For double interventions, all combinations made up of HAART components have the higher and same comparative effectiveness, followed by a combination of condom use with either PrEP and male circumcision while the combination of PrEP and male circumcision has the least comparative effectiveness.
- We note that as the number of interventions are integrated into a package of HIV services, the impact of such packages increases. For instance, combined HAART and male circumcision is more effective than an intervention involving HAART alone.

3.9.2 Assessment of comparative effectiveness using the controlled endemic value of HIV Prevalence

No.	Indicator of Intervention effectiveness	Calculated $I_{H-L-eff}$	CEL	Calculated $I_{H-M-eff}$	CEM	Calculated $I_{H-H-eff}$	CEH
1	Baseline HIV Prevalence (I_H)	4,249.41	1	4,249.41	1	4,249.41	1
2	FIs induced endemic value of HIV Prevalence (I_{H_γ})	4,249.28	4	4,248.94	4	4,246.63	5
3	RTIs induced endemic value of HIV Prevalence (I_{H_c})	4,249.28	4	4,248.94	4	4,246.63	5
4	PIs induced endemic value of HIV Prevalence (I_{H_κ})	4,249.28	4	4,248.94	4	4,246.63	5
5	PrEP induced endemic value of HIV Prevalence (I_{H_ϕ})	4,249.31	2	4,249.22	2	4,249.13	2
6	Condom use induced endemic value of HIV Prevalence (I_{H_σ})	4,249.15	8	4,248.52	8	4,244.08	8
7	Male circumcision induced endemic value of HIV Prevalence (I_{H_ν})	4,249.31	2	4,249.22	3	4,249.13	2

8	FIs and RTIs induced endemic value of HIV Prevalence ($I_{H_{\gamma\epsilon}}$)	4,249.09	9	4,247.78	11	4,218.80	11
9	FIs and PIs induced endemic value of HIV Prevalence ($I_{H_{\gamma\kappa}}$)	4,249.09	9	4,247.78	11	4,218.80	11
10	RTIs and PIs induced endemic value of HIV Prevalence ($I_{H_{\epsilon\kappa}}$)	4,249.09	9	4,247.78	11	4,218.80	11
11	PrEP and Condom use induced endemic value of HIV Prevalence ($I_{H_{\phi\sigma}}$)	4,249.02	12	4,248.06	9	4,241.30	9
12	PrEP and Male circumcision induced endemic value of HIV Prevalence ($I_{H_{\phi\nu}}$)	4,249.19	7	4,248.93	7	4,248.60	4
13	Condom use and male circumcision induced endemic value of HIV Prevalence ($I_{H_{\sigma\nu}}$)	4,249.02	12	4,248.06	9	4,241.30	9
14	HAART induced endemic value of HIV Prevalence ($I_{H_{\gamma\epsilon\kappa}}$)	4,248.82	14	4,244.89	14	3,940.56	14
15	HAART and PrEP induced endemic value of HIV Prevalence ($I_{H_{\gamma\epsilon\kappa\phi}}$)	4,248.54	15	4,241.99	15	3,662.32	15

16	HAART and condom use induced endemic value of HIV Prevalence ($I_{H_{\gamma\epsilon\kappa\sigma}}$)	4,248.31	17	4,237.22	18	1,157.44	18
17	HAART and male circumcision induced endemic value of HIV Prevalence ($I_{H_{\gamma\epsilon\kappa\nu}}$)	4,248.54	15	4,241.99	15	3,662.32	15
18	HAART-PrEP and Condom use induced endemic value of HIV Prevalence ($I_{H_{\gamma\epsilon\kappa\phi\sigma}}$)	4,247.92	19	4,229.97	19	-1,623.31	19
19	HAART- PrEP and male circumcision induced endemic value of HIV Prevalence ($I_{H_{\gamma\epsilon\kappa\phi\nu}}$)	4,248.19	18	4,237.35	17	3,133.66	17
20	HAART- condom use and male circumcision induced endemic value of HIV Prevalence ($I_{H_{\gamma\epsilon\kappa\sigma\nu}}$)	4,247.92	19	4,229.97	19	-1,623.31	19
21	HAART- PrEP- condom use and male circumcision induced endemic value of HIV Prevalence ($I_{H_{\gamma\epsilon\kappa\phi\sigma\nu}}$)	4,247.42	21	4,218.38	21	-6,906.75	21

Table 3.4: Results of the assessment of comparative effectiveness of six HIV/AIDS interventions using the HIV Prevalence (I_H) as an indicator of intervention effectiveness when each of the six preventive interventions is assumed to have: (a) low efficacy of 0.30, (b) medium efficacy of 0.60, and (c) high efficacy of 0.90.

Table (3.4) shows the results of the comparative effectiveness of six HIV/AIDS interventions when intervention-induced endemic value of HIV Prevalence is considered as an indicator of intervention effectiveness. From (3.4) we deduce the following results regarding comparative effectiveness of 20 different HIV/AIDS interventions considered:

- For single HIV/AIDS comprising of monotherapy associated with HAART's three drug classes, condom use, male circumcision and pre-exposure prophylaxis (PrEP), we note that unlike the case where the basic reproduction number was used as an indicator of effectiveness where drugs showed high impact, condom use have the highest comparative effectiveness for all efficacy levels (0.30, 0.60 and 0.90), followed by three classes of HAART which are tied at the same rank whereas male circumcision maintains its position as the intervention with the least comparative effectiveness, as was the case in the previous explanation for the effective basic reproduction number. For instance, it is evident from the table that $I_{H_\sigma} > (I_{H_\gamma} = I_{H_\epsilon} = I_{H_\kappa}) > I_{H_\nu}$. The results implies that when HIV/AIDS has firmly established in the population, condom use becomes the only reliable intervention for preventing further spread of the disease. We also note that when the effect of HAART's component drugs are considered using this type of between-host model, their effects will be the same since they will be acting to reduce one parameter N_i and this is despite of the fact that previous studies have shown in which these drug classes are shown to act differently in controlling HIV infection dynamics.
- For double HIV/AIDS interventions comprising the combination of any of the six health interventions, we note that double interventions have benefits far more exceeding those associated with mono-interventions. Furthermore, we note that the combination of condoms with either PrEP or male circumcision have the highest comparative effectiveness, followed by combinations involving HAART components (FIs & RTIs, FIs & PIs and RTIs & PIs) whereas the combination of PrEP and male circumcision have the lowest comparative effectiveness. This is because $(I_{H_{\phi\sigma}} = I_{H_{\sigma\nu}}) < (I_{H_{\gamma\epsilon}} = I_{H_{\gamma\kappa}} = I_{H_{\epsilon\kappa}}) < I_{H_{\phi\nu}}$.
- For interventions comprising three or more of the six health interventions under consideration, we note that intervention effectiveness, with regard to intervention - induced HIV Prevalence, increases with an increase in efficacy as well as the number of interventions added to the combination package.

3.9.3 Assessment of comparative effectiveness using the controlled endemic value of Community Viral Load

No.	Indicator of Intervention effectiveness	Calculated $V_{H-L-eff}$	CEL	Calculated $V_{H-M-eff}$	CEM	Calculated $V_{H-H-eff}$	CEH
1	Baseline Community Viral Load (V_H)	183,255,699.62	1	183,255,699.62	1	183,255,699.62	1
2	FIs induced endemic value of CVL (V_{H_γ})	128,274,990.00	8	73,294,280.38	8	18,313,570.76	8
3	RTIs induced endemic value of CVL (V_{H_ϵ})	128,274,990.00	8	73,294,280.38	8	18,313,570.76	8
4	PIs induced endemic value of CVL (V_{H_κ})	128,274,990.00	8	73,294,280.38	8	18,313,570.76	8

5	PrEP induced endemic value of CVL (V_{H_ϕ})	183,251,699.89	2	183,247,700.15	2	183,243,700.42	2
6	Condom use induced endemic value of CVL (V_{H_σ})	183,244,750.50	5	183,217,380.44	5	183,025,899.40	5
7	Male circumcision induced endemic value of CVL (V_{H_v})	183,251,699.89	2	183,247,700.15	2	183,243,700.42	2
8	FIs and RTIs induced endemic value of CVL ($V_{H_{\gamma\epsilon}}$)	89,788,493.27	11	29,309,712.69	11	1,819,357.88	11
9	FIs and PIs induced endemic value of CVL ($V_{H_{\gamma\kappa}}$)	89,788,493.27	11	29,309,712.69	11	1,819,357.88	11
10	RTIs and PIs induced endemic value of CVL ($V_{H_{\epsilon\kappa}}$)	89,788,493.27	11	29,309,712.69	11	1,819,357.88	11
11	PrEP and Condom use induced endemic value of CVL ($V_{H_{\phi\sigma}}$)	183,239,036.76	6	183,197,383.77	6	182,905,979.35	6
12	PrEP and Male circumcision induced endemic value of CVL ($V_{H_{\phi v}}$)	183,246,500.23	4	183,234,901.01	4	183,220,901.94	4
13	Condom use and male circumcision induced endemic value of CVL ($V_{H_{\sigma v}}$)	183,239,036.76	6	183,197,383.77	6	182,905,979.35	6
14	HAART induced endemic value of CVL ($V_{H_{\gamma\epsilon\kappa}}$)	62,847,945.55	14	11,715,885.61	14	169,936.59	14
15	HAART and PrEP induced endemic value of CVL ($V_{H_{\gamma\epsilon\kappa\phi}}$)	62,843,945.82	15	11,707,886.14	15	157,937.39	15

16	HAART and condom use induced endemic value of CVL ($V_{H_{\gamma\epsilon\kappa\sigma}}$)	62,840,436.33	17	11,694,717.55	18	49,914.64	18
17	HAART and male circumcision induced endemic value of CVL ($V_{H_{\gamma\epsilon\kappa\nu}}$)	62,843,945.82	15	11,707,886.14	15	157,937.39	15
18	HAART-PrEP and Condom use induced endemic value of CVL ($V_{H_{\gamma\epsilon\kappa\phi\sigma}}$)	62,834,722.59	19	11,674,720.88	19	-70,005.41	19
19	HAART- PrEP and male circumcision induced endemic value of CVL ($V_{H_{\gamma\epsilon\kappa\phi\nu}}$)	62,838,746.17	18	11,695,086.99	17	135,138.91	17
20	HAART- condom use and male circumcision induced endemic value of CVL ($V_{H_{\gamma\epsilon\kappa\sigma\nu}}$)	62,834,722.59	19	11,674,720.88	19	-70,005.41	19
21	HAART- PrEP- condom use and male circumcision induced endemic value of CVL ($V_{H_{\gamma\epsilon\kappa\phi\sigma\nu}}$)	62,827,294.72	21	11,642,726.21	21	-297,853.51	21

Table 3.5: Results of the assessment of comparative effectiveness of HIV/AIDS preventive interventions using the CVL (V_H) as an indicator of treatment effectiveness when each of the six preventive interventions is assumed to have: (a) low efficacy of 0.30, (b) medium efficacy of 0.60, and (c) high efficacy of 0.90.

Table (3.5) shows the results for the assessment of comparative effectiveness of the 20 HIV/AIDS interventions obtained using the intervention-induced endemic community viral load, (V_H) as the indicator of intervention effectiveness. From (3.5), we deduce the following results regarding comparative effectiveness of the 20 different HIV/AIDS interventions considered:

- For single HIV/AIDS interventions the three drug classes (FIs, RTIs and PIs) has the highest comparative effectiveness, followed by condom use and the lastly, by PrEP and male circumcision.
- For double HIV/AIDS interventions comprising of two combinations, we deduce that drug classes have the highest comparative effectiveness, followed by the combinations of condom use with either male circumcision or PrEP and

then the combination of male circumcision and PrEP with the lowest comparative effectiveness.

- When we considered a combination of HAART with either PrEP, condom use or male circumcision, we notice that adding condom use to HAART presents the potential for an effective HIV package as compared with adding PrEP or male circumcision to HAART.

3.10 Summary

In this chapter we developed a mathematical model that describes the transmission dynamics of HIV/AIDS at the population level. The model takes into consideration the role of community pathogen load as we assumed that individual viral loads can be pooled together to determine the community's level of infectiousness. The model was analysed and its main properties were established. In particular, we showed the local and global stability of the disease free equilibrium (DFE) and endemic equilibrium point (EEP) associated with the model. After performing the sensitivity analysis based on two model metrics (R_0 and V_H) and identification of model parameters that are worthy targeting for effective control of HIV/AIDS transmission, we then introduced improvements to the model. Three metrics derived from analysing the model were then used to carry out a comparative effectiveness assessment of HIV/AIDS control strategies. The comparative assessment showed that attempts to compare drug classes using the between-host model is a futile endeavour as long as the model is designed to capture the dynamics that occur at population scale. In particular, we failed to differentiate the effectiveness of the 3 drug classes. Therefore, the current model also share the same weakness as the previous within-host model presented in Chapter (2). Consequently, there is need to develop a multi-scale model that links the within-host and between-host scales so as to pave way for a meaningful insight regarding the comparative effectiveness of different medical and public health interventions. In the next Chapter, we will present a multiscale modelling framework for linked within-host and between-host with the goal to simultaneously carry out a comparative effectiveness assessment of HIV/AIDS interventions that are implemented at different scales (for instance medical intervention scale domains (operative at within-host scale) and public health interventions scale (operative at between-host scale). This entails developing a framework for linking the within-host and between-host disease dynamics and use of the resulting multiscale model to carry out mathematical analysis to identify high-level intervention strategies. This inturn will ensure effective management and control mechanisms of HIV/AIDS disease transmission.

Chapter 4

Multiscale Modelling of HIV/AIDS Disease System

4.1 Introduction

Infectious diseases continue to pose a major threat to human health. Although advances in medicine and public health have helped control many endemic diseases, World Health Organisation (WHO) study on the global burden of diseases indicates that by 2002, infectious diseases were the cause for more than one-quarter of approximately 57 million deaths worldwide (WHO et al., 2004). In addition, approximately two-thirds of all deaths in developing countries among children younger than 5 years of age are due to infectious diseases (WHO, 2005). In order to respond effectively to the growing health threats of infectious diseases such as HIV/AIDS, tuberculosis, malaria and the transfer of these health risks there is need to identify and implement high-impact health interventions for the control, elimination and even eradication of infectious diseases. Mathematical modelling and cluster randomized controlled trials (Boily et al., 2012; Cori et al., 2014) can be useful in characterizing the preventive effect of health interventions at the population level. One of the latest preventive health intervention that has been adopted for HIV/AIDS control, elimination and even eradication is Treatment as Prevention (TasP) which is based on the understanding that the single most important risk factor in determining the likelihood of HIV transmission is an HIV infected individual's plasma viral load. With effective treatment, plasma viral load can be greatly reduced for HIV infected individuals thereby significantly preventing severe disease, death and onward transmission (both heterosexual transmission and mother-to-child transmission) of HIV. Encouraged by results from TasP in HIV/AIDS (Das et al., 2011; Montaner et al., 2010; Granich et al., 2009; Fang et al., 2004; Cohen et al., 2012; Smith et al., 2012; Wilson, 2012; Delva et al., 2012), researchers are now also considering TasP as an approach for trying to deal with many other infectious diseases such as malaria (McMorrow et al., 2011; Johnston et al., 2014; Tseroni et al., 2015; Gerardin et al., 2015; John, 2016; Maude et al., 2012; El-Sayed et al., 2007; Kiszewski, 2010; Tanner et al., 2015; Chaccour et al., 2013; Greenwood, 2006), neglected tropical diseases (Smits, 2009; Keenan et al., 2013; Bockarie et al., 2013; Mbah et al., 2013), tuberculosis (Griffith et al., 2007; Disease Control, (CDC, et al., 2000; Halsey et al., 1998) and many other infectious diseases (Yamshchikov et al., 2009; Webster et al., 2014). In all of these infectious diseases, the use of TasP as a preventive health intervention is based on the fact that the transmission of an infectious disease system can be prevented by treating infected individuals so that they become less likely to transmit the infection to others. However, there is need to assess the comparative effectiveness of this public health intervention when implemented in combination with other health interventions at the community scale. Since treatment is administered at within-host scale while

other health interventions such as male condom use, male circumcision (Mukandavire and Garira, 2007a; Mukandavire et al., 2007) for HIV/AIDS, indoor residual spraying (IRS) and insecticide-treated nets (ITNs) (Griffin et al., 2010) for malaria and water supply, water quality, sanitation, and hygiene (WASH) intervention systems (Fewtrell et al., 2005; Fung, 2014) for diarrhea and cholera are implemented at between-host scale, mathematical models that link the within-host and between-host scales of infection can better inform public health policies on the comparative effectiveness of several health interventions which are implemented at different scale domains for the same infectious disease system.

One of the most important implementations research question in infectious disease prevention today is how to determine the specific contribution of each preventive intervention in an environment where these interventions are implemented as a combination. For sexually transmitted infectious disease systems such as HIV/AIDS (with for example, preventive health interventions that include TasP, condom use, male circumcision, voluntary testing and counseling, HIV/AIDS health education, pre-exposure prophylaxis, and post-exposure prophylaxis), these interventions have individual level, pairwise level and population/community level benefits. In this study, 'efficacy' and 'comparative effectiveness' are words used to describe the individual level and population level benefits of health interventions respectively. The efficacy of an infectious disease system preventive health intervention denotes the degree of protection against infection experienced by one individual benefiting directly from the health intervention, such as the degree of protection afforded to a man who is circumcised (Mukandavire and Garira, 2007a; Mukandavire et al., 2007) for HIV/AIDS or the degree of protection afforded to an individual using insecticide-treated nets (ITNs) (Griffin et al., 2010) for malaria. However, comparative effectiveness also sometimes called relative effectiveness or relative impact of an infectious disease system preventive intervention is more complex, as it incorporates the population level effects which include both direct and indirect benefits of applying the intervention to some of these individuals in the community. This makes the relationship between individual-level efficacy and population level comparative effectiveness of preventive health interventions of an infectious disease system very difficult to determine from empirical studies alone. In this study we define comparative effectiveness or relative effectiveness or relative impact of a health intervention or a combination of health interventions as the extend to which a health intervention or a combination of health interventions does better than harm at population level than an alternative health intervention or a combination of health interventions. At the individual level, the efficacy of each of the health interventions can be evaluated with sufficient follow-up during individual level randomized controlled trials (I-RCTs) or using single scale models. In the context of I-RCTs, it will not be possible to assess the comparative effectiveness of each of these interventions at the population level because at this level the comparative effectiveness of each of the interventions can be very different from its observed efficacy in I-RCTs. This is because for I-RCTs, it will not be possible to capture the full spectrum of benefits from the use of an intervention which includes a combination of direct effects on those receiving the intervention, and indirect effects on those who benefit from reduced exposure because others received the intervention (sometimes called community immunity or herd immunity in the case of vaccines). In addition, single scale models would also have problems originating from scale mismatch especially when single scale models at between-host scale are used to evaluate the population-level impact of interventions operating at within-host scale such as drugs and vaccines. An alternative would be

to use community-based randomized controlled trials (C-RCTs) (Boily et al., 2008; Donner and Klar, 2000) also sometimes called cluster randomized controlled trials in which whole communities are randomly allocated to receive either the intervention or the control condition. However, C-RCTs will also present some problems because their design, implementation and interpretation of results obtained from them can be quite challenging (Boily et al., 2008; Donner and Klar, 2000; Padian et al., 2010; Boily et al., 2007). In addition, C-RCTs cannot be used to assess the comparative effectiveness of each of the health interventions when they are implemented as a combination because they are currently not designed to establish differences between the different health intervention components as this would involve larger trials with multiple arms with the potential of using factorial designs (Boily et al., 2012). One of the best viable options proposed in this study is to use multiscale modelling to assess the comparative effectiveness of health interventions based on efficacy data from I-RCTs. Therefore, the explicit purpose of this study is to develop a new multiscale modelling framework for linking the within-host and between-host scale submodels of a directly transmitted infectious disease system in which the between-host scale disease dynamics are influenced by the within-host scale disease dynamics, and not the other way, and use it to assess the comparative effectiveness of health interventions at community level in an environment in which the health interventions are implemented as a combination comprising of several of them in which some of them operate at within-host scale while others operate at between-host scale using efficacy data.

In order to use model-based tools to assess the comparative effectiveness of health interventions that are implemented at different scale domains in the control, elimination and even eradication of infectious disease systems, we need to develop new analytic frameworks that incorporate appropriate metrics for assessing the community's level of infectiousness. This requires us to, first of all, develop models that correctly represent the transmission of infectious disease systems. Despite the fact that transmission of an infectious disease system is a consequence of processes acting on at least two different scales, i.e., within-host and between-host scales (Handel and Rohani, 2015; Garira et al., 2014; Gog et al., 2015), there has been little attempt to develop models that characterize transmission of infectious disease systems based on integrating these two scales of infection. In particular, there are three ways in which the transmission of an infectious disease system is regulated by the within-host scale processes, that is, when the immune system impacts the dynamics of an infectious disease system in a population. First, by regulating pathogen dynamics at within-host scale. Second, by affecting herd immunity at between-host scale. Finally, by altered immuno-demography through a change in the immune status due to age, disease or therapy. For example, in the case of altered immuno-demography through a change in immune status due to disease alone, we note that tuberculosis (TB) control has markedly deteriorated throughout the world since the late 1980s because of the destructive effects of HIV on the immune system (Currie et al., 2003). In addition, a number of studies on infectious disease systems have established that transmission of infectious diseases depends critically on within-host scale processes. In particular, these studies established that the transmission potential of an infectious host increases with increasing pathogen load in the infected host (Handel and Rohani, 2015), although the actual functional relationship between infectivity and pathogen load may vary considerably depending on the infectious disease system

under consideration. The hypothesis that host infectiousness depends on within-host scale pathogen load has been confirmed in a number of studies. Valuable insights were initially gained from studies of HIV-1 in discordant couples (Mellors et al., 1996; Gray et al., 2001). Further, some studies on HIV and dengue virus transmission established a sigmoid functional relationship between host infectiousness and within-host scale pathogen load (Quinn et al., 2000; Fraser et al., 2007; Lange and Ferguson, 2009; Mellors et al., 1996; Nguyen et al., 2013). Other studies which have also confirmed a similar functional relationship between host infectiousness and within-host scale pathogen load include (Jeffery and Eyles, 1955) for malaria, (Pesko et al., 2009; Seblova et al., 2013; Miller et al., 2014) for Visceral leishmaniasis and Chikungunya, (Wen et al., 2013) for hepatitis B, (Kaplan et al., 1996; Li et al., 2004) for human T lymphotropic virus, (Lawley et al., 2008; Lawley et al., 2009) for *Salmonella* and *Clostridium difficile* and (Matthews et al., 2006) for *Escherichia coli*. Although these studies established strong evidence regarding the role of pathogen load on transmission at an individual level, limited population-level information exists that demonstrates the effect of pathogen load on the transmission of infectious diseases at the community level. While this study's overall aim is to develop a new class of nested multiscale models that can be used to assess the comparative effectiveness of a combination of health interventions administered and implemented at different scale domains of an infectious disease system, the study is also intended to establish proof-of-principle about the effect of pathogen load on transmission of infectious diseases at community level.

Current modelling approach to assess the comparative effectiveness of health interventions on the transmission dynamics of infectious diseases is based on the assumption that the most ideal scale to develop such models for assessing the comparative effectiveness of health interventions administered and operating at between-host scale such as condoms, and male circumcision (Mukandavire and Garira, 2007a; Mukandavire et al., 2007) for HIV/AIDS, IRS and ITNs (Griffin et al., 2010) for malaria and WASH intervention systems (Fewtrell et al., 2005; Fung, 2014) for diarrhea and cholera is the between-host scale with such models being based on compartmentalizing hosts into susceptible, exposed, infected, recovered (SEIR) and variations of this paradigm (e.g. SI, SIS, SIR, etc.). Similarly, such a modelling approach also recognizes that the most ideal scale for assessing the relative impact of health interventions applied at the within-host scale such as drugs and vaccines for HIV (Magombedze et al., 2008; Wang et al., 2016), malaria (Chiyaka et al., 2008), TB (Magombedze et al., 2006) and influenza (Vegvari et al., 2016; Hadjichrysanthou et al., 2016) is the within-host scale with such models being based on compartmentalizing various types of immune cells (immune responses) and various types of target cells including the population of invading pathogen as well as the effect of therapeutic interventions on the invading pathogen occurring in different anatomical compartments of the human body and some molecular determinants of the disease system. However, when the comparative effectiveness of these interventions which operate at different scale domains are assessed together as combination intervention, the analytic tools currently used to assess them are predominantly those based on single scale between-host forecasting models, based on compartmentalizing hosts into susceptible, exposed, infected, recovered (SEIR), and variations of this paradigm (e.g. SI, SIS, SIR etc.) without explicitly incorporating the effects of within-host scale which also determines the transmission process of the infectious disease. Many problems in the use of such single scale models in guiding optimal drug design and assessment of the comparative effectiveness of health interventions

on infectious disease transmission originate from scale mismatch between the scale at which infectious disease processes occur and the scale at which decisions on them are made as well as scale mismatch between the scale at which the health interventions are implemented and the scale at which decisions on them are made. This is because infectious diseases are often critically influenced by interactions of several processes occurring at a wide variety of spatial and temporal scales associated with molecular, cellular, tissue, organ, organism, community and ecosystem levels of biological organization. For example, in the context of clinical trials, focusing entirely on a single scale is likely to miss interactions between processes occurring at the different scale domains, which are critically important in determining the choice of suitable endpoints during the planning of clinical trials of candidate interventions. Given that good endpoints in clinical trials should reflect the action of the health intervention on the underlying cause of the disease at appropriate scale domain, it is essential that assessments of comparative effectiveness of health interventions be explicit regarding the scale domains to be integrated and in which the interventions are implemented in order to avoid the problem of scale mismatch between the scale at which the intervention operates and the scale at which decisions on it are made. For example, disease processes such as pathogen replication with the host, exploitation of host resources such as nutrients and other vital molecules (e.g. nucleic acids for virus replication), immune evasion, infectiousness, the antimicrobial activity of drugs and vaccines and evolution of resistance mechanisms against treatment happen at the within-host scale. At the same time the spread of pathogens among hosts, the influence of environmental factors such as climate, the population dynamics of reservoir hosts, the spread of drug-resistant strains among hosts, and the influence of cultural, social and behavioural factors on susceptibility of hosts and the impact of some health interventions such as male condom use and male circumcision for HIV/AIDS are all dimensions of infectious disease transmission processes which occur at the between-host scale.

The analytic gap created by using single scale models in assessing the comparative effectiveness of health interventions operating at different scale domains of an infectious disease system may be overcome by developing appropriate multi-scale models - the all-encompassing quantitative representation of infectious disease systems that can lay bare the mechanisms of transmission of disease systems and enable individual health interventions to be assessed at the appropriate scale domain at which they operate while linked to effects of other health interventions at other appropriate scale domains and levels of organization of an infectious disease system. Such models allow progressively greater spatial, temporal, or causal detail of infectious disease systems to be considered as the scales become finer. The development of multiscale models of infectious diseases in this way is even more possible now than ever before because infectious disease study has entered a new era dominated by the "omics" (Daefler, 2013; Durmuş et al., 2015; Schulze et al., 2015; Nourani et al., 2015) as a result of the advent of high-throughput experimental technologies producing patient-specific data, establishing a complete cascade from genome, transcriptome, proteome, metabolome and physiome to health, forming a multi-scale, multi-science system that can assist in establishing the molecular basis of diseases. Further, recent advances in multiscale modelling integrating within-host and between-host scales of infectious disease systems such as (Vickers and Osgood, 2014) for Chlamydia, (Ogunjimi et al., 2015) for Chickenpox, (Wang and Wang, 2017) for Cholera, (Feng et al., 2013; Feng et al., 2015) for *Toxoplasma gondii*, (Garira et al., 2014) for schistosomiasis and other environmentally transmitted infectious disease

systems, (Martcheva, 2011; Martcheva et al., 2015a) for paratuberculosis, (Handel et al., 2013; Lukens et al., 2014; Dang et al., 2016) for influenza, (Legros and Bonhoeffer, 2016; McKenzie and Bossert, 2005; Yang, 2000; Chiyaka et al., 2007) for malaria, (Martcheva and Li, 2013; Lou et al., 2015; Dorp et al., 2014) for HIV/AIDS and (Kostova, 2007; Vickers and Osgood, 2007; Feng et al., 2012) for other viral infections have demonstrated the need for this systems approach to the study of infectious diseases. In an effort to satisfy this need we develop a new multiscale modelling framework that incorporates the concept of community pathogen load. However, there is still widespread lack of knowledge on the mathematical techniques for the representation and construction of multiscale models of infectious disease systems. The central idea in multi-scale modelling is to divide a modelling problem such as an infectious disease system into a family of sub-models that exist at different scales and then attempt to study the problem at these scales while simultaneously linking the submodels across these scales. We, therefore, define multiscale modelling as a modelling methodology in which a collection of partial models or sub-models from at least two different scales are integrated into a single model using a wide range of methodologies. However, this divide-and-rule strategy poses new challenges in terms of strategies for problem decomposition and solution strategy, scale separation and coupling, integration and coupling of submodels of different or same formalism and validation of multiscale models. There is an urgent need to develop mathematical modelling approaches to integrate models at different scales for infectious disease systems. Such multi-scale approaches are essential for producing quantitative models of infectious disease systems that can be used to assess the impact of health interventions and their implementation. At the same time, developing methodologies to integrate between scales will lead to a much deeper understanding of the universal and generic features of infectious disease systems. In this Chapter, we develop a multiscale modelling framework for linking the within-host and between-host submodels of an infectious disease system.

At the centre of the multiscale modelling framework presented in this study is the idea of using community pathogen load as the standard metric for assessing the community's level of infectiousness and disease transmission probability and as an indicator of the effectiveness of health interventions at community level. Using the strong evidence regarding the role of pathogen load on transmission of infectious diseases at individual level (Quinn et al., 2000; Fraser et al., 2007; Lange and Ferguson, 2009; Mellors et al., 1996; Nguyen et al., 2013; Pesko et al., 2009; Seblova et al., 2013; Miller et al., 2014; Wen et al., 2013; Kaplan et al., 1996; Li et al., 2004; Lawley et al., 2008; Lawley et al., 2009; Matthews et al., 2006), we upscale individual host infectiousness (within-host scale pathogen load) to define population-level infectiousness (community pathogen load) for directly transmitted infectious disease systems. Therefore, the incorporation of community pathogen load variable into the multiscale model as presented in this study arises from the need to represent the transmission of an infectious disease system more accurately at the population level. The usefulness of such simple mechanistic multiscale models is that they are predictive models for community pathogen load which is also useful as a proximal marker for infectious disease incidence and potential epidemic propagation (Das, 2014). The concept of community pathogen load is a new concept which has been recently adopted as a new public health measure which is an aggregate biomarker of a community's pathogen burden over a specific time period. At operational level, this measure has now been incorporated into national HIV/AIDS strategy by many governments starting with British Columbia (Canada), then the

US, Uganda and then France, as one of the most widely used public health metric to assess the impact of Treatment as Prevention (TasP) as a health intervention in the context of HIV/AIDS (Kranzer et al., 2013; Das et al., 2010; Abu-Raddad et al., 2013; Herbeck et al., 2014; Jain et al., 2014; Abu-Raddad and Awad, 2014; Castel et al., 2012; Miller et al., 2013; Das et al., 2011; Montaner et al., 2010; Granich et al., 2009; Palombi et al., 2012; Das et al., 2013; Estill et al., 2012; Disease Control et al., 2011; Landis et al., 2013). We define the term community pathogen load as an aggregation of individual pathogen loads of hosts (humans, animals, vectors, plants) infected with a particular pathogen (virus, protozoan, helminth, bacteria, fungus, prion) in a particular geographical location or community at a particular time.

Although the use of community-wide pathogen pool/load as a population-level metric of disease transmission potential has of late been used in multiscale modelling of environmentally transmitted infectious disease systems (see for example (Garira et al., 2014) and references therein), few multiscale modelling studies, have assessed this proposition thoroughly in relationship to directly transmitted infectious disease systems (Herbeck et al., 2014). Therefore, in this study our starting hypothesis is that by using the concept of community pathogen load in modelling directly transmitted infectious disease systems, we can, apart from developing a new multiscale modelling framework for this category of infectious diseases be developing a modelling science base for directly transmitted infectious disease systems (where the inside-host environment's biological entities such as cells, organs, body fluids, whole body, etc. are the reservoir of infective pathogen) that is comparable or similar to an existing modelling science base for environmentally transmitted infectious diseases (where the outside-host geographical environment's physical entities such as soil, air, fomites/contact surfaces, water, etc. are the reservoir of infective pathogen) where pathogen load in the environment is explicitly incorporated into the model. The usefulness of such an approach is that apart from it being a model-based and cost-effective way of determining community pathogen load for planning purposes without having to solely depend on empirical data (see for example (Disease Control et al., 2011) in the case of HIV/AIDS) only which is sometimes costly to obtain, it facilitates a common modelling framework for infectious disease systems with mixed modes of transmission (i.e. directly and environmentally transmitted infectious disease systems) so that methods and approaches for analyzing environmentally transmitted infectious disease systems such as the calculation of reproductive numbers (Bani-Yaghoub et al., 2012) are applicable to directly transmitted infectious disease systems. Typical examples of infectious disease systems with mixed modes of transmission are cholera and some co-infections such HIV-TB coinfection. In the case of cholera, for example, we note that cholera epidemics are often initially driven by environmental transmission, and once sufficient numbers of individuals are infected in the community, the epidemic dynamics is then driven by direct transmission (human-to-human contact) with environmental transmission also still playing a role. By using CPL as a common metric for disease transmission for both environmentally transmitted and directly transmitted infectious disease systems, disease impact and program outcomes can be fairly compared for these infections with different modes of transmission, and planning and policy decisions can be based on a more level assessment of the comparative effectiveness of health interventions. Currently, model-based determination of community pathogen load is not feasible for directly transmitted infectious disease systems because existing single scale models for population surveillance of directly transmitted infectious disease systems build on basic SI, SIS, SIR, etc. which are either age-structured or sex-structured do not

explicitly incorporate a measure of pathogen load.

4.2 Multiscale Model Development

In order to illustrate the application of the proposed new method for developing nested multiscale models of infectious disease systems and its utility, we develop a multiscale model for HIV/AIDS transmission dynamics as a paradigm in this section. This is a directly transmitted infectious disease system for which the primary mode of transmission is through direct contact (sexual contact) between hosts. In the context of HIV/AIDS, viral load has of late been increasingly used as a tool to monitor treatment adherence, to track viral replication within the body, to reduce the risk of HIV transmission, to inform epidemiological surveillance, and to map the virus at a population level (community viral load) (Kranzer et al., 2013; Das et al., 2010; Abu-Raddad et al., 2013; Herbeck et al., 2014; Jain et al., 2014; Abu-Raddad and Awad, 2014; Castel et al., 2012; Miller et al., 2013; Das et al., 2011; Montaner et al., 2010; Granich et al., 2009; Fang et al., 2004; Palombi et al., 2012; Das et al., 2013; Estill et al., 2012; Disease Control et al., 2011; Landis et al., 2013). For HIV/AIDS, the single-scale models based on compartmentalizing hosts into susceptible, exposed, infected, (SEI), and variations of this paradigm (e.g. SI etc.) would require incorporating the probability of transmission per unprotected sex act. However, recent studies of HIV/AIDS transmission (Quinn et al., 2000; Fraser et al., 2007; Gray et al., 2001) recorded very different rates of unprotected sex despite similar transmission rates whose dependence on viral load was similar. These studies established that the probability of transmission per unprotected sexual act would be unreliable in characterizing HIV/AIDS transmission. Therefore, the use of community viral load as a new metric of the community's level of infectiousness is an attempt to model the transmission of HIV/AIDS more accurately. In the following subsection, we develop two independent submodels for HIV/AIDS transmission dynamics at two scales, one at within-host scale and the other at between-host scale and then integrate them into a single multiscale model in subsection 4.2.2. We further simplify the integrated multiscale model of HIV/AIDS transmission dynamics by reducing its dimension through slow and fast time scale analysis in subsection 4.2.3.

4.2.1 The two Submodels of HIV/AIDS Transmission Dynamics

1. *Between-human scale HIV/AIDS transmission dynamics:* This submodel is described by an SI model. This submodel is based on monitoring the dynamics of two populations which are susceptible humans S_H , and infected humans I_H so that the total human population is given by $N_H = S_H + I_H$. We make the following assumptions for this submodel.
 - i. There is only heterosexual transmission of HIV/AIDS in the community.
 - ii. The infected human host does not recover from HIV infection.
 - iii. The transmission parameter $\widetilde{\beta}_H$ is a function of the number of infected humans so that $\widetilde{\beta}_H = \widetilde{\beta}_H(I_H)$.
 - iv. The dynamics of S_H and I_H are assumed to occur at slow time scale, t compared to the within-host scale HIV transmission dynamics submodel variables so that $S_H = S_H(t)$ and $I_H = I_H(t)$.

These assumptions lead to the following submodel for the between-host scale HIV/AIDS transmission dynamics.

$$\text{Between-host submodel : } \begin{cases} 1. \frac{dS_H(t)}{dt} = \Lambda_H - \widetilde{\beta}_H(I_H)S_H(t) - \mu_H S_H(t), \\ 2. \frac{dI_H(t)}{dt} = \widetilde{\beta}_H(I_H)S_H(t) - [\mu_H + \widetilde{\delta}_H]I_H(t). \end{cases} \quad (4.1)$$

The first equation in submodel system (4.1) describes the dynamics of susceptible humans. The population of susceptible humans is assumed to increase at a constant rate Λ_H through birth. This population is depleted through HIV infection of susceptible humans at a variable rate $\widetilde{\beta}_H(I_H)$ and natural death at a constant rate μ_H . The second equation in submodel system (4.1) describes the dynamics of HIV infected humans. This population increases through infection of susceptibles and decreases through natural death at rate μ_H and disease-induced death at rate $\widetilde{\delta}_H$.

2. *Within-host scale HIV infection dynamics:* We develop the within-host scale submodel of HIV-1 infection dynamics, which assumes interaction of the following four populations: susceptible CD4+ T cells (T_s), infected CD4+ T cells where virions have only entered the cytoplasm but without transcription that has occurred (T_c), infected CD4+ T cells which are a result of successful transcription (T_v), and the HIV pathogen (V_h). The within-host scale submodel used in this study is a simplified version of a more elaborate model developed in (Magombedze et al., 2008). In (Magombedze et al., 2008), we developed a within-host model for HIV-1 transmission that incorporates three distinct stages in the infection cycle of HIV-1: (a) entry of HIV-1 into the cytoplasm of CD4+ T cells, (b) transcription of HIV-1 RNA to DNA within CD4+ T cells, and (c) production of HIV-1 viral particles within CD4+ T cells. Here we simplify the model in (Magombedze et al., 2008) by making the following assumptions.

- i. There is no immune response in the infected human host.
- ii. There is no proliferation of CD4+ T cells due to antigenic stimulation.
- iii. There is no loss of CD4+ T cells through apoptosis due to the bystander effect induced by HIV proteins.
- iv. The within-host scale infection processes occur at fast time scale, s compared to the between-host scale HIV/AIDS submodel variables so that $T_s = T_s(s)$, $T_c = T_c(s)$, $T_v = T_v(s)$ and $V_h = V_h(s)$.

Taking into account these assumptions, the submodel for the HIV population dynamics at within-host scale is proposed to be

$$\text{Within-host submodel : } \begin{cases} 1. \frac{dT_s(s)}{ds} = \Lambda_s - \beta_h V_h(s)T_s(s) - \mu_s T_s(s), \\ 2. \frac{dT_c(s)}{ds} = \beta_h V_h(s)T_s(s) - [\alpha_c + \mu_c]T_c(s), \\ 3. \frac{dT_v(s)}{ds} = \alpha_c T_c(s) - [\alpha_v + \mu_v]T_v(s), \\ 4. \frac{dV_h(s)}{ds} = N_v \alpha_v T_v(s) - [\alpha_h + \mu_h]V_h(s). \end{cases} \quad (4.2)$$

Equation (1) of submodel (4.2) describes the dynamics of susceptible CD4+ T cells. In this equation, the first term Λ_s models the supply of CD4+ T cells from the thymus. The second term represents the collision, fusion, and entry of HIV virions into the cytoplasm of CD4+ T cells at a rate β_h . The parameter β_h models three mechanisms (Magombedze et al., 2008): that is, (a) the rate at which virus and target cells collide, (b) the fraction of cells which are activated and hence susceptible to infection, and (c) the fraction of interactions between activated CD4+ T cells and virus which results in successful entry of virions into the cytoplasm of CD4+ T cells (Magombedze et al., 2008). Transcription is modelled separately in equation (2) of submodel (4.2) by α_c . The last term represents the natural death of susceptible CD4+ T cells at rate μ_s . Equation (2) of submodel (4.2) describes the dynamics of CD4+ T cells that have been exposed to the virus (i.e., that have allowed viral entry into their cytoplasm). The first term on the right-hand side of equation (2) of submodel (4.2) is from the second term of equation (1) and models the rate of increase of CD4+ T cells where HIV has just entered the cytoplasm but await transcription of HIV RNA to DNA to occur. This equation describes the transition stage that the successful infection process of CD4+ T cells passes through before transcription occurs. Successful collisions result in the entry of viral particles in the CD4+ T cells. After entry of viral particles into the CD4+ T cells, the virus uses the CD4+ T cell machinery to replicate; then transcription of viral RNA to DNA occurs at rate α_c . Here α_c represents three processes in the HIV-1 infection cycle (Magombedze et al., 2008) which are: (a) reverse transcription, (b) viral DNA and host DNA integration and (c) transcription that results in production of many copies of HIV. As in (Magombedze et al., 2008) this equation describes the intermediate stage that the infection process goes through before the CD4+ T cells become productively infected. The last term models the death of exposed CD4+ T cells at rate μ_c during this transient stage. Equation (3) of submodel (4.2) models the dynamics of HIV infected CD4+ T cells that have moved from the exposed class after RNA to DNA transcription. The first term represents an increase in infected CD4+ T cells from the second term of equation (2). The second and last terms represent the bursting and natural death of infected CD4+ T cells at rates α_v and μ_v respectively. Equation (4) of submodel (4.2) models the dynamics of the viral load within an infected individual. The first term describes the increase of new virions from the bursting of infected CD4+ T cells. The second term models the rate of excretion of infectious virions from cells and tissues of the human body into the blood plasma at a rate α_h . The last term represents the natural decay of viral particles at rate μ_h .

We combine these submodels into a single integrated multiscale model in the following subsection.

4.2.2 Integration of the two Submodels into a Single Multiscale Model

Having presented the two submodels that separately describe the transmission of HIV/AIDS at the two different scales (within-host and between-host scale) in the community we now show how to integrate them into a single multiscale model. Based on our previous experience of developing multiscale models for environmentally transmitted infectious disease systems (Garira et al., 2014), we know that in general individual infectiousness V_h , links the within-host scale to between-host scale while exposure $\tilde{\beta}_H(I_H)$, links between-host scale to the within-host scale (Garira et

al., 2014). We apply these ideas to the current problem where the within-human scale submodel is unidirectionally coupled to the between-host scale HIV/AIDS transmission dynamics submodel. The integration of the two submodels is achieved in two steps. The first step in the integration of the two submodels presented in subsection (4.2.1) is to make assumptions about the relationship between the independent variables of the within-human virus population dynamics which are T_s and V_h and the parameters of the between-host scale HIV transmission dynamics submodel which are $\widetilde{\beta}_H(I_H)$ and $\widetilde{\delta}_H$. The second step involves applying ecosystems concepts to the within-human HIV population dynamics where we consider HIV infected humans as homogeneous and unevenly distributed individual microbial ecosystems (Rynkiewicz et al., 2015; Lofgren et al., 2016; Sicard et al., 2014) or simply homogeneous and unevenly distributed microbial habitats (Lofgren et al., 2016) to derive the appropriate equations. Details of the specific derivations and assumptions are as follows.

1. In the context of HIV infection, when the human host is considered as an ecosystem (Rynkiewicz et al., 2015; Lofgren et al., 2016; Sicard et al., 2014), then host survival or death can be considered as a suitable metric of the emergent ecosystem property owing to HIV and CD4 T cells interaction within an infected individual since the virus and CD4+ T cell populations are responsible for morbidity and mortality. So we assume that the disease induced death rate of humans in the between-host scale submodel (4.1) is an emergent ecosystem property due to HIV and is a function of the within-human scale HIV and CD4+ T cell population dynamics so that $\widetilde{\delta}_H$ becomes $\widehat{\delta}_H$ where $\widehat{\delta}_H = \widehat{\delta}_H(V_h, T_s)$.
2. Further, we assume that the transmission parameter in the between-host scale HIV transmission dynamics submodel, $\widetilde{\beta}_H(I_H)$ is not just a function of the infected human population alone $I_H(t)$, but of both the between-host scale infected human population $I_H(t)$ and within-host scale virus population $V_h(s)$ (individual host infectiousness) so that $\widetilde{\beta}_H(I_H)$ becomes $\widehat{\beta}_H$ where $\widehat{\beta}_H = \widehat{\beta}_H(V_h(s)I_H(t))$. The net effect of this assumption is to upscale individual human infectiousness $V_h(s)$ to population level or community level infectiousness so that the transmission parameter $\widehat{\beta}_H$ is now a function of the product of within-host scale viral load $V_h(s)$ and the population of infected individuals $I_H(t)$ which is, $V_h(s)I_H(t)$. In addition the quantity $V_h(s)I_H(t)$ is a new variable at between-host scale which we now denote by $V_H(t)$ so that $V_H(t) = V_h(s)I_H(t)$. Here $V_H(t)$ is the total infectious reservoir of humans in the community which we refer to in this study as community viral load. In terms of community viral load, the transmission parameter $\widetilde{\beta}_H$, for between-host scale HIV/AIDS transmission dynamics submodel becomes $\widehat{\beta}_H = \widehat{\beta}_H(V_H(t))$. We further assume a Holling type II functional form of the function $\widehat{\beta}_H(V_H)$ so that the force of infection, denoted here by $\lambda_H(t)$, associated with HIV infectivity to humans at community scale becomes

$$\lambda_H(t) = \widehat{\beta}_H(V_H(t)) = \frac{\beta_H V_H(t)}{V_0 + V_H(t)} \quad (4.3)$$

where β_H is the exposure to community viral load per unit time through sexual contact and $V_H(t)$ is the community viral at the time of sexual contact while

$$\lambda_H[V_H(t)] = \frac{V_H(t)}{V_0 + V_H(t)}, \quad (4.4)$$

is probability that a random heterosexual contact with a person in a particular community will infect the individual with HIV in that community. In the expressions (4.3) and (4.4) V_0 is the community viral load that yields 50 percent chance of getting a human host infected with HIV after a random sexual contact in a particular community. In this study, we interpret the quantity $\frac{1}{V_0}$ as a measure of the community's susceptibility to HIV infection. We assume that every community's HIV/AIDS transmission dynamics is characterized by a different susceptibility coefficient $\frac{1}{V_0}$, to HIV infection which is intrinsic to that community and that this susceptibility coefficient is dependent on many factors which include existence of co-infections, strength of the health system and nutritional status of the community. Together these factors will lead to a particular susceptibility coefficient $\frac{1}{V_0}$, for a given community if no health interventions are implemented to reduce it such as male circumcision and pre-exposure prophylaxis. We also note that $V_H(t)$ is a new variable at between-host scale which we have just introduced. In order to derive the differential equation governing the dynamics of $V_H(t)$, we again appeal to the ideas of an ecosystem approach to the within-human virus population dynamics (Rynkiewicz et al., 2015; Lofgren et al., 2016; Sicard et al., 2014). The ecosystem approach to the within-human virus population dynamics will enable us to couple the new epidemiological variable $V_H(t)$, to the within-human virus population dynamics. In particular it enables us to couple the differential equation for $V_H(t)$ to the differential equation for $V_h(s)$ at the within-human scale. From sub-model system (4.2), we know that the differential equation for $V_h(s)$ is

$$\frac{dV_h(s)}{ds} = N_v \alpha_v T_v(s) - [\alpha_h + \mu_h] V_h(s). \quad (4.5)$$

Applying the ecosystem concepts in (Rynkiewicz et al., 2015; Lofgren et al., 2016; Sicard et al., 2014) to the within-human population dynamics of HIV, we assume that infected humans in a particular geographical location or community are small homogeneous and unevenly distributed habitats or environments in which HIV survives and multiply until it becomes infectious to susceptible humans. So at any time s , each of these habitats is contaminated at a rate α_h since this is the rate at which infectious HIV is excreted from cells and tissues of the human body into the blood plasma within each of the infected humans and becomes infectious to susceptible humans. Now since at any time t we have a total of $I_H(t)$ of these homogeneous habitats/environments with each of these habitats being contaminated with an average of $V_h(s)$ virions, then the rate of change of community viral load $V_H(t)$, in the entire habitat/environment (community) made of of $I_H(t)$ homogeneous and unevenly distributed habitats/environments in the community becomes

$$\frac{dV_H(t)}{dt} = V_h(s) \alpha_h I_H(t) - \widehat{\alpha}_H(V_h, T_s) V_H(t), \quad (4.6)$$

where $\widehat{\alpha}_H(V_h, T_s)$ is the community-wide elimination of the total infectious reservoir of humans V_H so that it takes an average of $\frac{1}{\widehat{\alpha}_H(V_h, T_s)}$ days from the time of start of the HIV/AIDS epidemic in a community to the time when everyone's plasma viral load in the community is suppressed to below detection

limit in which case $V_H = 0$ and the probability of transmission of HIV/AIDS in the community given by equation 4.4 becomes zero. But since current drugs cannot cure HIV $V_H = 0$ denotes the case where every infected individual's viral load in the community is suppressed to below detection limit in which case we assume that every infected individual on HIV drug therapy in the community with plasma viral load suppressed to below detection limit due to drug therapy is non-infectious (Vernazza et al., 2008). Further, since $V_H(t)$ is the total infectious reservoir of humans in a particular community defined here as community viral load, then $\frac{1}{\widehat{\alpha}_H(V_h, T_s)}$ is the average time to suppress every infected individual's viral load in the community to below detection limit and render all infected humans in a particular community non-infectious. Therefore, for the eradication of HIV (complete absence of the infectious agent) in the community, the theoretical solution is that if it was possible to treat all infected individuals and suppress their viral loads to below detection limit and render them non-infectious for a period longer than the life-span of an HIV infected person (which on average is $\frac{1}{\mu_H + \delta_H}$) then HIV/AIDS would be eradicated in the community and transmission would completely stop. Taking into account the above derivations and assumptions the between-host scale HIV/AIDS transmission dynamics submodel becomes

$$\left\{ \begin{array}{l} 1. \frac{dS_H(t)}{dt} = \Lambda_H - \frac{\beta_H V_H(t)}{V_0 + V_H(t)} S_H(t) - \mu_H S_H(t), \\ 2. \frac{dI_H(t)}{dt} = \frac{\beta_H V_H(t)}{V_0 + V_H(t)} S_H(t) - [\mu_H + \widehat{\delta}_H(V_h, T_s)] I_H(t), \\ 3. \frac{dV_H(t)}{dt} = V_h(s) \alpha_h I_H(t) - \widehat{\alpha}_H(V_h, T_s) V_H(t). \end{array} \right. \quad (4.7)$$

Community viral load (CVL) $V_H(t)$, which is also a measure of the total infectious reservoir of humans in the community and burden of disease, is defined in this study as an aggregate population-level biomarker of a community's viral burden over a specific time period.

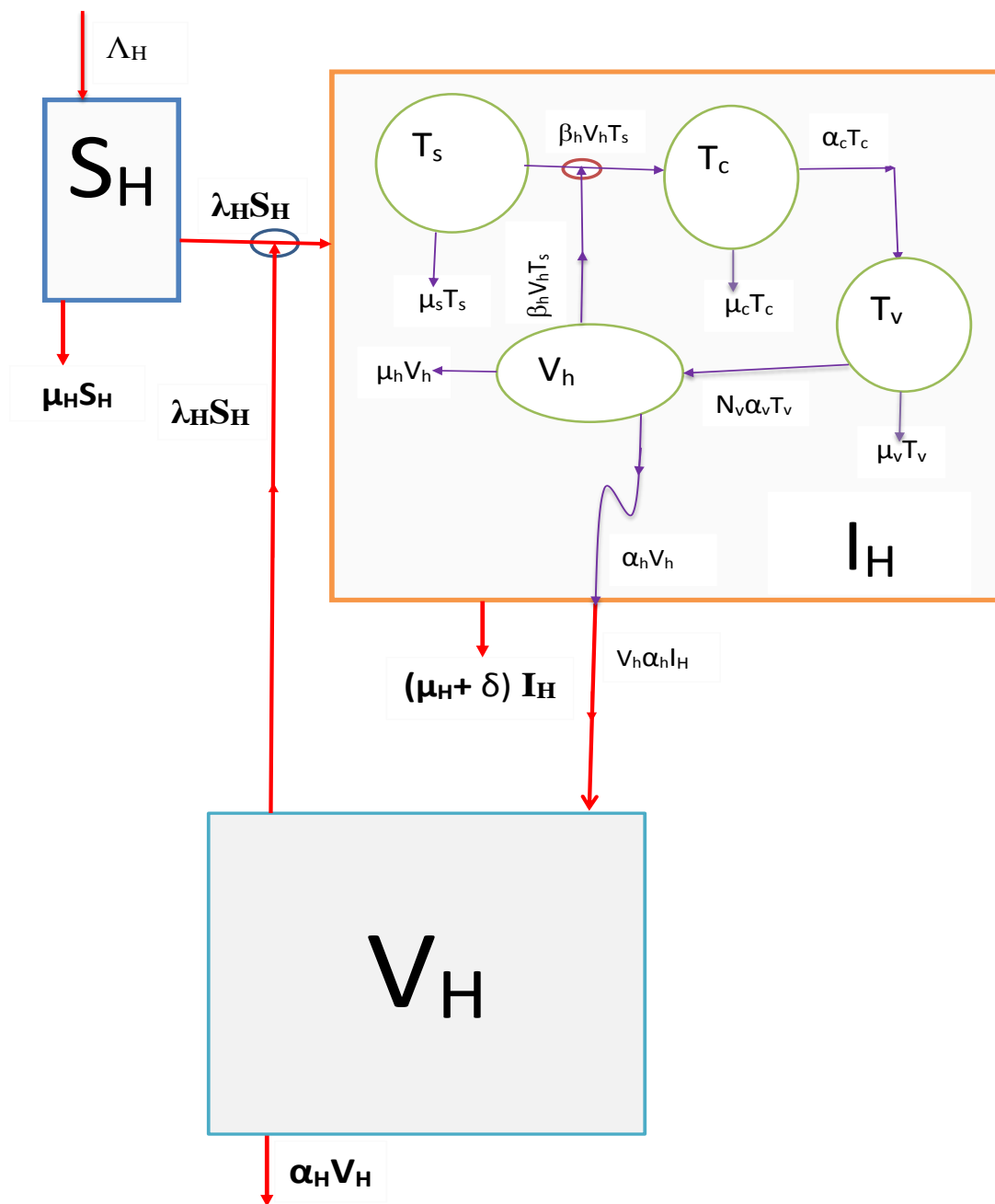
Putting together all the various derivations and assumptions the complete multiscale model for HIV transmission dynamics from human-to-human becomes

$$\left\{ \begin{array}{l} 1. \frac{dT_s(s)}{ds} = \Lambda_s - \beta_h V_h(s) T_s(s) - \mu_s T_s(s), \\ 2. \frac{dT_c(s)}{ds} = \beta_h V_h(s) T_s(s) - [\alpha_c + \mu_c] T_c(s), \\ 3. \frac{dT_v(s)}{ds} = \alpha_c T_c(s) - [\alpha_v + \mu_v] T_v(s), \\ 4. \frac{dV_h(s)}{ds} = N_v \alpha_v T_v(s) - [\alpha_h + \mu_h] V_h(s), \\ 5. \frac{dS_H(t)}{dt} = \Lambda_H - \lambda_H(t) S_H(t) - \mu_H S_H(t), \\ 6. \frac{dI_H(t)}{dt} = \lambda_H(t) S_H(t) - [\mu_H + \widehat{\delta}_H(V_h, T_s)] I_H(t), \\ 7. \frac{dV_H(t)}{dt} = V_h(s) \alpha_h I_H(t) - \widehat{\alpha}_H(V_h, T_s) V_H(t), \end{array} \right. \quad (4.8)$$

where

$$\lambda_H(t) = \frac{\beta_H V_H(t)}{V_0 + V_H(t)}. \quad (4.9)$$

We derived the multiscale model system (4.8) by making the assumption that humans are small homogeneous and unevenly distributed habitats/environments in which HIV survives and multiply to become infectious. This assumption has the importance of establishing a modelling science base for directly transmitted infectious disease systems that is comparable to an existing modelling science base for environmentally transmitted infectious diseases where the community pathogen load in the environment is explicitly incorporated into the model. The conceptual diagram of the full multiscale model of HIV/AIDS transmission dynamics is shown in Figure 4.1. As shown in Figure 4.1, we note that the similarity between directly transmitted and environmentally transmitted infectious disease systems comes from the fact that in both cases there is excretion of the infectious agent into some environment in the community. In the case of HIV/AIDS disease system considered in this work as a paradigm, the excretion of the infectious agent (HIV) (at an assumed rate α_h) is into inside-host environment's biological entity (blood plasma) while in conventional environmentally transmitted infectious disease systems the excretion of the infectious agent will be into the geographical environment's physical entities such as soil, water, air, etc.



chch

Figure 4.1: A conceptual diagram of the full multiscale model of HIV/AIDS transmission dynamics. In this Figure δ_H stands for $\widehat{\delta}_H(V_h, T_s)$ and α_H stands for $\widehat{\alpha}_H(V_h, T_s)$.

This type of modelling framework enables us to develop multiscale models for directly transmitted infectious disease systems without focusing on who infects who in a particular community but only addressing the question about how often are individuals infected in a particular community. This is also the approach taken when modelling environmentally transmitted infectious disease (see for example (Chiyaka and GARIRA, 2009; Hartley et al., 2005) and references therein) in that the question of who infects who does not arise. Data on who infects who in directly transmitted infectious disease systems are difficult to obtain. On the other hand, there is considerable amount of data available on the effects of pathogens within an individual host and the resulting responses of the host immune system, and including data

on the distribution of the infectious diseases within host populations (for example, the total number of infections and the rates of new infections) which are not being adequately applied to good effect in infectious disease modelling. To date, the potential for modelling directly transmitted infectious disease systems incorporating community pathogen load (i.e. by only addressing the question about how often are individuals infected in a particular community) is not being adequately tapped. The incorporation of CPL in the multiscale modelling framework presented in this study is the major selling point of this modelling framework in which we want to develop a model-based tool to assess the comparative effectiveness of health interventions at population level while capturing the full spectrum of benefits from the use of an intervention which include direct benefits on those individuals receiving the intervention and indirect effects on those who benefit from reduced exposure as a result of reduction in CPL or reduction in contact with CPL because others have received the intervention.

4.2.3 Simplifying the Complete Multiscale Model for HIV/AIDS Transmission Dynamics

One of the difficulties in analysing the multiscale model system (4.8) is that the within-human submodel is in terms of a fast time scale s , while the between-host scale submodel is in terms of a slow time scale t . Another difficulty is that the disease induced death rate $\widehat{\delta}_H$ and the rate of suppression of community viral load $\widehat{\alpha}_H$ are assumed to be a functions of within-host scale variables $V_h(s)$ and $T_v(s)$, that is, $\widehat{\delta}_H = \widehat{\delta}_H(V_h, T_s)$ and $\widehat{\alpha}_H = \widehat{\alpha}_H(V_h, T_s)$. However, we do not know the explicit functional forms of $\widehat{\delta}_H(V_h, T_s)$ and $\widehat{\alpha}_H(V_h, T_s)$. Thus, the two major difficulties with the multiscale model given by (4.8) is timescale mismatch between the within-host scale submodel timescale and the between-host scale submodel timescale as well as the inability to properly account for emergent phenomena. In order to overcome the problem of timescale mismatch between the within-host scale submodel timescale and the between-host scale submodel timescale, we simplify the multiscale model by making a slow and fast time scale analysis. Consider the within-human submodel (4.2) and re-written here for quick reference as

$$\left\{ \begin{array}{l} \frac{dT_s(s)}{ds} = \Lambda_s - \beta_h V_h(s) T_s(s) - \mu_s T_s(s), \\ \frac{dT_c(s)}{ds} = \beta_h V_h(s) T_s(s) - [\alpha_c + \mu_c] T_c(s), \\ \frac{dT_v(s)}{ds} = \alpha_c T_c(s) - [\alpha_v + \mu_v] T_v(s), \\ \frac{dV_h(s)}{ds} = N_v \alpha_v T_v(s) - [\alpha_h + \mu_h] V_h(s). \end{array} \right. \quad (4.10)$$

We can re-write the model system (4.10) using the slow time scale t by assuming a relation between the fast and slow time-scales to be $t = \epsilon s$ where $0 < \epsilon \ll 1$, so that the within-human scale HIV transmission dynamics submodel can be re-written in terms of the slow time-scale as follows:

$$\left\{ \begin{array}{l} 1. \epsilon \frac{dT_s(t)}{dt} = \Lambda_s - \beta_h V_h(t) T_s(t) - \mu_s T_s(t), \\ 2. \epsilon \frac{dT_c(t)}{dt} = \beta_h V_h(t) T_s(s) - [\alpha_c + \mu_c] T_c(t), \\ 3. \epsilon \frac{dT_v(t)}{dt} = \alpha_c T_c(t) - [\alpha_v + \mu_v] T_v(t), \\ 4. \frac{dV_h(t)}{dt} = N_v \alpha_v T_v(t) - [\alpha_h + \mu_h] V_h(t). \end{array} \right. \quad (4.11)$$

In the within-host scale model system (4.11), ϵ is a constant highlighting the fast time scale of the within-human scale submodel compared to the slow time scale of the between-host scale HIV/AIDS transmission dynamics submodel. Since $0 < \epsilon \ll 1$, we set $\epsilon = 0$ so that the within-human scale HIV transmission dynamics submodel becomes independent of time and we get:

$$\left\{ \begin{array}{l} 1. \Lambda_s - \beta_h V_h T_s - \mu_s T_s = 0, \\ 2. \beta_h V_h T_s - [\alpha_c + \mu_c] T_c = 0, \\ 3. \alpha_c T_c - [\alpha_v + \mu_v] T_v = 0, \\ 4. N_v \alpha_v T_v - [\alpha_h + \mu_h] V_h = 0. \end{array} \right. \quad (4.12)$$

From the algebraic equations (4.12) we get

$$\left\{ \begin{array}{l} 1. T_s = \frac{\alpha_h + \mu_h}{\beta_h} \cdot \frac{\alpha_c + \mu_c}{\alpha_c} \cdot \frac{\alpha_v + \mu_v}{N_v \alpha_v} = \frac{\Lambda_s}{\mu_s \mathfrak{R}_0}, \\ 2. T_c = \frac{\alpha_h + \mu_h}{\alpha_c} \cdot \frac{\alpha_v + \mu_v}{N_v \alpha_v} \cdot \frac{\mu_s}{\beta_h} \left[\frac{\beta_h}{\alpha_h + \mu_h} \cdot \frac{\Lambda_s}{\mu_s} \cdot \frac{\alpha_c}{\alpha_c + \mu_c} \cdot \frac{N_v \alpha_v}{\alpha_v + \mu_v} - 1 \right] = \frac{\Lambda_s (\mathfrak{R}_0 - 1)}{\mathfrak{R}_0 (\alpha_c + \mu_c)}, \\ 3. T_v = \frac{1}{N_v \alpha_v} \cdot \frac{\mu_s}{\beta_h} \left[\frac{\beta_h}{\alpha_h + \mu_h} \cdot \frac{\Lambda_s}{\mu_s} \cdot \frac{\alpha_c}{\alpha_c + \mu_c} \cdot \frac{N_v \alpha_v}{\alpha_v + \mu_v} - 1 \right] = \frac{\mu_s (\mathfrak{R}_0 - 1)}{N_v \alpha_v \beta_h}, \\ 4. V_h = \frac{\mu_s}{\beta_h} \left[\frac{\beta_h}{\alpha_h + \mu_h} \cdot \frac{\Lambda_s}{\mu_s} \cdot \frac{\alpha_c}{\alpha_c + \mu_c} \cdot \frac{N_v \alpha_v}{\alpha_v + \mu_v} - 1 \right] = \frac{\mu_s}{\beta_h} [\mathfrak{R}_0 - 1]. \end{array} \right. \quad (4.13)$$

In the equation (4.13)

$$\mathfrak{R}_0 = \frac{\beta_h}{\alpha_h + \mu_h} \cdot \frac{\Lambda_s}{\mu_s} \cdot \frac{\alpha_c}{\alpha_c + \mu_c} \cdot \frac{N_v \alpha_v}{\alpha_v + \mu_v}, \quad (4.14)$$

is the within-host scale basic reproductive number. Therefore, a consequence of the slow and fast time scale analysis here is that the within-host scale submodel (4.10) is reduced to algebraic equations as given by equation (4.12) which can be solved to get some values as given by expressions in equation (4.13) which feed into the parameters and variables of the between-host scale submodel as follows.

$$\left\{ \begin{array}{l} 1. \frac{dS_H(t)}{dt} = \Lambda_H - \lambda_H(t)S_H(t) - \mu_H S_H(t), \\ 2. \frac{dI_H(t)}{dt} = \lambda_H(t)S_H(t) - [\mu_H + \widehat{\delta}_H(V_h, T_s)] I_H(t), \\ 3. \frac{dV_H(t)}{dt} = V_h \alpha_h I_H(t) - \widehat{\alpha}_H(V_h, T_s) V_H(t). \end{array} \right. \quad (4.15)$$

From the model system (4.15), we note that the total infectious reservoir of humans (community viral load) $V_h(s)V_H(t)$ is now approximated by $V_h I_V(t)$. Using the notation that

$$\left\{ \begin{array}{l} 1. N_h = V_h, \text{ a composite constant parameter,} \\ 2. \delta_H = \widehat{\delta}_H(V_h, T_s), \text{ a constant parameter,} \\ 3. \alpha_H = \widehat{\alpha}_H(V_h, T_s), \text{ a constant parameter,} \end{array} \right. \quad (4.16)$$

then the full multiscale model (4.8) of HIV/AIDS transmission dynamics is simplified to become

$$\left\{ \begin{array}{l} 1. \frac{dS_H(t)}{dt} = \Lambda_H - \lambda_H(t)S_H(t) - \mu_H S_H(t), \\ 2. \frac{dI_H(t)}{dt} = \lambda_H(t)S_H(t) - [\mu_H + \delta_H] I_H(t), \\ 3. \frac{dV_H(t)}{dt} = N_h \alpha_h I_H(t) - \alpha_H V_H(t). \end{array} \right. \quad (4.17)$$

where,

$$\left\{ \begin{array}{l} 1. \lambda_H = \frac{\beta_H V_H}{V_0 + V_H}, \\ 2. N_h = \frac{\mu_s}{\beta_h} \left[\frac{\beta_h}{\alpha_h + \mu_h} \cdot \frac{\Lambda_s}{\mu_s} \cdot \frac{\alpha_c}{\alpha_c + \mu_c} \cdot \frac{N_v \alpha_v}{\alpha_v + \mu_v} - 1 \right] = \frac{\mu_s}{\beta_h} [\mathfrak{R}_0 - 1]. \end{array} \right. \quad (4.18)$$

Under the flow described by the simplified multiscale model system (4.17), the non-negative octant \mathbb{R}_+^3 is positively invariant; thus we have the following result.

Theorem 4.2.1. *Let $(S_H(t), I_H(t), V_H(t))$ be the solution of the multiscale model system (4.17), with initial conditions $(S_H(0), I_H(0), V_H(0))$ and the compact set*

$$\Omega = \left\{ (S_H, I_H, V_C) \in \mathbb{R}_+^3, F_H \leq \frac{\Lambda_H}{\mu_H}, F_V \leq \frac{N_h \alpha_h \Lambda_H}{\mu_H \alpha_H} \right\}. \quad (4.19)$$

Under the flow described by model system (4.17), Ω is a positively invariant set that attracts all solutions in \mathbb{R}_+^3 .

Proof. Consider the following Lyapunov function candidate:

$$F = (F_H, F_V) = (S_H + I_H, V_H). \quad (4.20)$$

The time derivative of F is given by

$$\begin{aligned} \frac{dF}{dt} &= \left(\frac{dF_H}{dt}, \frac{dF_V}{dt} \right) = (S_H + I_H, V_H), \\ &= (\Lambda_H - \mu_H S_H - \mu_H I_H - \delta_H I_H, N_h \alpha_H I_H - \alpha_H V_H). \end{aligned} \quad (4.21)$$

This gives

$$\begin{cases} \frac{dF_H}{dt} = \Lambda_H - \mu_H F_H - \delta_H I_H \leq \Lambda_H - \mu_H F_H \leq 0, \text{ for } F_H \geq \frac{\Lambda_H}{\mu_H}, \\ \frac{dF_V}{dt} = N_h \alpha_h I_H - \alpha_H F_V \leq N_h \alpha_h F_H - \alpha_H F_V \leq 0, \text{ for } F_V \geq \frac{N_h \alpha_h \Lambda_H}{\mu_H \alpha_H}. \end{cases} \quad (4.22)$$

From equation (4.22), we have $\frac{dF}{dt} \leq 0$ which implies that Ω is an invariant set. By solving equation (4.22) we have

$$0 \leq (F_H, F_V) \leq \left(F_H(0)e^{-\mu_H t} + \frac{\Lambda_H}{\mu_H} [1 - e^{-\mu_H t}], F_V(0)e^{-\alpha_H t} + \frac{N_h \alpha_h \Lambda_H}{\mu_H \alpha_H} [1 - e^{-\alpha_H t}] \right), \quad (4.23)$$

where $F_H(0)$ and $F_V(0)$ represent the initial values of $F_H(t)$ and $F_V(t)$. Thus as $t \rightarrow \infty$,

$$0 \leq (F_H, F_V) \leq \left(\frac{\Lambda_H}{\mu_H}, \frac{N_h \alpha_h \Lambda_H}{\mu_H \alpha_H} \right), \quad (4.24)$$

where $\mathfrak{R}_0 > 1$ since $N_h = \frac{\mu_s}{\beta_h} [\mathfrak{R}_0 - 1]$. Thus whenever $\mathfrak{R}_0 > 1$, Ω is an attractive positively invariant set. This completes the proof. \square

4.3 Analysis of the Baseline Multiscale Model

4.3.1 The Disease-free Equilibrium and the Reproductive Number

We obtain the disease-free equilibrium point of the multiscale model system (4.17) by setting its left-hand side equal to zero and also assume that $I_H = V_H = 0$. Thus we get

$$E_0 = (S_H^0, I_H^0, V_H^0) = \left(\frac{\Lambda_H}{\mu_H}, 0, 0 \right), \quad (4.25)$$

where E_0 denotes the disease-free equilibrium of the model system (4.17). The local asymptotic stability of E_0 can be established using the basic reproductive number. The basic reproductive number \mathcal{R}_0 , defined as the average number of secondary infections produced by single infectious host, introduced into a totally susceptible population is one of the important tools in the analysis of disease outbreak. For multiscale models that integrate the within-host scale and the between-host scale, this threshold quantity is a combined function of pathogen dynamics at within-host scale and between-host scale. This implies that in order to get an accurate reproductive number from a mathematical model, we need to develop a multiscale model that integrates relevant scales for the phenomenon of the infectious disease system being investigated. For most infectious disease systems, if $\mathcal{R}_0 < 1$, then the infectious disease system will disappear with time, whereas if $\mathcal{R}_0 > 1$, the infectious

disease system will persist at endemic levels. In the context of HIV/AIDS infection, the quantity \mathcal{R}_0 defines the expected number of human infections generated by a single infected human introduced in a completely susceptible community of hosts. The basic reproductive number characterizing the transmission of an infectious disease system can be calculated from a compartmental model by using either the next generation matrix (NGM) approach (Diekmann et al., 1990; Driessche and Watmough, 2002) or the next generation operator (NGO) approach (Castillo-Chavez et al., 2002). In this study, we calculate the basic reproduction number of the multiscale model system (4.17) by using the next generation matrix approach (Driessche and Watmough, 2002). In this case, the second and the third equations of the multiscale model system (4.17) form a subsystem that describes the generation and transition of infectious humans and the community viral load that are used to calculate \mathcal{R}_0 . The Jacobian matrix associated with the linearized subsystem evaluated at the disease free equilibrium point, E_0 , of the multiscale model system (4.17) is given by

$$J(E_0) = \begin{bmatrix} -(\mu_H + \delta_H) & \frac{\beta_H \Lambda_H}{V_0 \mu_H} \\ N_h \alpha_h & -\alpha_H \end{bmatrix}. \quad (4.26)$$

Then, $J(E_0)$ is decomposed into two matrices F and V such that $J(E_0) = F - V$, where F is the transmission and non-negative matrix describing the generation of secondary infections, and V is the transition and non-singular matrix, describing the changes in individual states such as removal by death, recovery or excretion of HIV into the blood plasma by infected humans in the community. Following (Bani-Yaghoub et al., 2012), we can give two different biological interpretations of the disease compartments and hence different next generation matrices from (4.26), to get two different \mathcal{R}_0 expressions for the compartmental multiscale model (4.17) as follows.

- i. Assume that the community viral load is an extended state of host infectiousness: This assumption holds since we upscaled individual host infectiousness $V_h(s)$ to population level infectiousness $V_H(t)$. In this case the shedding of HIV (i.e. $N_h \alpha_h$) into the blood plasma is placed in the V matrix rather than the F matrix, so that matrices F and V become

$$F_I = \begin{bmatrix} 0 & \frac{\beta_H \Lambda_H}{V_0 \mu_H} \\ 0 & 0 \end{bmatrix}, \quad V_I = \begin{bmatrix} (\mu_H + \delta_H) & 0 \\ -N_h \alpha_h & \alpha_H \end{bmatrix}, \quad (4.27)$$

and the next generation matrix, M_I is given by

$$M_I = F_I V_I^{-1} = \begin{bmatrix} \frac{N_h \alpha_h \beta_H \Lambda_H}{\mu_H \alpha_H (\mu_H + \delta_H) V_0} & 0 \\ 0 & 0 \end{bmatrix}. \quad (4.28)$$

The basic reproductive number is the spectral radius (dominant eigenvalue) of the matrix $F_I V_I^{-1}$, that is, $\mathcal{R}_0^I = \rho(F_I V_I^{-1})$. Therefore, in this case, the basic reproduction number of the multiscale model system (4.17) becomes

$$\mathcal{R}_0^I = \frac{N_h \alpha_h \beta_H \Lambda_H}{\mu_H \alpha_H (\mu_H + \delta_H) V_0} = \mathcal{R}_{0HC} \cdot \mathcal{R}_{0CH}. \quad (4.29)$$

- ii. *The community is assumed to act as a reservoir of the infective pathogen:* This assumption also holds since $N_h\alpha_h$ is the rate that describes how much viral load each infected individual contributes to the community viral load during his/her entire period of infectiousness. In this case, the shedding rate of HIV (i.e. $N_h\alpha_h$) into the blood plasma is placed in the F matrix rather than the V matrix, so that matrices F and V derived from matrix (4.26) become

$$F_{II} = \begin{bmatrix} 0 & \frac{\beta_H\Lambda_H}{V_0\mu_H} \\ N_h\alpha_h & 0 \end{bmatrix}, \quad V_{II} = \begin{bmatrix} (\mu_H + \delta_H) & 0 \\ 0 & \alpha_H \end{bmatrix}, \quad (4.30)$$

and the next generation matrix, M_{II} is given by

$$M_{II} = F_{II}V_{II}^{-1} = \begin{bmatrix} 0 & \frac{\beta_H\Lambda_H}{\alpha_H\mu_H V_0} \\ \frac{N_h\alpha_h}{(\mu_H + \delta_H)} & 0 \end{bmatrix}. \quad (4.31)$$

The basic reproductive number is also the spectral radius (dominant eigenvalue) of the matrix $F_{II}V_{II}^{-1}$, that is, $\mathcal{R}_0^{II} = \rho(F_{II}V_{II}^{-1})$. Therefore, in this case, the basic reproduction number of the multiscale model system (4.17) becomes

$$\mathcal{R}_0^{II} = \sqrt{\frac{N_h\alpha_h\beta_H\Lambda_H}{\mu_H\alpha_H(\mu_H + \delta_H)V_0}} = \sqrt{\mathcal{R}_{0HC} \cdot \mathcal{R}_{0CH}}. \quad (4.32)$$

The two basic reproductive numbers \mathcal{R}_0^I and \mathcal{R}_0^{II} given by equations (4.29) and (4.32), respectively are interpreted as follows.

- Consider a single newly infected human host entering an HIV/AIDS disease-free community. This individual is still present and infectious and the expected amount of infectious reservoir contributed to the total infectious reservoir of humans in the community (community viral load) by each infected human host during his/her entire period of infectiousness is approximately

$$\mathcal{R}_{0HC} = \frac{N_h\alpha_h}{(\mu_H + \delta_H)}. \quad (4.33)$$

This quantity depends on the average viral load in the human body N_h which is excreted into the blood plasma at a rate α_h of an infected individual, where it becomes infectious to other humans during sexual contact during an individual's entire period of infectiousness and N_h is a composite parameter which in this study is interpreted as the endemic value of the within-human scale viral load V_h which we have already determined from the within-human HIV transmission dynamics submodel as

$$\begin{cases} N_h &= \frac{\mu_s}{\beta_h} \left[\frac{\beta_h}{\alpha_h + \mu_h} \cdot \frac{\Lambda_s}{\mu_s} \cdot \frac{\alpha_c}{\alpha_c + \mu_c} \cdot \frac{N_v\alpha_v}{\alpha_v + \mu_v} - 1 \right] = \frac{\mu_s}{\beta_h} [\mathfrak{R}_0 - 1], \\ \mathfrak{R}_0 &= \frac{\beta_h}{\alpha_h + \mu_h} \cdot \frac{\Lambda_s}{\mu_s} \cdot \frac{\alpha_c}{\alpha_c + \mu_c} \cdot \frac{N_v\alpha_v}{\alpha_v + \mu_v}. \end{cases} \quad (4.34)$$

Therefore, in the expression for \mathcal{R}_{0HC} , $N_h\alpha_h$ is the rate that describes how much an infected human contributes to the community viral load (the total infectious reservoir of humans in the community) during his/her entire period of

infectiousness while $\frac{1}{(\mu_H + \delta_H)}$ is the average viral carriage time by each infected human (i.e. the average life span of an HIV infected individual).

- Similarly, consider a single infectious dose of HIV entering an infectious viral load-free community with susceptible humans at equilibrium. This infectious dose is still present and infectious and the expected number of infected humans arising from each infectious dose of HIV is approximately

$$R_{0CH} = \frac{\Lambda_H \beta_H}{\mu_H \alpha_H V_0}. \quad (4.35)$$

This partial reproductive number depends on the supply rate of susceptible humans Λ_H , the average life span of each susceptible human host $\frac{1}{\mu_H}$, the rate of sexual contact of the susceptible humans with the infectious reservoir of humans β_H , the average time it takes to suppress the infectious reservoir of humans in the community to below detection levels $\frac{1}{\alpha_H}$ and the the susceptibility coefficient to HIV infection in the community $\frac{1}{V_0}$, where V_0 is the community viral load that results in 50% of the people being infected.

From equations (4.29) and (4.32) we deduce that the HIV/AIDS basic reproductive number \mathcal{R}_0 is composed of between-host scale disease parameters and within-human scale parameters. Therefore, most reproductive numbers of infectious diseases currently reported in literature which are calculated from single scale (between-host scale) may not be accurate enough since they do not take into account the selective pressure on the pathogen exhibited by the host's immune system (a within-host scale phenomenon) that tends to increase the pathogen's fitness by optimizing the reproductive number of the disease at population level (between-host scale) (Gog et al., 2015). We note that since our work in the example of HIV/AIDS disease system as a paradigm is focused on assessing the comparative effectiveness of five HIV/AIDS interventions (TasP composed of three drug classes, male condom use, and male circumcision), the outcome of our results will not be dependent on the choice of the reproductive from these two basic reproductive numbers (R_0^I and R_0^H). Therefore, because of its simplicity, we shall use in all that follows (unless stated otherwise) $R_0 = R_0^I$ as the basic reproductive of the multiscale model (4.17).

4.3.2 Local stability of DFE

For determining the local stability of disease-free equilibrium (DFE) of the model system (4.17), we linearize equations of the system (4.17). In order to obtain a Jacobian matrix we evaluate the linearized system at the DFE, denoted here by E_0 where

$$E_0 = \left(\frac{\Lambda_H}{\mu_H}, 0, 0 \right), \quad (4.36)$$

to get

$$J(E_0) = \begin{pmatrix} -\mu_H & 0 & -\frac{\beta_H \Lambda_H}{V_0 \mu_H} \\ 0 & -(\mu_H + \delta_H) & \frac{\beta_H \Lambda_H}{V_0 \mu_H} \\ 0 & N_h \alpha_h & -\alpha_H \end{pmatrix}, \quad (4.37)$$

as previously defined. We prove the stability of DFE by calculating the eigenvalues (λ_i , $i = 1, 2, 3$) of the above Jacobian matrix (4.37). The characteristic equation from which we can derive the eigenvalues is

$$(-\mu_H - \lambda)[\lambda^2 + a_1\lambda + a_2] = 0, \quad (4.38)$$

where

$$\begin{cases} a_1 = \mu_H + \delta_H + \alpha_H, \\ a_2 = (\mu_H + \delta_H)\alpha_H(1 - \mathcal{R}_0). \end{cases} \quad (4.39)$$

It is clear from equation (4.38) that one of the eigenvalues is $\lambda = -\mu_H$. Now to determine the nature of the remaining two eigenvalues we use the polynomial

$$P(\lambda) = \lambda^2 + a_1\lambda + a_2 = 0. \quad (4.40)$$

To do this, we use the Routh-Hurwitz criteria. In this case, we define the following Hurwitz matrices (H_j , $j = 1, 2$) whose elements are the coefficients of the characteristic polynomial in $P(\lambda)$ given by equation (4.40) as

$$H_1 = \begin{pmatrix} a_1 \end{pmatrix}, \quad H_2 = \begin{pmatrix} a_1 & 1 \\ 0 & a_2 \end{pmatrix}. \quad (4.41)$$

Evaluating the determinant of H_1 , we obtain

$$\det(H_1) = |a_1| = a_1 = \mu_H + \delta_H + \alpha_H > 0. \quad (4.42)$$

Similarly, the determinant of H_2 is given by

$$\det(H_2) = \begin{vmatrix} a_1 & 1 \\ 0 & a_2 \end{vmatrix} = a_1 a_2 = (\mu_H + \delta_H + \alpha_H)\alpha_H(\mu_H + \delta_H)(1 - \mathcal{R}_0). \quad (4.43)$$

From equation (4.39) it can be noticed that all the coefficients a_1 and a_2 of the polynomial $P(\lambda)$ are greater than zero whenever $\mathcal{R}_0 < 1$ and $\mathfrak{R}_0 > 1$. Furthermore, all the determinants of matrices H_1 and H_2 are positive if and only if $\mathcal{R}_0 < 1$ and whenever $\mathfrak{R}_0 > 1$. Hence all the roots of the polynomial $P(\lambda)$ are either negative or have negative real parts if $\mathcal{R}_0 < 1$ and whenever $\mathfrak{R}_0 > 1$. These results are summarized by the following theorem.

Theorem 4.3.1. *The disease-free equilibrium point of the multiscale model system (4.17) is locally asymptotically stable if $\mathcal{R}_0 < 1$ and whenever $\mathfrak{R}_0 > 1$.*

Theorem (4.3.1) implies that it may not be necessary to eradicate HIV in every HIV infected individual in order to eliminate HIV/AIDS in a community since elimination of HIV/AIDS can happen for $\mathfrak{R}_0 > 1$. This implies that HIV/AIDS may be eliminated from a community even with current drugs which do not cure infected individuals but at best only function to suppress the individuals' viral loads to below detection limit and render the individuals less likely to transmit HIV in the community.

4.3.3 Global stability of DFE

We determine the global stability of DFE of the multiscale model system (4.17) by using the next generation operator approach (Castillo-Chavez et al., 2002). Thus the

system (4.17) can be re-written in the form

$$\begin{cases} \frac{dX}{dt} = F(X, Z), \\ \frac{dY}{dt} = G(X, Z), \end{cases} \quad (4.44)$$

where

- $X = S_H$ represents a compartment of uninfected components, and
- $Z = (I_H, V_H)$ represents all compartments of infected and infectious components.

Let

$$E_0 = (X^*, 0) = \left(\frac{\Lambda_H}{\mu_H}, 0, 0 \right), \quad (4.45)$$

denote the disease-free equilibrium (DFE) of the multiscale model system (4.17). For E_0 to be globally asymptotically stable, the following conditions (H1) and (H2) must be satisfied.

H1. For $\frac{dX}{dt} = F(X, 0)$, X^* is globally asymptotically stable (g.a.s),

H2. $G(X, Z) = AZ - \hat{G}(X, Z)$, $\hat{G}((X, Z) \geq 0$ for $(X, Z) \in \mathbb{R}_+^3$ where $A = D_Z G(X^*, 0)$ is an M-matrix and \mathbb{R}_+^3 is the region where the model makes biological sense.

In our case

$$F(X, 0) = [\Lambda_H - \mu_H S_H], \quad (4.46)$$

and the matrix A is given by

$$A = \begin{bmatrix} -(\mu_H + \delta_H) & \frac{\beta_H \Lambda_H}{\mu_H V_0} \\ N_h \alpha_h & -\alpha_H \end{bmatrix}, \quad (4.47)$$

and

$$\hat{G}(X, Z) = \begin{bmatrix} \left(\frac{\Lambda_H}{\mu_H V_0} - \frac{S_H}{V_0 + V_H} \right) \beta_H V_H \\ 0 \end{bmatrix}. \quad (4.48)$$

Since $\frac{\Lambda_H}{\mu_H V_0} \geq \frac{S_H}{V_0 + V_H}$, it is clear that $\hat{G}(X, Z) \geq 0$ for all $(X, Z) \in \mathbb{R}_+^3$. It is also clear that A is an M-matrix, since the off diagonal elements of A are non-negative. We state a theorem which summarizes these results.

Theorem 4.3.2. *The fixed point*

$$E_0 = (X^*, 0) = \left(\frac{\Lambda_H}{\mu_H}, 0, 0 \right), \quad (4.49)$$

is globally asymptotically stable equilibrium of model system (4.17) if $\mathcal{R}_0 < 1$ and whenever $\mathcal{R}_0 > 1$ and the assumptions (H1) and (H2) are satisfied.

4.3.4 The Endemic Equilibrium State

Let $E = (S_H, I_H, V_H)$, denote the endemic equilibrium point of the multiscale model system (4.17). At the endemic equilibrium point, each of the three variables is constant such that the rate of change of each of the model variables is zero. Thus, we set the left-hand side of the equations of the model system (4.17) equal to zero and determine the non-trivial solution of the resulting algebraic equations which gives

$$\left\{ \begin{array}{l} 1. S_H = \frac{\Lambda_H}{\lambda_H + \mu_H}, \\ 2. I_H = \frac{\lambda_H}{(\mu_H + \delta_H)} \cdot \frac{\Lambda_H}{\mu_H + \lambda_H}, \\ 3. V_H = \frac{N_h \alpha_h I_H}{\alpha_H}. \end{array} \right. \quad (4.50)$$

We note the following about the endemic equilibrium given by expressions in (4.50).

- ▶ From the first expression in equation (4.50) we note that the susceptible human population at endemic equilibrium is equal to the average time of stay in susceptible class $\frac{1}{\mu_H + \lambda_H}$ and the rate at which new susceptible individuals are entering the susceptible class through natural birth Λ_H . Individuals leave the susceptible class either through infection due to physical sexual contact in the community viral load at rate λ_H or through natural death at rate μ_H .
- ▶ We also note from the second expression in equation (4.50) that the infected human population at the endemic equilibrium point is equal to the average time of stay in the infected class $\frac{1}{\mu_H + \delta_H}$, the rate at which susceptible individuals become infected λ_H , the average time of stay in susceptible class $\frac{1}{\mu_H + \lambda_H}$ and the rate at which new susceptible individuals are entering the susceptible class through natural birth Λ_H .
- ▶ Furthermore, we deduce from the third expression in equation (4.50) that the endemic value of community viral load is determined by the rate at which infected human population excretes HIV into the blood plasma $N_h \alpha_h$, the number of infected hosts I_H , and the rate of elimination of viral load α_H in the community.

We have been talking about the endemic equilibrium of model system (4.17) without saying anything about its existence. The endemic equilibrium for model system (4.17) given by equation (4.50) only exists for $\mathcal{R}_0 > 1$ and whenever $\mathfrak{R}_0 > 1$; thus we have the following result.

Theorem 4.3.3. *The endemic equilibrium for the multiscale model system (4.17) given by expression (4.50) exists if $\mathcal{R}_0 > 1$ and whenever $\mathfrak{R}_0 > 1$.*

Proof. Showing the existence of the endemic equilibrium given by expression (4.50) is straightforward. To determine the existence of the endemic equilibrium point given by equation (4.50), we first of all express S_H and I_H in terms of V_H in the form

$$\left\{ \begin{array}{l} S_H(V_H) = \frac{\Lambda_H(V_0 + V_H)}{\mu_H V_0 + (\mu_H + \beta_H)V_H}, \\ I_H(V_H) = \frac{\mu_H \beta_H V_H}{(\mu_H + \delta_H) [\mu_H V_0 + (\mu_H + \beta_H)V_H]}. \end{array} \right. \quad (4.51)$$

Substituting the expressions in equations (4.51) into the equation for V_H which is

$$\frac{dV_H(t)}{dt} = N_h \alpha_h I_H - \alpha_H V_H, \quad (4.52)$$

at the endemic equilibrium, we obtain

$$V_H = \frac{\mu_H V_0 (\mathcal{R}_0 - 1)}{(\mu_H + \beta_H)}, \quad (4.53)$$

for the community viral load endemic equilibrium value where

$$\mathcal{R}_0 = \frac{\mu_s (\mathcal{R}_0 - 1) \alpha_h \Lambda_H \beta_H}{\beta_h (\mu_H + \delta_H) \mu_H \alpha_H V_0}. \quad (4.54)$$

We can easily deduce from equations (4.53) and (4.54) that only a single positive endemic equilibrium point exists for $\mathcal{R}_0 > 1$ and whenever $\mathcal{R}_0 > 1$. Therefore, we conclude that there exists only one unique endemic equilibrium point for model system (4.17) given by equation (4.50) for $\mathcal{R}_0 > 1$ and whenever $\mathcal{R}_0 > 1$. \square

In addition, since \mathcal{R}_0 is a function of both within-host scale and between-host scale parameters, the expressions (4.51), (4.52) and (4.54) confirm the unidirectional coupling structure of the multiscale model given by (??) in which the within-host scale submodel influences the between-host scale submodel and not the other way round.

4.3.5 Local Stability of the Endemic Equilibrium

Theorem 4.3.3 has established the existence of a unique endemic equilibrium for the simplified multiscale model system (4.17) without providing any information about its stability. Here, we determine the local stability of the endemic steady state given by equation (4.50) of the multiscale model system (4.17) by using the center manifold theory (Carr, 1981). The center manifold theory has been used to determine the local stability of non-hyperbolic equilibrium points. For the convenience of interpretation of the stability, Theorem 4.1 in Castillo-Chavez and Song (Castillo-Chavez and Song, 2004), reproduced here as Theorem 4.3.4 for convenience, will be used to show the local asymptotic stability of the endemic equilibrium point (4.50).

Theorem 4.3.4. Consider the following general system of ordinary differential equations with parameter ϕ :

$$\frac{dx}{dt} f(x, \phi), \quad f : \mathbb{R}^n \longrightarrow \mathbb{R}, \quad f : \mathbb{C}^2(\mathbb{R}^2 \times \mathbb{R}), \quad (4.55)$$

where 0 is an equilibrium point of the system (4.17), (i.e., $f(0, \phi) = 0, \quad \forall \quad \phi$), and assume that

- (1) $A = D_x f(0, 0) = \left(\frac{\partial f_i(0, 0)}{\partial x_i} \right)$ is a linearization of the system around the equilibrium 0 with ϕ evaluated at 0 ;
- (2) Zero is a simple eigenvalue of A and other eigenvalues of A have negative real part;
- (3) Matrix A has a left eigenvector denoted by \mathbf{u} and a right eigenvector denoted by \mathbf{v} , corresponding to the zero eigenvalue.

Let f_k be the k th component of f and

$$\begin{cases} a = \sum_{k,i,j=1}^n u_k v_i v_j \frac{\partial^2 f_k}{\partial x_i \partial x_j}(0, 0), \\ b = \sum_{k,i,j=1}^n u_k v_i \frac{\partial^2 f_k}{\partial x_i \partial \phi}(0, 0). \end{cases} \quad (4.56)$$

The local dynamics of the system around the equilibrium point 0 is totally governed by the signs of a and b .

- (i) $a > 0, b > 0$, when $\phi < 0$ with $|\phi| \ll 1$, 0 is locally asymptotically stable, and there exists a positive unstable equilibrium; when $0 < \phi \ll 1$, 0 is unstable and there exists a negative and locally asymptotically stable equilibrium.
- (ii) $a < 0, b < 0$, when $\phi < 0$ with $|\phi| \ll 1$, 0 is unstable; when $0 < \phi \ll 1$, 0 is locally asymptotically stable, and there exists a positive unstable equilibrium point.
- (iii) $a > 0, b < 0$, when $\phi < 0$ with $|\phi| \ll 1$, 0 is unstable and there exists a locally asymptotically stable negative equilibrium; when $0 < \phi \ll 1$, 0 is stable and a positive unstable equilibrium appear.
- (iv) $a < 0, b > 0$, when ϕ changes from negative to positive, 0 changes its stability from stable to unstable. Correspondingly a negative unstable equilibrium becomes positive and locally asymptotically stable.

In our case, we use the above theorem by making the following change of variables, $S_H = x_1, I_H = x_2, V_H = x_3$. Further, we let $\phi = \beta^*$, where β^* is considered as the bifurcation parameter. Letting $\beta^* = \beta_H$ and consider $R_0 = 1$, and solve for β^* , we obtain

$$\beta^* = \sqrt{\frac{\mu_H(\mu_H + \delta_H)V_0\alpha_H}{N_h\alpha_h\Lambda_H}}. \quad (4.57)$$

We further use the vector notation $\mathbf{x} = (x_1, x_2, x_3)^T$ so that the model system (4.17) can be written in the form

$$\frac{d\mathbf{x}}{dt} = \mathbf{F}(\mathbf{x}, \beta^*), \quad (4.58)$$

where

$$\mathbf{F} = (f_1, f_2, f_3), \quad (4.59)$$

so that:

$$\begin{cases} \dot{x}_1 = \Lambda_H - \frac{\beta^* x_3 x_1}{V_0 + x_3} - \mu_H x_1, \\ \dot{x}_2 = \frac{\beta^* x_3 x_1}{V_0 + x_3} - (\mu_H + \delta_H)x_2, \\ \dot{x}_3 = N_h \alpha_h x_2 - \alpha_H x_3. \end{cases} \quad (4.60)$$

The Jacobian matrix associated with the system of equations (4.60) evaluated at the disease-free equilibrium (E_0) is given by

$$J(E_0) = \begin{pmatrix} -\mu_H & 0 & -\frac{\beta^* \Lambda_H}{V_0 \mu_H} \\ 0 & -(\mu_H + \delta_H) & \frac{\beta^* \Lambda_H}{V_0 \mu_H} \\ 0 & N_h \alpha_h & -\alpha_H \end{pmatrix}. \quad (4.61)$$

The Jacobian matrix (4.61) of the model system (4.60) has a left eigenvector $\mathbf{u} = (u_1, u_2, u_3)$, where

$$\begin{cases} u_1 = 0, \\ u_2 = \frac{N_h \alpha_h}{\mu_H + \delta_H}, \\ u_3 = 1. \end{cases} \quad (4.62)$$

Further, the Jacobian matrix (4.61) of the model system (4.60) has a right eigenvector given by $\mathbf{v} = (v_1, v_2, v_3)$, where

$$\begin{cases} v_1 = \frac{-\beta^* \Lambda_H}{V_0 \mu_H^2}, \\ v_2 = \frac{\beta^* \Lambda_H}{(\mu_H + \delta_H) \mu_H V_0}, \\ v_3 = 1. \end{cases} \quad (4.63)$$

The non-zero second order mixed derivatives of F with respect to each variable used to determine the sign of a are,

$$\begin{cases} \frac{\partial^2 f_1}{\partial x_3^2} = \frac{2\beta^* \Lambda_H}{V_0^2 \mu_H}, \\ \frac{\partial^2 f_2}{\partial x_3^2} = -\frac{2\beta^* \Lambda_H}{V_0^2 \mu_H}. \end{cases} \quad (4.64)$$

Furthermore, the non-zero partial derivatives with respect to variables and β^* , used to determine the sign of b are,

$$\begin{cases} \frac{\partial^2 f_1}{\partial x_3 \partial \beta^*} = -\frac{\Lambda_H}{\mu_H V_0}, \\ \frac{\partial^2 f_2}{\partial x_3 \partial \beta^*} = \frac{\Lambda_H}{\mu_H V_0}. \end{cases} \quad (4.65)$$

Substituting expressions (4.62), (4.63), (4.64) and (4.65) into equation (4.56), we get

$$\begin{cases} a = \frac{-2\alpha_H}{V_0} \cdot \frac{N_h \alpha_h}{\mu_H + \delta_H} \cdot \frac{\Lambda_H \beta^*}{\mu_H \alpha_H V_0} = \frac{-2\alpha_H \mathcal{R}_0}{V_0} < 0, \\ b = \frac{N_h \alpha_h}{\mu_H + \delta_H} \cdot \frac{\Lambda_H \beta^*}{\mu_H V_0} = \frac{\alpha_H \mathcal{R}_0}{\beta^*} > 0, \end{cases} \quad (4.66)$$

where,

$$\mathcal{R}_0 = \frac{\mu_s(\mathfrak{R}_0 - 1)\alpha_h\Lambda_H\beta_H}{\beta_h(\mu_H + \delta_H)\mu_H\alpha_H V_0}. \quad (4.67)$$

Thus, $a < 0$ and $b > 0$ whenever $\mathfrak{R}_0 > 1$. Using Theorem 4.3.4, item (iv), we conclude that the HIV endemic steady state of model system (4.60) is locally asymptotically stable which only holds for $\mathcal{R}_0 > 1$ but close to 1 and whenever $\mathfrak{R}_0 > 1$. These results are summarized by the following theorem.

Theorem 4.3.5. *The HIV/AIDS endemic steady state of model system (4.60) guaranteed by Theorem 4.3.4 is locally asymptotically stable for $\mathcal{R}_0 > 1$ near 1 and whenever $\mathfrak{R}_0 > 1$.*

4.3.6 Sensitivity Analysis of the Transmission Metrics of Baseline Multi-scale Model

In order to use the multiscale model given by (4.17) to obtain results that can be used to inform HIV/AIDS prevention and treatment policy we used parameters from published literature to parameterize it. The parameters are listed in Table 2.1 and 3.1. However, because of the uncertainty surrounding these parameters, we conducted a sensitivity analysis study to assess the sensitivity of four HIV/AIDS transmission metrics derived from the multiscale model given by (4.17) to all the 16 parameters in the multiscale model. The four HIV/AIDS transmission metrics derived from the multiscale model are: the basic reproductive number \mathcal{R}_0 , the within-host scale basic reproductive number \mathfrak{R}_0 , the endemic value of the community viral load V_H , and the endemic value of the within-host scale viral load V_h . However, since the within-host scale submodel is not influenced by the between-host scale submodel in the multiscale model, the sensitivity assessment of \mathfrak{R}_0 and V_h to the multiscale model parameters only measures the sensitivity of model output to parameters at a single scale (within-host scale). In general if a model (multiscale or single scale) is highly sensitive to parameters on which there is little reliable data, then such a model is of limited use. In the worst case scenario, such a model is even considered dangerous in decision making. On the other hand, if a parameter has little material influence on key outputs of the model (which in this case are \mathcal{R}_0 , V_H , \mathfrak{R}_0 and V_h), the uncertainty about the value of that parameter does not detract the value of the model in decision making. However, parameters which are known to vary in real life and to which disease dynamics model output is sensitive are also useful in a totally different way in that they provide 'critical points' for disease control, elimination or even eradication which should be monitored and controlled during a disease outbreak.

The sensitivity analysis of the four HIV/AIDS transmission metrics (\mathcal{R}_0 , V_H , \mathfrak{R}_0 and V_h), with respect to all the 16 parameters will assist in informing HIV/AIDS prevention and treatment policy by using high impact preventive health interventions. There are several ways of conducting sensitivity analysis (Hamby, 1994), all of which give slightly different sensitivity ranking. In this study, we use the approach given in (Helton et al., 1985; Pannell, 1997; Arriola and Hyman, 2007; Chitnis et al., 2008; Van Damme and Van Herck, 2007). This approach is the backbone of all other sensitivity analysis techniques and gives the normalized forward sensitivity index, which is also sometimes called the elasticity. For the four HIV/AIDS transmission metrics, \mathcal{R}_0 , V_H , V_h , and \mathfrak{R}_0 the normalized sensitivity index with respect to a parameter P is given by

$$S_{\Gamma_i}^P = \frac{\partial \Gamma_i}{\partial P} \times \frac{P}{\Gamma_i}, \quad i = V_H, \mathcal{R}_0, V_h, \mathfrak{R}_0, \quad (4.68)$$

where

$$\left\{ \begin{array}{l} V_H = \frac{\mu_H V_0 (R_0 - 1)}{(\mu_H + \beta_H)}, \\ \mathcal{R}_0 = \frac{N_h \alpha_h \beta_H \Lambda_H}{\mu_H \alpha_H (\mu_H + \delta_H) V_0} = \frac{\mu_s (\mathfrak{R}_0 - 1) \alpha_h \Lambda_H \beta_H}{\beta_h (\mu_H + \delta_H) \mu_H \alpha_H V_0}, \\ V_h = \frac{\mu_s}{\beta_h} \left[\frac{\beta_h}{\alpha_h + \mu_h} \cdot \frac{\Lambda_s}{\mu_s} \cdot \frac{\alpha_c}{\alpha_c + \mu_c} \cdot \frac{N_v \alpha_v}{\alpha_v + \mu_v} - 1 \right] = \frac{\mu_s}{\beta_h} [\mathfrak{R}_0 - 1], \\ \mathfrak{R}_0 = \frac{\beta_h}{\alpha_h + \mu_h} \cdot \frac{\Lambda_s}{\mu_s} \cdot \frac{\alpha_c}{\alpha_c + \mu_c} \cdot \frac{N_v \alpha_v}{\alpha_v + \mu_v}. \end{array} \right. \quad (4.69)$$

SL. No.	Parameter	Sensitivity index of \mathcal{R}_0	Sensitivity index of V_H	Sensitivity index of \mathfrak{R}_0	Sensitivity index of V_h
1.	β_H	1	0.000116	-	-
2.	Λ_H	1	1.0000496	-	-
3.	V_0	-1	-0.0000496	-	-
4.	μ_H	-1.250	-0.250	-	-
5.	δ_H	-0.75	-0.75	-	-
6.	α_H	-1	-1.0000496	-	-
7.	α_h	0.9434	0.9434	-0.05660	-0.05660
8.	β_h	0.0000878	0.0000878	1	0.0000878
9.	μ_s	-0.0000878	-0.0000878	-1	-0.0000878
10.	μ_h	-0.9435	-0.9435	-0.9434	-0.943
11.	Λ_s	1.0000878	1.000137	1	1.0000878
12.	α_c	0.9781	0.9781	0.9780	0.97808
13.	μ_c	-0.9781	-0.9781	-0.9780	-0.9781
14.	α_v	0.6251	0.6251	0.6250	0.6250
15.	μ_v	-0.6251	-0.6251	-0.625	-0.6250
16.	N_v	1.0000878	1.000137	1	1.0000878

Table 4.1: Results of the assessment of the sensitivity of the four HIV/AIDS transmission metrics (\mathcal{R}_0 , V_H , \mathfrak{R}_0 and V_h) to the baseline HIV multiscale model parameters.

Table (4.1) shows results of the assessment of the sensitivity of the four HIV/AIDS transmission metrics to the baseline HIV multiscale model (4.17)'s parameters. From the sensitivity indices in Table (4.1), we deduce the following results.

- a. The first six values of sensitivity indices in Table (4.1) are associated with between-host scale disease parameters only. We note from these values that the sensitivity of \mathcal{R}_0 to the four of these between-host scale parameters Λ_H , V_0 , β_H and α_H is relatively high and the same. However, the sensitivity of V_H to the same parameters is variable, with V_H being least sensitive to V_0 and β_H while remaining highly sensitive and having approximately the same sensitivity to Λ_H and α_H as for \mathcal{R}_0 . Thus V_H is more robust with respect to the parameters V_0 and β_H . Further, both \mathcal{R}_0 and V_H are significantly sensitive to μ_H and δ_H (natural and HIV/AIDS induced death rates). Since \mathcal{R}_0 characterizes transmission of HIV/AIDS at the start of the epidemic while V_H characterizes transmission of HIV/AIDS when the disease is now endemic in a community, we make the following conclusions regarding the sensitivity of \mathcal{R}_0 and V_H to the between-host scale HIV/AIDS transmission parameters:

- ▶ Since both \mathcal{R}_0 and V_H are significantly sensitive to Λ_H , α_H , μ_H and δ_H , this implies that care should be taken in improving the accuracy of these between-host scale parameters during data collection if the validity and utility of the multiscale model of HIV/AIDS transmission given by (4.17) is to be improved.
 - ▶ Since β_H measures contact rate with community viral load and V_0 measures susceptibility of the community to HIV infection, we infer that β_H is modified by condom use (since condoms reduce contact with the virus) while V_0 is modified by male circumcision and pre-exposure prophylaxis (since these two interventions do not reduce contact with the virus but reduce susceptibility to infection by the virus).
 - ▶ Since V_H is less sensitive to β_H and V_0 while \mathcal{R}_0 is significantly sensitive to β_H and V_0 , this can imply that condoms and male circumcision are more effective in controlling the transmission of HIV/AIDS at the start of the epidemic than when the disease is already endemic in the community.
 - ▶ Since both \mathcal{R}_0 and V_H are significantly sensitive to Λ_H (supply rate of susceptibles) and α_H (reduction rate of community viral load), we note that Λ_H is modified by HIV/AIDS health education that targets youths to delay the age of sexual activity while α_H is modified by treatment as prevention (TasP) which reduces the amount of virus in infected individuals and resulting in reduction in community viral load. We therefore conclude that these two interventions are equally important in reducing transmission of HIV/AIDS both at the start of the epidemic and when the disease is endemic in the community.
- b. The remaining 10 parameters in Table (4.1) are associated with within-host scale disease parameters. Considering the effect of these within-host scale parameters on the output of the multiscale model given by (4.17), we note that both \mathcal{R}_0 and V_H are significantly sensitive to all of them except β_h and μ_s . Thus \mathcal{R}_0 and V_H are most robust with respect to β_h and μ_s . We make the following deductions regarding the assessment of the sensitivity of \mathcal{R}_0 and V_H with respect to within-host scale parameters.
- ▶ Since \mathcal{R}_0 and V_H are significantly sensitive to 8 of 10 within-host scale parameters which are α_h , μ_h , Λ_s , α_c , μ_c , α_v , μ_v and N_v , this implies that care must also be taken in improving the accuracy of these within-host scale parameters during data collection if the validity and utility of the multiscale model of HIV/AIDS transmission given by (4.17) is to be improved.
 - ▶ From results in Magombedze et al., 2008, we know that 3 of the 10 within-host scale parameters (β_h , α_c and N_v) are modified by different classes of antiretroviral drugs. For these three parameters β_h is modified by fusion inhibitors (FIs), α_c is modified by reverse transcriptase inhibitors (RTIs) while N_v is modified by protease inhibitors Magombedze et al., 2008. From the assessment of the sensitivity of \mathcal{R}_0 and V_H to these three parameters, we note that they are most sensitive to N_v , followed by α_c while they are all least sensitive to β_h . This may imply that PIs have the highest effectiveness in controlling HIV/AIDS transmission followed by RTIs with FIs having the least effectiveness in controlling the transmission of HIV/AIDS at community level.

- ▶ From the assessment of the sensitivity of \mathcal{R}_0 and V_H to three additional parameters (Λ_s , μ_v and μ_h), we note that both \mathcal{R}_0 and V_H are also significantly sensitive to all these three within-host scale parameters while having the highest sensitivity to Λ_s . A common feature of all these parameters is that they are linked to known effects of immune response to HIV infection (Magombedze et al., 2008). We therefore, infer that all these three parameters are likely to be modified by a vaccine that improves supply of CD4+ T cells (associated with Λ_s) whose effects may include direct killing of infected cells (associated with μ_v) and direct degradation of the virus (associated with μ_h). We conclude that a vaccine that improves the supply of CD4T+ cells will likely yield the highest benefits in reducing the transmission of HIV/AIDS at community level.
 - ▶ However, we note that contrary to our expectation that an increased supply of immune cells (that is, CD4+ T cells), will reduce both \mathcal{R}_0 and V_H at community, the results of the assessment of the sensitivity of both \mathcal{R}_0 and V_H to Λ_s show that these two HIV/AIDS transmission metrics will increase with increasing Λ_s . We think that this anomaly is a result of the weakness and limitation of our multiscale model given by (4.17), where we did not incorporate the two conflicting roles of CD4+ T cells which include being target cells as well as orchestrating immune response to HIV infection.
- c. For the within-host scale submodel given by (4.2), whose dynamics is not influenced by the between-host scale submodel sensitivity analysis was implemented by assessing the sensitivity of \mathfrak{R}_0 and V_h to all the ten within-host scale model parameters and we note that both \mathfrak{R}_0 and V_h have the same and high sensitivity to 7 of the 10 within-host scale parameters (μ_h , Λ_s , α_c , μ_c , α_v , μ_v and N_v) similar to that of both \mathcal{R}_0 and V_H . Therefore, we note that in general, the sensitivity of multiscale model output given by (4.17) and the within-host scale submodel output given by (4.2) are comparable. Thus, similar to our conclusions for the multiscale model, we conclude that care must be taken in improving the accuracy of these parameters during data collection if the validity and utility of the within-host scale given by (4.2) used in building up the multiscale model given by (4.17) is to be improved.

Overall, we note that the assessment of the sensitivity of all the four HIV/AIDS transmission metrics which are the basic reproductive number \mathcal{R}_0 , the within-host scale basic reproductive number \mathfrak{R}_0 , the endemic value of the community viral load V_H , and the endemic value of the within-host scale viral load V_h to the multiscale model parameters was useful with respect to guiding data collection for model parameterization and to identify parameters which are crucial in the control of the HIV/AIDS epidemic.

4.3.7 The Influence of Within-host Scale on Between-host Scale HIV/AIDS Transmission Dynamics

The multiscale model given by (4.17) is unidirectionally coupled in that only the within-host scale submodel influences the between-host scale submodel and not the other way round. We have already illustrated the influence of the within-host scale submodel on the between-host scale submodel in subsection (4.3.5) using analytical methods by the showing that the endemic values of the between-host scale variables S_H , I_H and V_H are functions of the within-host scale parameters. In this

subsection we use numerical simulations to verify this structure of the multiscale model. In particular, we illustrate the influence of within-host scale submodel parameters on the between-host scale submodel variables. The numerical simulations are conducted using the baseline parameter values given in Table (4.1). The multiscale model given by (4.17) has a total of 16 parameters of which 10 are within-host scale submodel parameters while the remaining 6 are between-host scale submodel parameter. However, we will only consider the influence of three within-host scale parameters which are β_h , α_c and N_v . We consider only these three parameters because of their relevancy to the work in this study where we consider the comparative effectiveness of the different classes of antiretroviral drugs and other interventions in the prevention and treatment of HIV/AIDS as a case study.

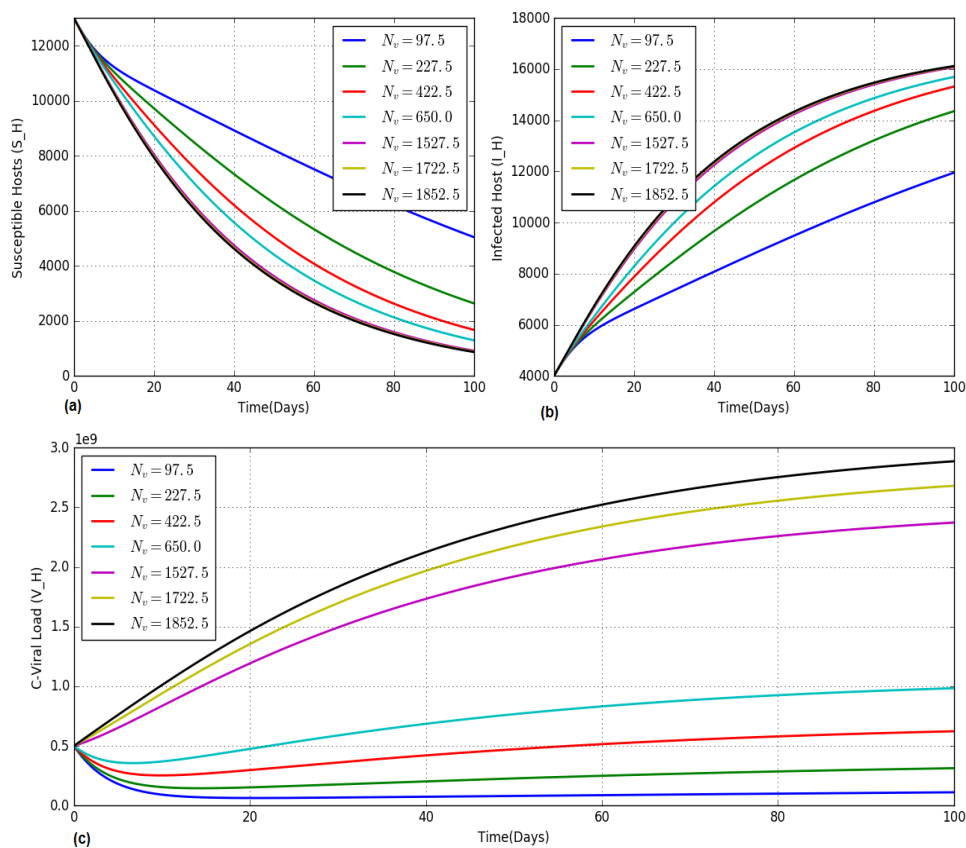


Figure 4.2: Effect of burst size of infected CD4+ T cells parameter (N_v) on (a) population of susceptible humans (S_H), (b) HIV/AIDS prevalence (I_H) and (c) community viral load (V_H) for different values of N_v : $N_v = 97.5$, $N_v = 227.5$, $N_v = 422.5$, $N_v = 650.0$, $N_v = 1,527.5$, $N_v = 1,722.5$, $N_v = 1,852.5$.

Figure (4.2) shows variation of (a) population of susceptible humans (S_H), (b) HIV/AIDS prevalence (I_H) and (c) community viral load (V_H) for different values of burst size of infected of CD4+ T cells (N_v): $N_v = 97.5$, $N_v = 227.5$, $N_v = 422.5$, $N_v = 650.0$, $N_v = 1,527.5$, $N_v = 1,722.5$, $N_v = 1,852.5$. The numerical results show that these three between-host scale variables (S_H , I_H , V_H) are significantly sensitive to within-host scale parameter N_v . The results also imply that as the average infected CD4+

T cell burst size increases, HIV/AIDS transmission in the community also increase. Therefore, antiretroviral drugs such as protease inhibitors that reduce the average infected CD4+ T cell burst size at within-host scale will likely reduce transmission of HIV at between-host scale.

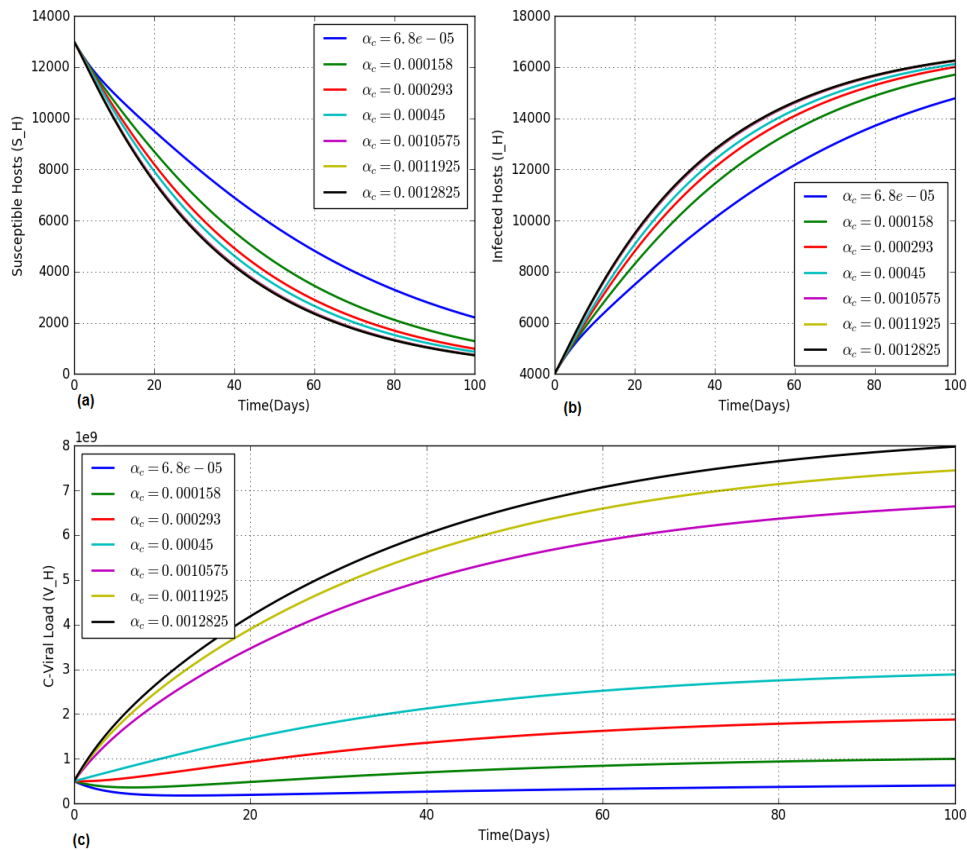


Figure 4.3: Effect of rate of transcription of HIV-1 RNA to DNA inside CD4+ T cells parameter (α_c) on (a) population of susceptible humans (S_H), (b) HIV/AIDS prevalence (I_H) and (c) community viral load (V_H), for different values of α_c : $\alpha_c = 6e^{-5}$, $\alpha_c = 0.000158$, $\alpha_c = 0.000293$, $\alpha_c = 0.00045$, $\alpha_c = 0.0010575$, $\alpha_c = 0.0011925$, $\alpha_c = 0.0012825$.

Figure 4.3 shows the time evolution of (a) susceptible humans (S_H), (b) HIV/AIDS prevalence (I_H), (c) community viral load (V_H), for different values of the rate of transcription of the HIV-1 RNA to DNA α_c : $\alpha_c = 6e^{-5}$, $\alpha_c = 0.000158$, $\alpha_c = 0.000293$, $\alpha_c = 0.00045$, $\alpha_c = 0.0010575$, $\alpha_c = 0.0011925$, $\alpha_c = 0.0012825$. The numerical results also show that the three between-host scale variables (S_H , I_H , V_H) are sensitive to within-host scale parameter α_c . Therefore, the results also imply that as the average rate of transcription of the HIV-1 RNA to DNA increases, HIV/AIDS transmission in the community also increase. Therefore, antiretroviral drugs such as reverse transcriptors inhibitors which block transcription of the HIV-1 RNA to DNA in an infected individual have potential community level benefits of reducing HIV/AIDS transmission at between-host scale apart from benefits to the infected individual.

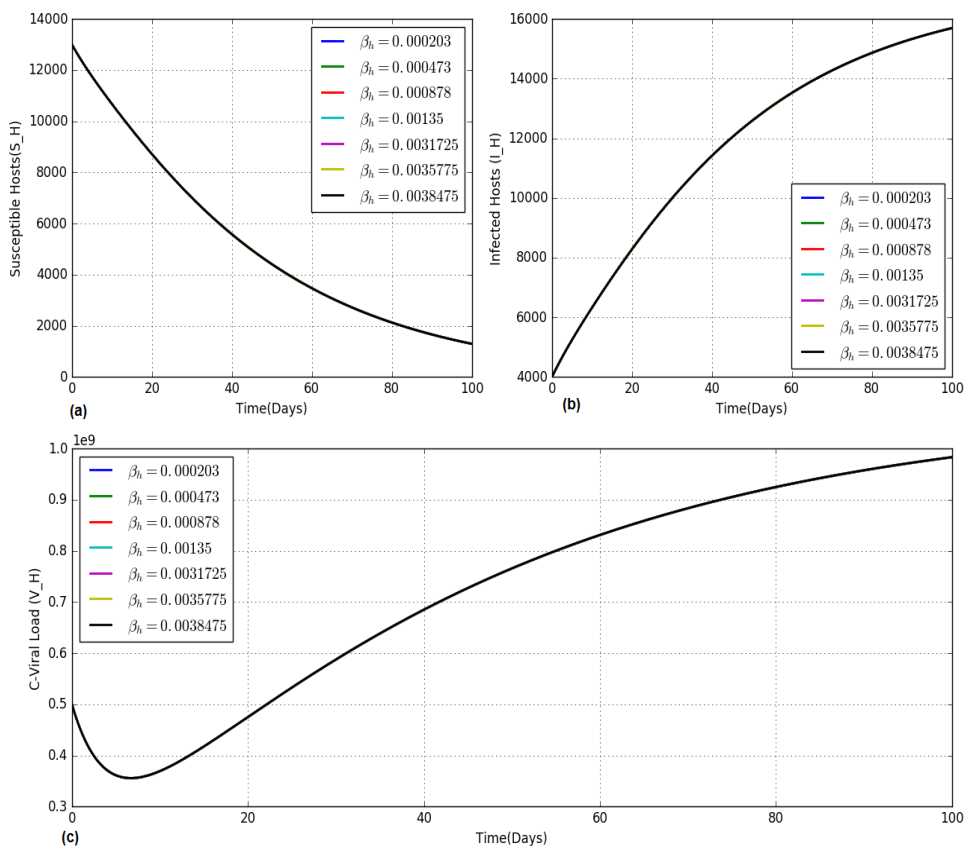


Figure 4.4: Effect of rate of virus entry into cytoplasm of CD4+ T cells (β_h) on (a) population of susceptible humans (S_H), (b) HIV/AIDS prevalence (I_H), (c) community viral load (V_H), for different values of β_h : $\beta_h = 0.000203$, $\beta_h = 0.000473$, $\beta_h = 0.000878$, $\beta_h = 0.00135$, $\beta_h = 0.0031725$, $\beta_h = 0.0035775$, $\beta_h = 0.0038475$.

Figure 4.4 shows changes in (a) population of susceptible humans (S_H), (b) HIV/AIDS prevalence (I_H), (c) community viral load (V_H), for different values of the rate of virus entry into the cytoplasm of CD4+ T cells β_h : $\beta_h = 0.000203$, $\beta_h = 0.000473$, $\beta_h = 0.000878$, $\beta_h = 0.00135$, $\beta_h = 0.0031725$, $\beta_h = 0.0035775$, $\beta_h = 0.0038475$. The numerical results show that the three between-host scale variables (S_H , I_H , V_H) have very low sensitivity to the within-host scale parameter β_h . These results are also in agreement with the results of the assessment of the sensitivity of endemic value of endemic value of community viral load and the effective reproductive in section 4.3.6 derived from the multiscale model system (4.17). Therefore, antiretroviral drugs such as fusion inhibitors which block virus entry into the cytoplasm of CD4+ T cells have minimal benefits at community level although they may have significant benefits individual level because \mathcal{R}_0 , the within-host scale basic reproductive number is highly sensitive to β_h as shown in section 4.3.6.

4.4 The Multiscale Model for HIV/AIDS Transmission with Combination Health Interventions

To ensure a comprehensive response to HIV/AIDS, many countries have adopted a number of intervention strategies such as TasP for STIs (Grosskurth et al., 1995; Kalichman et al., 2011; Hayes et al., 2010), male and female condoms (Mukandavire and Garira, 2007b; Ghys et al., 2002), HIV counseling and testing (Allen et al., 2003; Valdiserri, 1997), HIV/AIDS health education (Mukandavire and Garira, 2007a; Ford et al., 1996) use of safe injecting equipment, pre- and post- exposure prophylaxis, male circumcision (Auvert et al., 2005; Gray et al., 2007; Bailey et al., 2007; Mukandavire et al., 2007), TasP, law reform, community leadership, access to health services and political commitment (Vermund and Hayes, 2013; Brown et al., 2015; Brown et al., 2014; Blankenship et al., 2006; Gupta et al., 2008) with the most compelling goal of prevention of HIV infection which is crucial to the long-term goal of controlling and ultimately eliminating the HIV/AIDS pandemic. In this section we extend the baseline multiscale model developed in section 4.2 to incorporate HIV/AIDS combination interventions that include condom use, male circumcision and TasP composed of three drug classes (fusion inhibitors, protease inhibitors and reverse transcriptase inhibitors). In the context of the multiscale model given by (4.17) TasP is associated with the modification of the composite parameter N_h at within-host scale and the parameters δ_H and α_H at between-host scale since all these are directly modified as a result of TasP uptake, and male circumcision is associated with the modification of the susceptibility coefficient $\frac{1}{V_0}$, while condom use is directly associated with modification of β_H since these two parameters are also directly modified as a result of uptake of male circumcision and condom use as preventive interventions. We briefly describe the modifications to baseline multiscale model induced by these five interventions.

1. *TasP*: This is an intervention that is administered at within-host scale. In this study we consider that three categories of antiviral drugs are administered in TasP. These include fusion/entry inhibitors (FIs), which function by inhibiting viral entry into CD4 T cells (Briz et al., 2006; Moore and Doms, 2003; Moyle, 2003; Rockstroh and Mauss, 2004), and thereby by decreasing the infection rate β_h of CD4 T cells. They also include reverse transcriptase inhibitors (RTIs), which also function by inhibiting HIV RNA from being converted into DNA and thus blocking integration of the viral code into CD4 T cells (Adams et al., 2004), resulting in the modification of the parameter α_c . The third category of drugs includes protease inhibitors (PIs), whose mode of action involves preventing the assembly of key viral proteins after they have been produced by an infected cell thereby effectively reducing the number of infectious virus, N_v , produced by an infected cell. Therefore, administration of these three categories of anti-HIV-1 drugs results in the modification of the model parameters β_h , α_c and N_v which are part of the composite parameter N_h at within-host scale. Considering that fusion inhibitors (FIs) are administered, then rate of entry of virions into the cytoplasm of CD4+ T cells parameter β_h is modified to become $\beta_h(1 - \gamma)$, where γ is the efficacy of FIs and $0 < \gamma < 1$. The efficacy of FIs is defined as the probability with which FIs prevent entry of virions into the cytoplasm of CD4+ T cells. Now consider that reverse transcriptase inhibitors (RTIs) are administered. Then the rate of transcription of the HIV-1 RNA to DNA parameter α_c , is modified to become $\alpha_c(1 - \epsilon)$ where ϵ is the efficacy of RTIs and $0 < \epsilon < 1$. The efficacy of RTIs is also defined as the probability

with which RTIs abort reverse transcription of HIV-1 RNA to DNA and hence prevent successful infection of CD4+ T cells. If we also further assume that protease inhibitors (PIs) are administered, then the burst size parameter N_v is modified to become $N_v(1 - \kappa)$, where κ is the efficacy of PIs and $0 < \kappa < 1$. The efficacy of PIs is here defined as the probability with which they (PIs) render newly produced virions non-infectious. Therefore, the use of PIs will result in the production of non-infectious virus. Hence, while the multiscale model that incorporates the impact of TasP includes FIs, RTIs plus PIs does not explicitly include the five interacting populations which are: the uninfected CD4+ T cells (T_s , cells/mm³), infected CD4+ T cells where the virions have only entered the cytoplasm of the CD4+ T cells (T_i , cells/mm³), infected CD4+ T cell where transcription of the HIV-1 RNA to DNA has occurred (T_v , cells/mm³), infectious plasma viral load (V_h , copies/mm³) and non-infectious plasma viral load (V_n , copies/mm³) as expected from the within-host scale submodel (4.2), the antiviral drugs (RTIs, PIs and FIs) now only modify the composite parameter N_h in the simplified multiscale model (4.17) to become N_e where

$$N_e = \frac{\mu_s}{\beta_h(1 - \gamma)} \left[\frac{\beta_h(1 - \gamma)}{\alpha_h + \mu_h} \cdot \frac{\Lambda_s}{\mu_s} \cdot \frac{\alpha_c(1 - \epsilon)}{\alpha_c(1 - \epsilon) + \mu_c} \cdot \frac{N_v(1 - \kappa)\alpha_v}{\alpha_v + \mu_v} - 1 \right] = \frac{\mu_s}{\beta_h(1 - \gamma)} \left[\mathfrak{R}_e - 1 \right], \quad (4.70)$$

and

$$\mathfrak{R}_e = \frac{\beta_h(1 - \gamma)}{\alpha_h + \mu_h} \cdot \frac{\Lambda_s}{\mu_s} \cdot \frac{\alpha_c(1 - \epsilon)}{\alpha_c(1 - \epsilon) + \mu_c} \cdot \frac{N_v(1 - \kappa)\alpha_v}{\alpha_v + \mu_v}, \quad (4.71)$$

is the effective within-host scale reproductive number when TasP that includes FIs, RTIs plus PIs is used in a community. However, we note that the use of TasP which is applied and operating at within-host scale has other emergent properties whose effect manifest themselves at between-host scale through the parameters α_H and δ_H . Considering the approach in this study where we have derived the multiscale model for HIV/AIDS transmission dynamics (4.17) by considering the inside-host environmental scale of an infected human host as an ecosystem, then the suppression of community viral load at a rate α_H (i.e. host health) and host disease-induced death at a rate δ_H (i.e. host survival) are all metrics of emergent ecosystem properties owing to diverse impacts of HIV and CD4+ T cells on their host. Therefore, administration of the three categories of anti-HIV-1 drugs (FIs, RTIs and PIs) will have additional emergent effects at between-host scale which result in the modification of the multiscale model parameters δ_H and α_H . Considering that the three anti-HIV-1 drugs (FIs, RTIs and PIs) are administered at within-host scale, then rate of disease induced death rate parameter δ_H at between-host scale is modified to become $\delta_H(1 - \eta)$, where η is the efficacy of the emergent effect of TasP at community level owing to diverse impacts of these drugs on their host and $0 < \eta < 1$. The efficacy of the emergent effects of TasP in reducing disease induced death rate η , is defined as the probability with which TasP reduces disease induced death rate at community level. Further, assuming that the three anti-HIV-1 drugs (FIs, RTIs and PIs) are administered at within-host scale, then rate of community-wide suppression of the infectious reservoir of humans parameter α_H at between-host scale is modified to become $\alpha_H(1 + \varphi)$, where φ is the

4.4. The Multiscale Model for HIV/AIDS Transmission with Combination Health Interventions 99

efficacy of emergent effect of TasP at community level in increasing the reduction of community viral load owing to diverse impacts of these drugs on their host and $0 < \varphi < 1$. The efficacy of emergent effects of TasP in increasing community-wide elimination of viral load rate φ , is defined here as the probability with which TasP increases the rate of community-wide elimination of the infectious reservoir of humans $V_H(t)$.

- 2 *Male condom use*: Assuming male condoms are used in the community, then rate of contact with the community viral load parameter β_H is modified to become $\beta_H(1 - \sigma)$, where σ is the efficacy of male condoms and $0 < \sigma < 1$. The efficacy of condoms is defined as the probability with which male condoms prevent contact with the infectious reservoir of humans in the community.
- 3 *Male circumcision*: Assuming further, that male circumcision is also used as an HIV/AIDS preventive intervention, then the half saturation constant V_0 is modified to become $V_0(1 + \nu)$ where ν is the efficacy with which male circumcision reduces HIV infection susceptibility in the community and $0 < \nu < 1$. Overall, male circumcision and the use of male condoms in the community modify the force of infection $\lambda_H(t)$ in the simplified multiscale model (4.17) to become $\lambda_E(t)$ where

$$\lambda_E(t) = \frac{\beta_H(1 - \sigma)V_H(t)}{V_0(1 + \nu) + V_H(t)}. \quad (4.72)$$

Taking into all these modifications, the multiscale model that incorporates the effects of all the five HIV/AIDS interventions (TasP composed of three drug classes, condom use and male circumcision) becomes

$$\left\{ \begin{array}{l} 1. \frac{dS_H(t)}{dt} = \Lambda_H - \lambda_E(t)S_H(t) - \mu_H S_H(t), \\ 2. \frac{dI_H(t)}{dt} = \lambda_E(t)S_H(t) - [\mu_H + \delta_H(1 - \eta)]I_H(t), \\ 3. \frac{dV_H(t)}{dt} = N_e \alpha_h I_H(t) - \alpha_H(1 + \omega)I_H(t), \end{array} \right. \quad (4.73)$$

where,

$$\left\{ \begin{array}{l} \lambda_E = \frac{\beta_H(1 - \sigma)V_H}{V_0(1 + \nu) + V_H}, \\ N_e = \frac{\mu_s}{\beta_h(1 - \gamma)} \left[\frac{\beta_h(1 - \gamma)}{\alpha_h + \mu_h} \cdot \frac{\Lambda_s}{\mu_s} \cdot \frac{\alpha_c(1 - \epsilon)}{\alpha_c(1 - \epsilon) + \mu_c} \cdot \frac{N_v(1 - \kappa)\alpha_v}{\alpha_v + \mu_v} - 1 \right], \\ = \frac{\mu_s}{\beta_h(1 - \gamma)} [\mathfrak{R}_e - 1] = \frac{\mu_s}{\beta_h(1 - \gamma)} \cdot [(1 - \gamma)(1 - r_\epsilon)(1 - \kappa)\mathfrak{R}_0 - 1], \\ \mathfrak{R}_e = \frac{\beta_h(1 - \gamma)}{\alpha_h + \mu_h} \cdot \frac{\Lambda_s}{\mu_s} \cdot \frac{\alpha_c(1 - \epsilon)}{\alpha_c(1 - \epsilon) + \mu_c} \cdot \frac{N_v(1 - \kappa)\alpha_v}{\alpha_v + \mu_v} = (1 - \gamma)(1 - r_\epsilon)(1 - \kappa)\mathfrak{R}_0, \\ r_\epsilon = \frac{\epsilon\mu_c}{\alpha_c(1 - \epsilon) + \mu_c}. \end{array} \right. \quad (4.74)$$

SL. No.	Health Intervention	Mechanism of Intervention action	Modelling effect of intervention
1.	Treatment with FIs	Rate of virion entry into the cytoplasm of CD4+ T cells parameter β_h is reduced	$\beta_h \rightarrow \beta_h(1 - \gamma)$
2.	Treatment with PIs	Burst size parameter of infected CD4 T cells N_v is reduced	$N_v \rightarrow N_v(1 - \kappa)$
3.	Treatment with RTIs	Rate of transcription of the HIV-1 RNA to DNA parameter α_c is reduced	$\alpha_c \rightarrow \alpha_c(1 - \epsilon)$
4.	Condom use	Reduce contact rate β_H within community viral load	$\beta_H \rightarrow \beta_H(1 - \sigma)$
5.	male circumcision	Reduce susceptibility to HIV infection in the community by reducing the susceptibility coefficient $\frac{1}{V_0}$ and therefore increase V_0	$V_0 \rightarrow V_0(1 + \nu)$
6.	Overall TasP (RTIs, PIs, FIs)	Reduce disease induced death δ_H	$\delta_H \rightarrow \delta_H(1 - \eta)$
7.	Overall TasP (RTIs, PIs, FIs)	Increase rate of elimination of CVL α_H	$\alpha_H \rightarrow \alpha_H(1 + \varphi)$

Table 4.2: Summary of the action of health interventions on HIV/AIDS transmission dynamics.

A summary of the modifications of the multiscale model given by (4.17) due to effects of the five interventions is given in Table (4.2). In the following subsection, we analyse the multiscale model (4.73).

4.4.1 Analysis of the Multiscale Model With HIV/AIDS Combination Preventive Health Interventions

The equilibrium states of the multiscale model with HIV/AIDS preventive interventions are obtained by setting the right-hand side of multiscale model system (4.73) to zero. The disease-free equilibrium state of multiscale model system (4.73) is given by

$$\bar{E} = (\bar{S}_H, \bar{I}_H, \bar{V}_H) = \left(\frac{\Lambda_H}{\mu_H}, 0, 0 \right). \quad (4.75)$$

and an HIV preventive interventions induced endemic equilibrium state is given by

$$E = (S_H, I_H, V_H), \quad (4.76)$$

where

$$\left\{ \begin{array}{l} 1. S_H = \frac{\Lambda_H}{[\lambda_E + \mu_H]}, \\ 2. I_H = \frac{\lambda_E}{[\mu_H + \delta_H(1-\eta)]} \cdot \frac{\Lambda_H}{[\mu_H + \lambda_E]}, \\ 3. V_H = \frac{N_e \alpha_h I_H}{\alpha_H(1+\omega)}, \end{array} \right. \quad (4.77)$$

with λ_E and N_e defined in equation (4.74).

Therefore, we note from equation (4.77) that the use of the five HIV/AIDS preventive interventions (TasP composed of three drug classes which are fusion inhibitors, protease inhibitors and reverse transcriptase inhibitors, male condom use and male circumcision) have the following effects:

- ▶ The time of stay in the susceptible class when male circumcision and condom use are implemented given by $\frac{1}{[\lambda_E + \mu_H]}$, is greater than the time stay in the susceptible class in the counterfeit situation given by $\frac{1}{[\lambda_H + \mu_H]}$ when these two preventive interventions are not implemented. Therefore, use of male condoms and implementation of male circumcision reduces the number of new infections.
- ▶ The average life-span of the infected individuals increases from an average of $\frac{1}{[\mu_H + \delta_H]}$ when no TasP is implemented to an average of $\frac{1}{[\mu_H + \delta_H(1-\eta)]}$ when TasP is implemented.
- ▶ The community viral load is reduced since $N_e \alpha_h$, the rate at which infected individuals contribute to the community viral is reduced. This is because TasP reduces the amount of HIV in an infected individual from

$$N_h = \frac{\mu_s}{\beta_h} \left[\frac{\beta_h}{\alpha_h + \mu_h} \cdot \frac{\Lambda_s}{\mu_s} \cdot \frac{\alpha_c}{\alpha_c + \mu_c} \cdot \frac{N_v \alpha_v}{\alpha_v + \mu_v} - 1 \right], \quad (4.78)$$

when no TasP is implemented to a value of

$$N_e = \frac{\mu_s}{\beta_h(1-\gamma)} \left[\frac{\beta_h(1-\gamma)}{\alpha_h + \mu_h} \cdot \frac{\Lambda_s}{\mu_s} \cdot \frac{\alpha_c(1-\epsilon)}{\alpha_c(1-\epsilon) + \mu_c} \cdot \frac{N_v(1-\kappa)\alpha_v}{\alpha_v + \mu_v} - 1 \right], \quad (4.79)$$

when TasP is implemented.

- ▶ The time it takes for community-wide suppression of every infected individual's viral load in the community to below detection limit and render every HIV infected individual non-infectious $\frac{1}{\alpha_H}$ when no TasP is implemented to a value of $\frac{1}{\alpha_H(1+\omega)}$ when TasP is implemented.

Overall these five interventions (TasP composed of three drug classes, male condom use and male circumcision) have a preventive effect on severe disease, death and onward transmission of HIV/AIDS through reduced susceptibility to HIV infections (male circumcision), reduced contact with community viral load (male condom use), and reduced exposure to HIV (TasP) through reduction in community viral load.

Using the same method which was used to determine the basic reproductive number of the baseline multiscale model (4.17), it can be shown that the effective reproductive number of the modified multiscale model (4.73) is

$$\left\{ \begin{aligned} \mathcal{R}_E &= \frac{N_c \alpha_h \beta_H (1-\sigma) \Lambda_H}{\mu_H \alpha_H (1+\varphi) [\mu_H + \delta_H (1-\eta)] V_0 (1+\nu)}, \\ &= \frac{\mu_s (\mathfrak{R}_e - 1) \alpha_h \Lambda_H \beta_H (1-\sigma)}{\beta_h (1-\gamma) [\mu_H + \delta_H (1-\eta)] \mu_H \alpha_H (1+\varphi) V_0 (1+\nu)}, \\ &= \frac{\mu_s \left[(1-\gamma)(1-r_\epsilon)(1-\kappa) \mathfrak{R}_0 - 1 \right] \alpha_h \beta_H (1-\sigma) \Lambda_H}{\beta_h (1-\gamma) \left[\mu_H + \delta_H (1-\eta) \right] \mu_H \alpha_H (1+\varphi) V_0 (1+\nu)}, \end{aligned} \right. \quad (4.80)$$

where \mathfrak{R}_0 , \mathfrak{R}_e and r_ϵ have been previously defined.

Proving the existence of the intervention induced endemic equilibrium can easily be achieved by re-writing the endemic equilibrium value given by equation (4.77) in terms of parameters only to get

$$\left\{ \begin{aligned} S_H &= \frac{\Lambda_H \left[\beta_H (1-\sigma) + \mu_H \mathcal{R}_E \right]}{\mu_H \left[\mu_H + \beta_H (1-\sigma) \right] \mathcal{R}_E}, \\ I_H &= \frac{\Lambda_H \beta_H (1-\sigma) (\mathcal{R}_E - 1)}{\left[\mu_H + \delta_H (1-\eta) \right] \mathcal{R}_E \left[\mu_H + \beta_H (1-\sigma) \right]}, \\ V_H &= \frac{\mu_H V_0 (1+\nu) (\mathcal{R}_E - 1)}{\left[\mu_H + \beta_H (1-\sigma) \right]}. \end{aligned} \right. \quad (4.81)$$

From which we deduce that only a single positive endemic equilibrium point exists for $\mathcal{R}_E > 1$ and whenever $\mathfrak{R}_e > 1$. Therefore, we conclude that there exists only one unique endemic equilibrium point for model system (4.73) given by equation (4.50) for $\mathcal{R}_E > 1$ and whenever $\mathfrak{R}_e > 1$.

4.4.2 Assessing the comparative effectiveness of HIV/AIDS Combination Preventive interventions

In this subsection, we present results for the assessment of the comparative effectiveness of the five HIV/AIDS preventive interventions which include the three drug classes associated with TasP (PIs, FIs and RTIs), condom use and male circumcision using indicators of intervention effectiveness derived from the multiscale model with combination interventions given by (4.73). The three indicators of the effectiveness of the five HIV/AIDS health interventions are: (a) the effective reproductive number (\mathcal{R}_E), (b) the intervention induced endemic value of community viral load (V_H), and (c) the intervention induced endemic value of HIV/AIDS prevalence (I_H). For easy reference these indicators of the effectiveness of the HIV/AIDS preventive interventions which we refer to in this study as indicators of intervention effectiveness are given by

$$\left\{ \begin{array}{l} 1. \mathcal{R}_E = \frac{\mu_s \left[(1-\gamma)(1-r_e)(1-\kappa)\mathfrak{R}_0 - 1 \right] \alpha_h \beta_H (1-\sigma) \Lambda_H}{\beta_h (1-\gamma) \left[\mu_H + \delta_H (1-\eta) \right] \mu_H \alpha_H (1+\varphi) V_0 (1+\nu)}, \\ 2. V_H = \frac{\mu_H V_0 (1+\nu) (\mathcal{R}_E - 1)}{\left[\mu_H + \beta_H (1-\sigma) \right]}, \\ 3. I_H = \frac{\Lambda_H \beta_H (1-\sigma) (\mathcal{R}_E - 1)}{\left[\mu_H + \delta_H (1-\eta) \right] \mathcal{R}_E \left[\mu_H + \beta_H (1-\sigma) \right]}. \end{array} \right. \quad (4.82)$$

We use these quantities as indicators of intervention effectiveness to relate individual level efficacy to population/community level relative effectiveness of the five HIV/AIDS preventive interventions and some combination interventions derived from their use. In using these three quantities that characterize HIV/AIDS transmission dynamics at community level as indicators of intervention effectiveness, we assume that high values of these indicators of intervention effectiveness indicate the possibility of high transmission of HIV/AIDS in the community and that low values of these indicators of intervention effectiveness also indicate the possibility of low transmission of HIV/AIDS in the community. Tables (4.4), (4.5) and (4.6) show the results of the assessment of the comparative effectiveness of the five HIV/AIDS preventive interventions corresponding to efficacy values 0.3, 0.6 and 0.9 for each of the three indicators of intervention effectiveness (\mathcal{R}_E , V_H and I_H). Since we considered 14 different combinations of the 5 interventions, the comparative effectiveness of these interventions is measured on a scale from 1 to 14 with 1 denoting the lowest comparative effectiveness while 14 denotes the highest comparative effectiveness. Tables (4.3) shows the key to the interpretation of the results of the assessment of the comparative effectiveness of the five HIV/AIDS interventions and the resulting combination interventions given in Tables (4.4), (4.5) and (4.6). In what follows we discuss the results of the assessment of the comparative effectiveness of five HIV/AIDS interventions when each of the three indicators of intervention effectiveness is used (\mathcal{R}_E , V_H and I_H) separately.

No.	Key	Description/Meaning	Value/Range of Values
1.	Calculated V_H -L-eff	Calculated intervention induced endemic value of community viral load at low efficacy	Variable
2.	Calculated V_H -M-eff	Calculated intervention induced endemic value of community viral load at medium efficacy	Variable
3.	Calculated V_H -H-eff	Calculated intervention induced endemic value of community viral load at high efficacy	Variable
4.	Calculated \mathcal{R}_E -L-eff	Calculated intervention induced effective reproductive number value at low efficacy	Variable
5.	Calculated \mathcal{R}_E -M-eff	Calculated intervention induced effective reproductive number value at medium efficacy	Variable
6.	Calculated \mathcal{R}_E -H-eff	Calculated intervention induced effective reproductive number value at high efficacy	Variable
7.	Calculated I_H -L-eff	Calculated intervention induced endemic value of HIV prevalence at low efficacy	Variable
8.	Calculated I_H -M-eff	Calculated intervention induced endemic value of HIV prevalence at medium efficacy	Variable
9.	Calculated I_H -H-eff	Calculated intervention induced endemic value of HIV prevalence at high efficacy	Variable
10.	CEL	Comparative effectiveness at low efficacy	1-14
11.	CEM	Comparative effectiveness at medium efficacy	1-14
12.	CEH	Comparative effectiveness at high efficacy	1-14
13.	L-eff	Low efficacy value ($\gamma = \epsilon = \kappa = \sigma = \nu$)	0.30
14.	M-eff	Medium efficacy value ($\gamma = \epsilon = \kappa = \sigma = \nu$)	0.60
15.	H-eff	High efficacy value ($\gamma = \epsilon = \kappa = \sigma = \nu$)	0.90
16.	η, φ	Efficacy of emergent effects	Variable (0-1)

Table 4.3: Key for interpretation of the symbols used in the the description of results of the assessment of comparative effectiveness of HIV/AIDS interventions in Tables (4.4), (4.5) and (4.6) as well as the numerical values/ranges of values used in the calculations

1. Comparative effectiveness of the interventions using the effectiveness reproductive number as the indicator of intervention effectiveness.

No.	Indicator of Intervention effectiveness	Calculated \mathcal{R}_E -L-eff	CEL	Calculated \mathcal{R}_E -M-eff	CEM	Calculated \mathcal{R}_E -H-eff	CEH
1.	Basic reproductive number (R_0)	20,159.51	1	20,159.51	1	20,159.51	1
2.	FIs induced reproductive number (\mathcal{R}_{E_γ})	20,109.99	2	19,981.02	2	19,868.89	2
3.	RTIs induced reproductive number (\mathcal{R}_{E_c})	14,170.55	4	8,099.37	4	2,027.07	4
4.	PIs induced reproductive number (\mathcal{R}_{E_k})	14,076.99	7	7,992.41	7	1,986.89	7
5.	Condom Use induced reproductive number (\mathcal{R}_{E_σ})	14,111.66	6	8,063.80	6	2,015.95	5
6.	Male Circumcision induced reproductive number (\mathcal{R}_{E_v})	15,507.32	3	12,599.70	3	10,610.27	3
7.	FIs and RTIs induced reproductive number ($\mathcal{R}_{E_{\gamma c}}$)	14,137.71	5	8,082.11	5	2,008.62	6
8.	FIs and PIs induced reproductive number ($\mathcal{R}_{E_{\gamma k}}$)	14,044.36	8	7,975.35	8	1,968.50	8
9.	RTIs and PIs induced reproductive number ($\mathcal{R}_{E_{k c}}$)	9,896.39	10	3,232.85	10	200.86	10
10.	Condom use and male circumcision induced reproductive number ($\mathcal{R}_{E_{\sigma v}}$)	10,855.12	9	5,039.88	9	1,061.03	9
11.	HAART induced reproductive number ($\mathcal{R}_{E_{\gamma c k}}$)	9,874.75	11	3,224.87	11	184.94	11
12.	HAART and condom use induced reproductive number ($\mathcal{R}_{E_{\gamma c \sigma v}}$)	6,912.33	13	1,289.95	13	18.49	13
13.	HAART and male circumcision induced reproductive number ($\mathcal{R}_{E_{\gamma c k v}}$)	7,595.96	12	2,015.55	12	97.34	12
14.	HAART, condom use and male circumcision induced reproductive number ($\mathcal{R}_{E_{\gamma c k \sigma v}}$)	5,317.17	14	806.22	14	9.73	14

Table 4.4: Results of the assessment of comparative effectiveness of HIV/AIDS interventions using the effective reproductive number (\mathcal{R}_E) as the indicator of intervention effectiveness when each of the five interventions is assumed to have: (a) low efficacy of 0.30, (b) medium efficacy of 0.60, and (c) high efficacy of 0.90.

Table (4.4) shows the results of the assessment of the comparative effectiveness of the 14 different HIV/AIDS interventions obtained using \mathcal{R}_E as the indicator of intervention effectiveness. From Table (4.4), we deduce the following

results regarding comparative effectiveness of the 14 different interventions considered:

- a. From the single HIV/AIDS interventions comprising of monotherapy associated with TasP's three drug classes (PIs, FIs and RTIs), condom use and male circumcision, we note that PIs have the highest comparative effectiveness for all efficacy levels (0.3, 0.6 and 0.9) followed by condom use, then RTIs, followed by male circumcision with FIs having the lowest comparative effectiveness. This is because, from the values of the effective reproductive numbers in Table (4.4) we notice that $\mathcal{R}_{E_\kappa} < \mathcal{R}_{E_\sigma} < \mathcal{R}_{E_\epsilon} < \mathcal{R}_{E_\nu} < \mathcal{R}_{E_\gamma}$. Further, we note the following regarding the drug and non-drug HIV/AIDS interventions.
 - i. Among the three drug classes when used as monotherapy, PIs have the highest comparative effectiveness, with RTIs having the second highest comparative effectiveness while FIs have the lowest comparative since $\mathcal{R}_{E_\kappa} < \mathcal{R}_{E_\epsilon} < \mathcal{R}_{E_\gamma}$. These results are in agreement with the results obtained from sensitivity analysis where it was shown that \mathcal{R}_0 is most sensitive to viral burst size of infected CD4+ T cells parameter N_v (modified by PIs), followed by the rate of transcription of HIV-1 RNA to DNA parameter α_c (modified by RTIs), with \mathcal{R}_0 being least sensitive to rate of virus entry into cytoplasm of CD4+ T cells parameter β_h (modified by FIs).
 - ii. However, when the effectiveness of these three drugs is evaluated using the within-host scale effective reproductive number (\mathfrak{R}_e) as an indicator treatment effectiveness, FIs which were shown to have the lowest comparative effectiveness when using the therapy induced reproductive (\mathcal{R}_E) as the indicator of treatment effectiveness turn out to have the same effectiveness as PIs (see results in (Magombedze et al., 2008)). These results are also in agreement with those obtained from the sensitivity analysis of \mathfrak{R}_0 in this study where it was shown in subsection (4.3.6) that \mathfrak{R}_0 has the same sensitivity to N_v and β_h . These results imply that the effectiveness of an intervention evaluated at one scale may not necessarily be the same as its effectiveness at a different scale for the same efficacy value.
 - iii. When comparing condom use and male circumcision, the results indicate that condom use has a higher comparative effectiveness than male circumcision since $\mathcal{R}_{E_\sigma} < \mathcal{R}_{E_\nu}$.
 - iv. However, since male circumcision and pre-exposure prophylaxis have a similar mechanism (i.e. they both modify the same parameter V_0) in that they both reduce susceptibility to HIV/AIDS infection (unlike condoms which reduce contact with viral load), we expect that if the two interventions are assumed to have the same efficacy, male circumcision and pre-exposure prophylaxis will have the same comparative effectiveness. Since this study has established that condom use has a higher comparative effectiveness than male circumcision, we expect that for the same efficacy, condom use will have a higher comparative effectiveness than pre-exposure prophylaxis. This expectation is supported by results obtained in Mukandavire et al., 2016.
- b. We also considered the comparative effectiveness of these five interventions when they are implemented in combinations of two at a time. We

only considered four combination interventions which are FIs and RTIs, RTIs and PIs, PIs and FIs and condom use and male circumcision. From Table (4.4) we deduce that:

- i. The combination of PIs and RTIs has the highest comparative effectiveness, followed by the combination of condom use and male circumcision, while the comparative effectiveness FIs and PIs ranks third, with the comparative effectiveness of a combination FIs and RTIs ranking least since $\mathcal{R}_{E_{\kappa\epsilon}} < \mathcal{R}_{E_{\sigma v}} < \mathcal{R}_{E_{\kappa\gamma}} < \mathcal{R}_{E_{\gamma\epsilon}}$.
- ii. A very useful observation in terms of HIV/AIDS prevention and treatment policy from the results of the assessment of the comparative effectiveness of a combination of two drugs at a time is that the comparative effectiveness of PIs alone is higher than the comparative effectiveness of a combination of FIs and RTIs since $\mathcal{R}_{E_{\kappa}} < \mathcal{R}_{E_{\epsilon\gamma}}$ when each of the three drugs is assumed to have the same efficacy level.
- c. For a combination of three interventions, we only considered TasP with the three drug classes (FIs, PIs and RTIs) associated with HAART. The results from Table (4.4) show that HAART has a higher comparative effectiveness than any of the interventions comprising a combination of any two of them.
- d. For a combination of 4 interventions at a time, we considered only two scenarios which are HAART with condom use and HAART with male circumcision. The results show that HAART with condom use has a higher comparative effectiveness than HAART with male circumcision since $\mathcal{R}_{E_{\gamma\epsilon\kappa\sigma}} < \mathcal{R}_{E_{\gamma\epsilon\kappa v}}$.
- e. Lastly, we considered the comparative effectiveness of the HIV/AIDS interventions when all the five of them are implemented together. The results show that this combination has the highest comparative effectiveness than any of the other combination interventions considered in this study for the assumed efficacy levels.

We note that the main limitation of using \mathcal{R}_E as an indicator of intervention effectiveness is that it characterizes transmission of a disease at the start of the epidemic and therefore, the results of comparative effectiveness of HIV/AIDS interventions using \mathcal{R}_E as an indicator of intervention effectiveness may be of limited use when the disease is at endemic levels. In what follows we assess the comparative effectiveness of the five HIV/AIDS health interventions using the intervention induced endemic value of community viral load as an indicator of intervention effectiveness. This proposed indicator of intervention effectiveness characterizes the transmission of a disease when it is endemic in the community.

2. Comparative effectiveness of the interventions using the intervention induced endemic value of community viral load as the indicator of intervention effectiveness.

No.	Indicator of Intervention Effectiveness	Calculated V_H -L-eff	CEL	Calculated V_H -M-eff	CEM	Calculated V_H -H-eff	CEH
1.	Baseline endemic value of CVL (V_H)	268,762,245.49	1	268,762,245.49	1	268,762,245.49	1
2.	FIs induced endemic value of CVL ($V_{H\gamma}$)	268,101,947.56	5	266,382,547.44	5	264,887,505.57	5
3.	RTIs induced endemic value of CVL ($V_{H\epsilon}$)	188,914,721.35	6	107,971,039.03	6	27,012,441.82	6
4.	PIs induced endemic value of CVL ($V_{H\kappa}$)	187,667,363.56	8	106,545,019.51	8	26,476,751.36	8
5.	Condom use induced endemic value of CVL ($V_{H\sigma}$)	268,748,853.56	3	268,715,377.08	3	268,481,175.52	3
6.	Male circumcision induced endemic value of CVL ($V_{H\nu}$)	268,758,245.76	2	268,754,246.02	2	268,750,246.29	2
7.	FIs and RTIs induced endemic value of CVL ($V_{H\gamma\epsilon}$)	188,476,849.65	7	107,740,997.44	7	26,766,533.36	7
8.	FIs and PIs induced endemic value of CVL ($V_{H\gamma\kappa}$)	187,232,316.33	9	106,317,553.04	9	26,231,568.44	9
9.	RTIs and PIs induced endemic value of CVL ($V_{H\kappa\epsilon}$)	131,929,795.02	10	43,088,399.51	10	2,664,654.14	10
10.	Condom use and male circumcision induced endemic value of CVL ($V_{H\sigma\nu}$)	268,743,139.82	4	268,695,380.41	4	268,361,255.47	4
11.	HAART induced endemic value of CVL ($V_{H\gamma\epsilon\kappa}$)	131,641,266.71	11	42,982,097.32	11	2,452,374.46	11
12.	HAART and condoms induced endemic value of CVL ($V_{H\gamma\epsilon\kappa\sigma}$)	131,631,792.15	13	42,957,803.16	13	2,330,983.96	13
13.	HAART and male circumcision induced endemic value of CVL ($V_{H\gamma\epsilon\kappa\nu}$)	131,637,266.98	12	42,974,097.85	12	2,440,375.26	12
14.	HAART, condom use and male circumcision induced endemic value of CVL ($V_{H\gamma\epsilon\kappa\sigma\nu}$)	131,626,078.41	14	42,937,806.49	14	2,211,063.91	14

Table 4.5: Results of the assessment of comparative effectiveness of HIV/AIDS interventions using the intervention induced endemic value of community viral load (V_H) as the indicator intervention effectiveness when each of the five interventions is assumed to have: (a) low efficacy of 0.30, (b) medium efficacy of 0.60, and (c) high efficacy of 0.90.

Table (4.5) shows the results of the assessment of the comparative effectiveness of the 14 different HIV/AIDS interventions obtained using the intervention induced endemic value of community viral load, V_H , as the indicator of intervention effectiveness. From Table (4.5), we deduce the following results regarding the comparative effectiveness of the 14 different HIV/AIDS interventions considered:

- a. From the single HIV/AIDS interventions comprising of monotherapy associated with TasP's three drug classes (PIs, FIs and RTIs), condom use and male circumcision, we note that PIs still have the highest comparative effectiveness for all efficacy levels (0.3, 0.6 and 0.9) as in the case when we use \mathcal{R}_E as the indicator of intervention effectiveness. However, unlike in the case of using the effective reproductive number as an indicator of intervention effectiveness where condom use had the second highest comparative effectiveness, in this case, RTIs have the second highest comparative effectiveness, followed by FIs with the third highest comparative effectiveness, while the comparative effectiveness of condom use ranks fourth with male circumcision having the lowest comparative effectiveness. This is because from Table (4.5) we notice that $V_{H\kappa} < V_{H\epsilon} < V_{H\gamma} < V_{H\sigma} < V_{H\nu}$. These results imply that condom use and male circumcision would have a much higher impact in the curbing HIV/AIDS transmission at the start of the epidemic than would be the case when the disease is endemic in the community. However, the opposite is true for the three drug classes. Further, we also note the following regarding the drug and non-drug HIV/AIDS interventions.
 - i. Among the three drugs when used as monotherapy, we obtain similar ranking of the comparative effectiveness of these three drugs as those obtained when using the effective reproductive number as the indicator of the intervention effectiveness of the three drug classes in which PIs have the highest comparative effectiveness, with RTIs having the second highest comparative effectiveness while FIs have the lowest comparative effectiveness since $V_{H\kappa} < V_{H\epsilon} < V_{H\gamma}$. These results are also in agreement with the results obtained from sensitivity analysis where it was shown that V_H is most sensitive to viral burst size of infected CD4+ T cells parameter N_v (modified by PIs), followed by the rate of transcription of HIV-1 RNA to DNA parameter α_c (modified by RTIs), with V_H being least sensitive to rate of virus entry into cytoplasm of CD4+ T cells parameter β_h (modified by FIs).
 - ii. Further, although we did not use the within-host scale endemic viral load value (V_h) to evaluate the effectiveness of the three drug classes, we note that from the results of sensitivity analysis that V_h has different sensitivity to N_v (which is high and close to 1) and β_h (which is low and close to 0). When using \mathcal{R}_e to evaluate the comparative effectiveness of the three drug classes in (Magombedze et al., 2008), the results show that FIs and PIs have the same higher effectiveness at this scale than RTIs because $\mathcal{R}_e > (\mathcal{R}_\gamma = \mathcal{R}_\kappa)$. However, from the assessment of the sensitivity of V_h in subsection 4.3.6, V_h has highest sensitivity to N_v (modified by PIs), followed by α_c (modified by RTIs) while V_h is least sensitive to β_h (modified). We expect from these results of sensitivity analysis that $V_{h\kappa} < V_{h\epsilon} < V_{h\gamma}$. These results imply that for double therapy, a combination of PIs and FIs would be

the best for pre- and post-exposure prophylaxis, while RTIs and PIs would be the best combination for treatment in the chronic phase of HIV infection at within-host scale. These results further highlight the importance of scale when assessing the comparative effectiveness of health interventions.

- iii. When comparing condom use and male circumcision, the results are similar to those obtained using the effective reproductive as the indicator of intervention effectiveness in which condom use has a higher comparative effectiveness than male circumcision since $V_{H\sigma} < V_{H\nu}$.
 - iv. Therefore, we arrive at the same conclusion that since male circumcision and pre-exposure prophylaxis have a similar mechanism action (i.e. they modify the same parameter V_0) in that they both reduce susceptibility to HIV/AIDS infection (unlike condoms which reduce contact with viral load), we expect that for the two interventions (male circumcision and pre-exposure prophylaxis) would for the same efficacy, have the same comparative effectiveness. Since this study has established that condom use has a higher comparative effectiveness than male circumcision, we expect that for the same efficacy, condom use would have a higher comparative effectiveness than pre-exposure prophylaxis. This expectation is supported by results obtained in (Mukandavire et al., 2016).
- b. We also assessed the comparative effectiveness of these five interventions when they are implemented in combinations of two at a time using the intervention induced endemic value of community viral load as the indicator of intervention effectiveness. We only considered four combination interventions which are FIs and RTIs, RTIs and PIs, PIs and FIs and condom use and male circumcision. From Table (4.5) we deduce that:
- i. The combination of PIs and RTIs has the highest comparative effectiveness, followed by the combination of FIs and PIs while the comparative effectiveness of FIs and RTIs ranks third, with the comparative effectiveness of the combination of condom use and male circumcision ranking least.
 - ii. Another very useful observation in terms of HIV/AIDS prevention and treatment policy from the results of the assessment of the comparative effectiveness of a combination of two interventions at a time when using the intervention induced endemic value of community viral load as an indicator of intervention effectiveness is that the comparative effectiveness of PIs alone is higher than the comparative effectiveness of a combination of FIs and RTIs since $V_{H\kappa} < V_{H\epsilon\gamma}$ when each of the three drugs is assumed to have the same efficacy level. Further, the comparative effectiveness of PIs alone is also higher than the comparative effectiveness of a combination of condom use and male circumcision since $V_{H\kappa} < V_{H\sigma\nu}$ when each of the three interventions is assumed to have the same efficacy level.
- c. For a combination of three interventions, we only considered TasP with three drug classes (FIs, PIs and RTIs) associated with HAART. The results from Table (4.4) show that HAART has a higher comparative effectiveness than any of the interventions comprising a combination of any two of them.

- d. For a combination of 4 interventions at a time, we considered only two scenarios which are HAART with condom use and HAART with male circumcision. The results from Table (4.5) show that HAART with condom use has a higher comparative effectiveness than HAART with male circumcision since $V_{H\gamma\epsilon\kappa\sigma} < V_{H\gamma\epsilon\kappa\nu}$. These results are similar to those obtained using the effective reproductive number as the indicator of intervention effectiveness.
- e. Lastly, we considered the comparative effectiveness of the HIV/AIDS interventions when all the five of them are implemented together. The results also show that this combination has the highest comparative effectiveness than any of the other combination interventions for the assumed efficacy levels.

We note that the intervention induced endemic value of community viral load (V_H) characterizes HIV/AIDS transmission when the disease is at endemic levels in the community. This is unlike the effective reproductive number (\mathcal{R}_E) which characterizes transmission of a disease at the start of the epidemic. We, therefore, conclude that the assessment of the comparative effectiveness of HIV/AIDS interventions using the intervention induced endemic value of community viral load as the indicator of intervention effectiveness has more relevancy to HIV/AIDS prevention and treatment policy than those obtained using the effective reproductive number as the indicator of intervention effectiveness. Our study also sought to establish the relevance of using the intervention induced endemic value of prevalence (I_H) as an indicator of intervention effectiveness at the community level for HIV/AIDS transmission dynamics. The results are presented in Table 4.6.

3. *Comparative effectiveness of the interventions using the intervention induced endemic value of HIV/AIDS prevalence as the indicator of intervention effectiveness.*

No.	Indicator of Intervention Effectiveness	Calculated I_H -L-eff	CEL	Calculated I_H -M-eff	CEM	Calculated I_H -H-eff	CEH
1.	Baseline endemic value of Prevalence (I_H)	4,249.51	11	4,249.51	11	4,249.51	10
2.	FIs induced endemic value of HIV prevalence ($I_{H\gamma}$)	4,281.62	8	4,380.93	8	4,484.96	6
3.	RTIs induced endemic value of HIV prevalence ($I_{H\epsilon}$)	4,281.53	9	4,380.61	9	4,482.98	7
4.	PIs induced endemic value of HIV prevalence ($I_{H\kappa}$)	4,281.53	10	4,380.60	10	4,482.93	8
5.	Condom use induced endemic value of HIV prevalence ($I_{H\sigma}$)	4,249.29	13	4,248.76	13	4,245.06	12
6.	Male circumcision induced endemic value of HIV prevalence ($I_{H\nu}$)	4,249.44	12	4,249.38	12	4,249.32	11
7.	FIs and RTIs induced endemic value of HIV prevalence ($I_{H\gamma\epsilon}$)	4,314.13	5	4,414.74	5	4,518.72	2
8.	FIs and PIs induced endemic value of HIV prevalence ($I_{H\gamma\kappa}$)	4,314.13	6	4,414.74	6	4,518.68	3
9.	RTIs and PIs induced endemic value of HIV prevalence ($I_{H\kappa\epsilon}$)	4,314.00	7	4,413.92	7	4,498.47	5
10.	Condom use and male circumcision induced endemic value of HIV prevalence ($I_{H\sigma\nu}$)	4,249.20	14	4,248.45	14	4,243.17	13
11.	HAART induced endemic value of HIV prevalence ($I_{H\gamma\epsilon\kappa}$)	4,347.10	1	4,448.59	1	4,532.69	1
12.	HAART and condom use induced endemic value of HIV prevalence ($I_{H\gamma\epsilon\kappa\sigma}$)	4,346.78	3	4,446.07	3	4,308.33	9
13.	HAART and male circumcision induced endemic value of HIV prevalence ($I_{H\gamma\epsilon\kappa\nu}$)	4,346.96	2	4,447.76	2	4,510.52	4
14.	HAART, condom use and male circumcision induced endemic value of HIV ($I_{H\gamma\epsilon\kappa\sigma\nu}$) prevalence	4,346.59	4	4,444.00	4	4,086.68	14

Table 4.6: Results of the assessment of comparative effectiveness of HIV/AIDS interventions using the intervention induced endemic value of HIV/AIDS prevalence (I_H) as the population level indicator of intervention effectiveness when each of the five interventions is assumed to have: (a) low efficacy of 0.30, (b) medium efficacy of 0.60, and (c) high efficacy of 0.90.

Table 4.6 shows the results of the assessment of the comparative effectiveness of HIV/AIDS interventions using the intervention induced HIV/AIDS prevalence endemic value (I_H) as the population level indicator of intervention effectiveness when each of the five interventions is assumed to have: (a) low efficacy of 0.30, (b) medium efficacy of 0.60, and (c) high efficacy of 0.90. The results in Table 4.6 all serve to confirm that prevalence is an unreliable measure of HIV/AIDS transmission dynamics and is of limited use as an indicator of the effectiveness of HIV/AIDS health interventions.

- a. From the 14 single and combination HIV/AIDS interventions we notice from Table 4.6 HAART has the lowest comparative effectiveness. More surprising is that HAART has a lower comparative effectiveness than that of the counterfeit situation where there are no interventions (baseline transmission dynamics of HIV/AIDS). This contradicts studies that have clearly shown that HAART plays a significant role in controlling HIV transmission (Bezemer et al., 2010; Kato et al., 2013) compared to the counterfeit scenario without HAART. In addition, several other studies have also shown that the greater the coverage in the use of HAART, the greater the number of HIV infections averted and the lower the number of new HIV infections, incidences, and reproductive numbers (Dodd et al., 2010; Abbas et al., 2013; Cremin et al., 2013; Lima et al., 2008; Bärnighausen et al., 2012; Schwartländer et al., 2011). Therefore, the result that HAART has the lowest comparative effectiveness which is even lower than that of a counterfeit situation where there are no interventions can only be attributed to the fact that prevalence is an unreliable measure of transmission of HIV/AIDS and intervention effectiveness.
- b. The results from Table 4.6 also show that in general, for HAART, as efficacy increases, the comparative effectiveness of this combination therapy also decreases. This is also unrealistic because it establishes a positive correlation between HAART efficacy and HIV transmission. To date, several studies (Bezemer et al., 2010; Kato et al., 2013; Abbas et al., 2013; Velasco-Hernandez et al., 2002; Long et al., 2010; Xu et al., 2013) have established a negative correlation between HAART efficacy and HIV transmission. This further confirms that prevalence is an unreliable measure of transmission of HIV/AIDS and intervention effectiveness.
- c. Another result which also further confirms that prevalence is an unreliable measure of HIV/AIDS transmission is that for the 14 single and combination HIV/AIDS interventions given in Table 4.6, the results show that a combination of condom use and male circumcision has the highest comparative effectiveness. However, we also note from Table 4.6 that condom use alone and male circumcision alone has the second and third highest comparative effectiveness respectively. However, when each of these two interventions is implemented in combination with any of the three drug classes, the comparative effectiveness of such a combination decreases.

These observations regarding the assessment of the comparative effectiveness of HIV/AIDS interventions using prevalence as an indicator of intervention

effectiveness imply that the results obtained from modelling HIV/AIDS transmission dynamics using susceptible, exposed, infected, treated (SEIT) and variations of this paradigm which use prevalence as the metric for the community's level of infectiousness and transmission probability and as an indicator of intervention effectiveness are unreliable and of limited use in decision-making. We now summarize the results of the assessment of the comparative effectiveness of the HIV/AIDS interventions using all the three indicators of intervention effectiveness for each efficacy level.

4. Summary of results of assessment of comparative effectiveness of the interventions using all the three indicators of effectiveness at low efficacy.

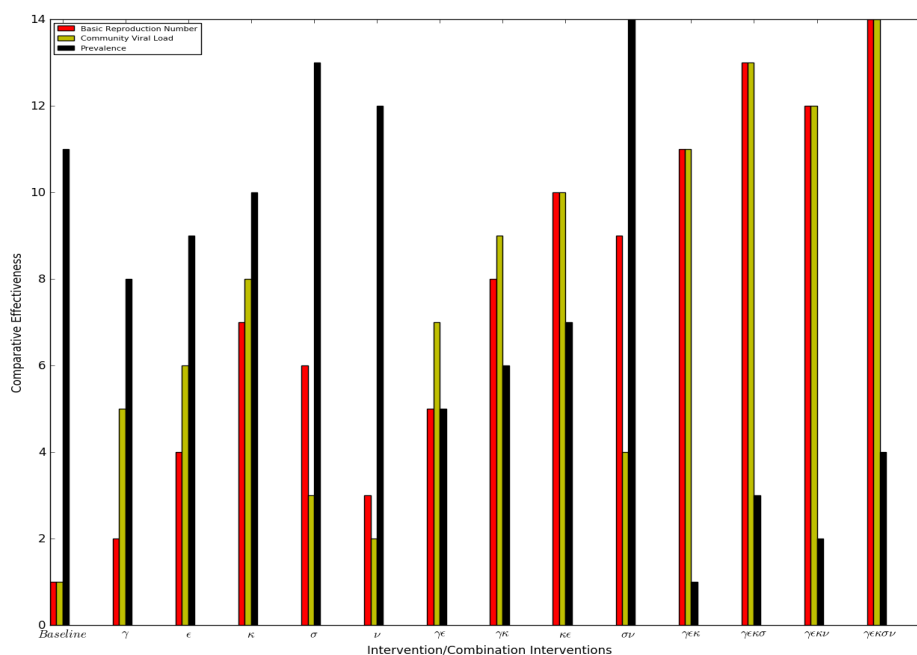


Figure 4.5: Histogram summarizing the results of the assessment of comparative effectiveness of HIV/AIDS interventions using the three different indicators of intervention effectiveness: (a) effective reproductive number (\mathcal{R}_E) - red colour, (b) intervention induced endemic value of community viral load (V_H) - gold colour, and (c) intervention induced HIV prevalence endemic value (I_H) - black colour, when each of the five different HIV/AIDS interventions is assumed to have a low efficacy of 0.30

Figure 4.5 summarizes the results of the assessment of the comparative effectiveness of the 14 different combination interventions when using all the three different indicators of intervention effectiveness: (a) effective reproductive number (\mathcal{R}_E) - red colour, (b) intervention induced endemic value of community viral load (V_H) - gold colour, and (c) intervention induced prevalence endemic value (I_H) - black colour, when each of the five different HIV/AIDS interventions is assumed to have a low efficacy of 0.30 using a histogram. The histogram shows that effective reproductive number and community viral load are the only realistic indicators of intervention effectiveness because they show that adding more interventions with demonstrated efficacy to existing efficacious interventions has additional benefits of improving the comparative

effectiveness of the combination intervention. This is unlike using prevalence as an indicator of intervention effectiveness which shows that adding more efficacious interventions to existing interventions with demonstrated efficacy may not yield any additional benefits or may even worsen the situation.

5. Summary of results of assessment of comparative effectiveness of the interventions using all the three indicators of effectiveness at medium efficacy.

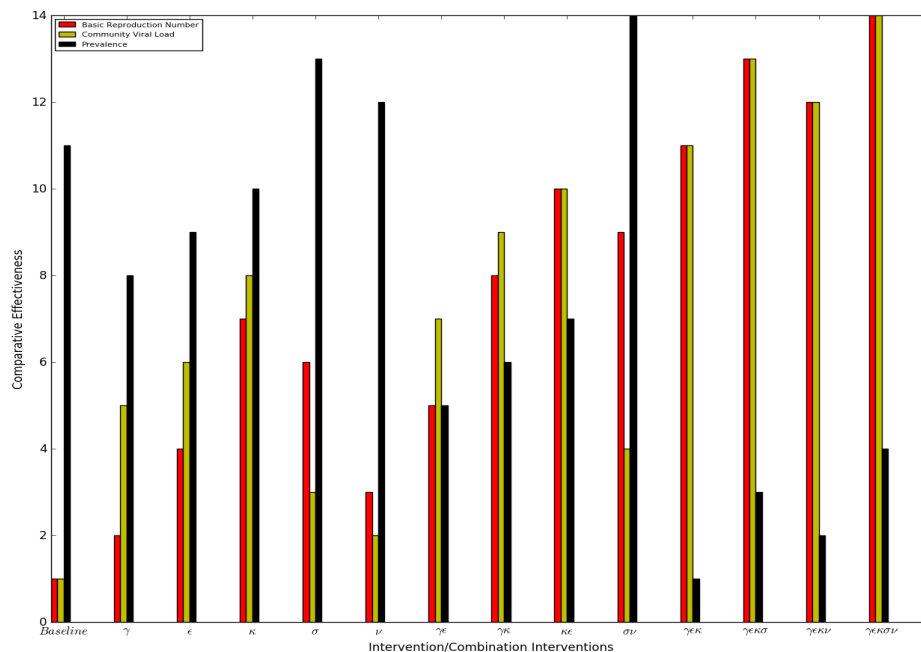


Figure 4.6: Histogram summarizing the results of the assessment of comparative effectiveness of HIV/AIDS interventions using the three different indicators of intervention effectiveness: (a) effective reproductive number (\mathcal{R}_E) - red colour, (b) intervention induced endemic value of community viral load (V_H) - gold colour, and (c) intervention induced HIV prevalence endemic value (I_H) - black colour, when each of the five different HIV/AIDS interventions is assumed to have a medium efficacy of 0.60

Figure 4.6 also summarizes the results of the assessment of the comparative effectiveness of the 14 different combination interventions when using all the three different indicators of intervention effectiveness: (a) effective reproductive number (\mathcal{R}_E) - red colour, (b) intervention induced endemic value of community viral load (V_H) - gold colour, and (c) intervention induced prevalence endemic value (I_H) - black colour, when each of the five different HIV/AIDS interventions is assumed to have an efficacy of 0.60 using a histogram. Like in Figure 4.5, the histogram shows that effective reproductive number and intervention induced endemic value of community viral load are the only realistic indicators of intervention effectiveness because they show that adding more interventions with demonstrated efficacy to existing efficacious interventions has additional benefits of improving the comparative effectiveness of the combination intervention. This is also unlike using prevalence as an indicator

of intervention effectiveness which shows that adding more efficacious interventions to existing interventions with demonstrated efficacy may not yield any additional benefits or may even worsen the situation.

6. Summary of results of assessment of comparative effectiveness of the interventions using all the three indicators of effectiveness at high efficacy.

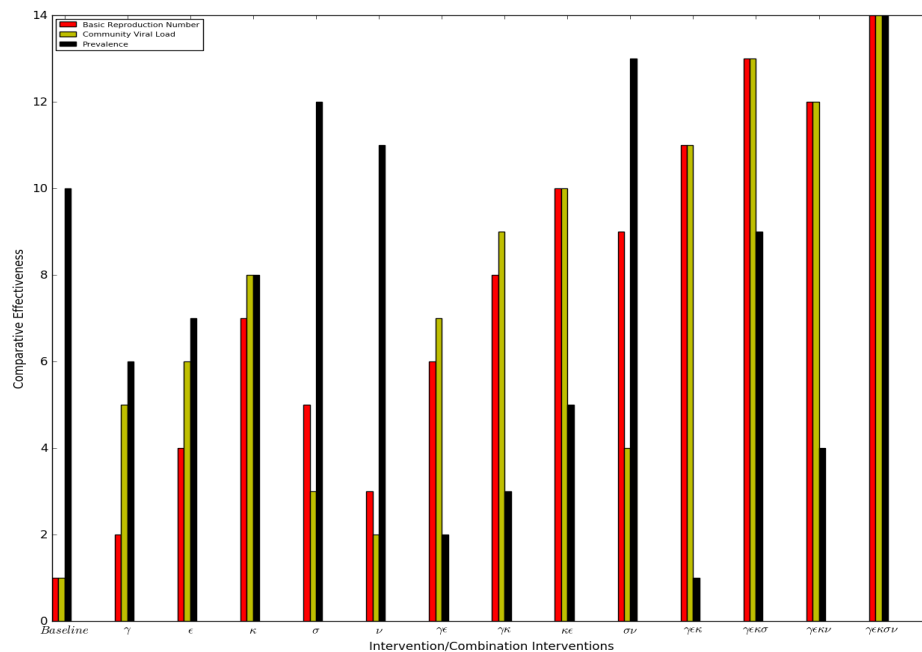


Figure 4.7: Histogram summarizing the results of the assessment of comparative effectiveness of HIV/AIDS interventions using the three different indicators of intervention effectiveness: (a) effective reproductive number (\mathcal{R}_E) - red colour, (b) intervention induced endemic value of community viral load (V_H) - gold colour, and (c) intervention induced HIV prevalence endemic value (I_H) - black colour, when each of the five different HIV/AIDS interventions is assumed to have a high efficacy of 0.90

Like in Figures 4.5 and 4.6, Figure 4.7 also summarizes the results of the assessment of the comparative effectiveness of the 14 different HIV/AIDS combination interventions when using all the three different indicators of intervention effectiveness: (a) effective reproductive number (\mathcal{R}_E) - red colour, (b) intervention induced endemic value of community viral load (V_H) - gold colour, and (c) intervention induced prevalence endemic value (I_H) - black colour, when each of the five different HIV/AIDS interventions is assumed to have an efficacy of 0.90 using a histogram. The histogram further confirms that prevalence is an unreliable indicator of intervention effectiveness which shows that adding more efficacious interventions to existing interventions with demonstrated efficacy may not yield any additional benefits or may even worsen the situation.

In summary, the main findings from the results of the assessment of the comparative effectiveness of the five HIV/AIDS preventive interventions and some of their possible combinations are that.

- ▶ For the assumed efficacy values the results show that PIs should be the mainstay of HAART.
- ▶ For the assumed efficacy values the results show that when implementing double therapy for treatment of HIV infected individuals a combination of FIs and PIs is more effective in pre-exposure prophylaxis than during the chronic phase of HIV infection while the opposite is true for a combination of PIs and RTIs.
- ▶ Condom use, male circumcision and pre-exposure prophylaxis are more effective in controlling the transmission dynamics of HIV/AIDS at the start of the epidemic than when the disease is endemic in the community while the opposite is true for TasP.
- ▶ In modelling HIV/AIDS transmission dynamics, community viral load (CVL) is a more reliable metric for the community's level of infectiousness and transmission probability and as well as an indicator of intervention effectiveness because (i) prevalence is not very informative, as the infectivity of individuals depend more on viral load than on whether one is infected or not; (ii) HIV incidence is difficult to measure directly; (iii) viral data is readily available or at least relatively easy to collect; and (iv) CVL combines information from both prevalence and impact of health interventions such as TasP and is potentially useful in predicting incidence.

However, we need to highlight that in the assessment of the various HIV/AIDS individual and combinations interventions, we could not use specific efficacy values for two reasons. First, efficacy values are normally given in terms of ranges with some of these ranges overlapping for different interventions. Secondly, for drug interventions, we only considered the comparative effectiveness for drug classes and yet efficacies are only available for specific drugs within each drug class. Overall, the results of comparative effectiveness of the various HIV/AIDS interventions and the associated combination interventions considered in this study are only useful in the context technical feasibility of control, or elimination or even eradication of HIV/AIDS in a particular community in which only the intensity of HIV/AIDS transmission is considered as the only factor that hinders successful control or elimination or even eradication of the epidemic. This is a limitation of our study and accordingly our results are preliminary. The modelling problem of considering comparative effectiveness in the context of operational feasibility of the successful control, elimination or even eradication of HIV/AIDS in which other aspects of effectiveness of an intervention such as coverage, cost-effectiveness, compliance, etc. are incorporated into the modelling is an interesting possible extension of the work in this paper which deserves careful attention and will be considered elsewhere.

4.5 Summary

In this Chapter, we presented a new method for developing a class of nested multiscale models of infectious disease systems that integrate within-host scale and between-host scale using community pathogen load (CPL) as the standard metric for the community's level of infectiousness and as an indicator of the effectiveness of health interventions. Three major steps were carried out in this chapter in developing the multiscale model for HIV/AIDS disease system. The first step in this approach is to define within-host and between-host submodels of the HIV/AIDS

disease system. The second step involved the integration of the two submodels into a single complete multiscale model. The third and final step involved to simplification of the multiscale model for the disease system using fast and slow time scale analysis. The result was a simple multiscale model which we then used to assess the comparative effectiveness of a combination of health interventions operating at different scale domains (within-host and between-host scale domains) of HIV/AIDS disease system. Most problems in using current model-based assessments of the comparative effectiveness of individual and combination interventions at community level using single scale models for population surveillance of infectious disease systems based on compartmentalizing hosts into susceptible, exposed, infected, recovered (SEIR), and variations of this paradigm (e.g. SI, SIS, SIR etc.) originate from scale mismatch between the scale at which a health intervention operates and the scale at which decisions on it are made. In this work, we successfully illustrated the utility of our multiscale modelling methodology by assessing the comparative effectiveness of HIV/AIDS preventive and treatment interventions.

Chapter 5

Discussion and Conclusions

The major contribution of this study to scientific knowledge is the development of a new nested multiscale modelling framework for HIV/AIDS disease system that can be used to assess the comparative effectiveness of health interventions with previously demonstrated efficacy for use with broader target populations or at a community level in anticipation of community-based randomized controlled trials. Multiscale modelling is central to characterizing the epidemiology of HIV/AIDS and infectious disease systems in general, developing new strategies for their control, informing disease management, identifying targets for new drugs and vaccines, and in turn evaluating the impact of these medical interventions. The proposed multiscale modelling approach uses community pathogen as a metric for the community's level of infectiousness and transmission probability as well as an indicator of intervention effectiveness. Obtaining measures of community pathogen load from a model provides a methodology that is cost-effective and can be used by public health officials to complement the use of empirical data which may, sometimes, not be readily available. CPL measurements can assist in monitoring and evaluating the implementation of health interventions and also provides an additional tool to assess the burden of disease at the community level. Furthermore, the utility of multiscale modelling framework was illustrated by developing a multiscale model for HIV/AIDS which we then used to assess the comparative effectiveness of HIV/AIDS combination prevention interventions that include TasP including three drug classes (PIs, FIs and RTIs), male condoms and male circumcision.

This multiscale modelling approach allowed the systematic examination of the comparative effectiveness of HIV/AIDS preventive interventions in ways that have not been easy in modelling studies that do not implement multiscale modelling in the analysis of the transmission dynamics of HIV/AIDS. While this study focused on HIV/AIDS, the multiscale modelling framework itself is general enough and is applicable to many other directly transmitted infectious diseases beyond the specific case of HIV/AIDS disease system. In addition, the approach proposed in this study can help public health planners and disease modellers to establish priorities in a rational way. For disease modellers, this modelling framework offers an alternative approach for modelling infectious diseases in a way that may better represent the transmission of an infectious disease, that is, based on community pathogen load. The approach develops an infectious disease modelling science base for directly transmitted infectious disease systems (where the inside-host environment's biological entities such as cells, tissues, organs, body fluids, whole body are the reservoir of infective pathogen) that is comparable to an existing modelling science base for environmentally transmitted infectious diseases (where the outside-host geographical environment's physical entities such as soil, air, fomites/contact surfaces, food

and water are the reservoir of infective pathogen) where pathogen load in the environment is explicitly incorporated into the model. For public health planners, this approach offers a model-based approach for assessing the comparative effectiveness of health interventions using community pathogen load as the indicator of intervention effectiveness.

However, like in all model development, our multiscale model is not without limitations. One limitation of the multiscale modelling framework presented in this study is that the within-host submodel is assumed to be in steady state compared to the between-host scale submodel. Treatment-as-prevention (TasP) targets potential transmitters by reducing the patients' virus load and thereby also their infectiousness. However, an onwards transmission may preferentially occur early after infection during the transient period (before an endemic level is attained) when the individual is unaware of his/her serologic status and may not have initiated treatment. Another limitation is that if one wanted to extend this model to multiple dimensions, the assumption that infected people contribute to CVL and that CVL affects the force of infection, which in turn causes new infections, intrinsically assumes that it is irrelevant who infects whom. This assumption is important in the context of our study where we wanted to incorporate indirect effects of health interventions as fully explained earlier on in this Chapter. However, the assumption that all infections come from the CVL would make it impossible to extend the model to include, for example, any sort of age-mixing or any associativity in the mixing between different sexual activity classes. Further, our parameters are not from a single epidemic setting. Therefore, the results obtained cannot be taken as characterizing a specific HIV/AIDS epidemic system in particular.

Bibliography

- Abbas, Ume L et al. (2013). "Antiretroviral therapy and pre-exposure prophylaxis: combined impact on HIV transmission and drug resistance in South Africa". In: *The Journal of infectious diseases* 208.2, pp. 224–234.
- Abu-Raddad, Laith J and Susanne F Awad (2014). "How does population viral load vary with the evolution of a large HIV epidemic in sub-Saharan Africa?" In: *AIDS (London, England)* 28.6, p. 927.
- Abu-Raddad, Laith J et al. (2013). "Have the explosive HIV epidemics in sub-Saharan Africa been driven by higher community viral load?" In: *AIDS (London, England)* 27.6, p. 981.
- Adams, Brian M et al. (2004). "Dynamic multidrug therapies for HIV: Optimal and STI control approaches". In: *Mathematical biosciences and engineering* 1.2, pp. 223–241.
- Ademiloye, AS et al. (2017). "Element-Free Multiscale Modeling Of Large Deformation Behavior Of Red Blood Cell Membrane With Malaria Infection". In: *bioRxiv*, p. 136648.
- Allen, Susan et al. (2003). "Sexual behavior of HIV discordant couples after HIV counseling and testing". In: *Aids* 17.5, pp. 733–740.
- Arriola, Leon M and James M Hyman (2007). "Being sensitive to uncertainty". In: *Computing in Science & Engineering* 9.2, pp. 10–20.
- Auvert, Bertran et al. (2005). "Randomized, controlled intervention trial of male circumcision for reduction of HIV infection risk: the ANRS 1265 Trial". In: *PLoS medicine* 2.11, e298.
- Bailey, Robert C et al. (2007). "Male circumcision for HIV prevention in young men in Kisumu, Kenya: a randomised controlled trial". In: *The lancet* 369.9562, pp. 643–656.
- Bani-Yaghoub, Majid et al. (2012). "Reproduction numbers for infections with free-living pathogens growing in the environment". In: *Journal of biological dynamics* 6.2, pp. 923–940.
- Bärnighausen, Till et al. (2012). "Economics of antiretroviral treatment vs. circumcision for HIV prevention". In: *Proceedings of the National Academy of Sciences* 109.52, pp. 21271–21276.
- Bezemer, Daniela et al. (2010). "27 years of the HIV epidemic amongst men having sex with men in the Netherlands: an in depth mathematical model-based analysis". In: *Epidemics* 2.2, pp. 66–79.
- Blankenship, Kim M et al. (2006). "Structural interventions: concepts, challenges and opportunities for research". In: *Journal of Urban Health* 83.1, pp. 59–72.
- Bockarie, Moses J et al. (2013). "Preventive chemotherapy as a strategy for elimination of neglected tropical parasitic diseases: endgame challenges". In: *Phil. Trans. R. Soc. B* 368.1623, p. 20120144.
- Boily, Marie-Claude et al. (2007). "Evaluating large-scale HIV prevention interventions: study design for an integrated mathematical modelling approach". In: *Sexually transmitted infections* 83.7, pp. 582–589.

- Boily, Marie-Claude et al. (2008). "Measuring the public-health impact of candidate HIV vaccines as part of the licensing process". In: *The Lancet infectious diseases* 8.3, pp. 200–207.
- Boily, Marie-Claude et al. (2012). "HIV treatment as prevention: considerations in the design, conduct, and analysis of cluster randomized controlled trials of combination HIV prevention". In: *PLoS medicine* 9.7, e1001250.
- Briz, Verónica et al. (2006). "HIV entry inhibitors: mechanisms of action and resistance pathways". In: *Journal of Antimicrobial Chemotherapy* 57.4, pp. 619–627.
- Brown, Graham et al. (2015). "Investigating combination HIV prevention: isolated interventions or complex system". In: *Journal of the International AIDS Society* 18.1.
- Brown, Jennifer L et al. (2014). "Combination HIV prevention interventions: the potential of integrated behavioral and biomedical approaches". In: *Current HIV/AIDS Reports* 11.4, pp. 363–375.
- Carr, J (1981). "Applications of Center Manifold Theory Applied Mathematical Sciences 35 Springer-Verlag". In: *New York*.
- Castel, Amanda D et al. (2012). "Use of the community viral load as a population-based biomarker of HIV burden". In: *Aids* 26.3, pp. 345–353.
- Castillo-Chavez, Carlos and Baojun Song (2004). "Dynamical models of tuberculosis and their applications". In: *Mathematical biosciences and engineering* 1.2, pp. 361–404.
- Castillo-Chavez, Carlos et al. (2002). "ON THE COMPUTATION OF R_0 AND ITS ROLE ON". In: *Mathematical approaches for emerging and reemerging infectious diseases: an introduction* 1, p. 229.
- CDC (2014 (accessed October 26, 2016)). *2013 Sexually Transmitted Diseases Surveillance*. URL: <http://www.cdc.gov/std/stats13/default.htm>.
- Chaccour, Carlos J et al. (2013). "Ivermectin to reduce malaria transmission: a research agenda for a promising new tool for elimination". In: *Malaria journal* 12.1, p. 153.
- Chitnis, Nakul et al. (2008). "Determining important parameters in the spread of malaria through the sensitivity analysis of a mathematical model". In: *Bulletin of mathematical biology* 70.5, pp. 1272–1296.
- Chiyaka, C et al. (2007). "Transmission model of endemic human malaria in a partially immune population". In: *Mathematical and computer modelling* 46.5, pp. 806–822.
- Chiyaka, Christinah et al. (2008). "Modelling immune response and drug therapy in human malaria infection". In: *Computational and Mathematical Methods in Medicine* 9.2, pp. 143–163.
- Chiyaka, Edward T and WINSTON GARIRA (2009). "Mathematical analysis of the transmission dynamics of schistosomiasis in the human-snail hosts". In: *Journal of Biological Systems* 17.03, pp. 397–423.
- Cohen, Myron S et al. (2012). "HIV treatment as prevention: debate and commentary—will early infection compromise treatment-as-prevention strategies?" In: *PLoS medicine* 9.7, e1001232.
- Conway, Jessica M and Alan S Perelson (2015). "Post-treatment control of HIV infection". In: *Proceedings of the National Academy of Sciences* 112.17, pp. 5467–5472.
- Cori, Anne et al. (2014). "HPTN 071 (PopART): a cluster-randomized trial of the population impact of an HIV combination prevention intervention including universal testing and treatment: mathematical model". In: *PloS one* 9.1, e84511.
- Cremin, Ide et al. (2013). "The new role of antiretrovirals in combination HIV prevention: a mathematical modelling analysis". In: *Aids* 27.3, pp. 447–458.

- Cuadros, Diego F et al. (2011). "Effect of variable transmission rate on the dynamics of HIV in sub-Saharan Africa". In: *BMC infectious diseases* 11.1, p. 216.
- Culshaw, Rebecca V and Shigui Ruan (2000). "A delay-differential equation model of HIV infection of CD4+ T-cells". In: *Mathematical biosciences* 165.1, pp. 27–39.
- Currie, Christine SM et al. (2003). "Tuberculosis epidemics driven by HIV: is prevention better than cure?" In: *Aids* 17.17, pp. 2501–2508.
- Daefler, S (2013). "Using Datasets for Modeling of Infectious Diseases". In: *Journal of Data Mining Genomics Proteomics* 13.119, p. 20160289.
- Dang, Yan-Xia et al. (2016). "Competitive exclusion in a multi-strain immuno-epidemiological influenza model with environmental transmission". In: *Journal of biological dynamics* 10.1, pp. 416–456.
- Das, M (2014). "Community Viral Load. In Encyclopedia of AIDS". In: *Nonlinear Dynamics* 68.3, pp. 1–10.
- Das, M et al. (2011). "Success of test and treat in San Francisco? Reduced time to virologic suppression, decreased community viral load, and fewer new HIV infections, 2004 to 2009". In: *18th conference on retroviruses and opportunistic infections*. Vol. 27.
- Das, Moupali et al. (2010). "Decreases in community viral load are accompanied by reductions in new HIV infections in San Francisco". In: *PloS one* 5.6, e11068.
- Das, Moupali et al. (2013). "Measuring the unknown: calculating community viral load among HIV-infected MSM unaware of their HIV status in San Francisco from National HIV Behavioral Surveillance, 2004-2011". In: *Journal of acquired immune deficiency syndromes (1999)* 63.2, e84.
- De Boer, Rob J et al. (2010). "Current estimates for HIV-1 production imply rapid viral clearance in lymphoid tissues". In: *PLoS Comput Biol* 6.9, e1000906.
- Delva, Wim et al. (2012). "HIV treatment as prevention: optimising the impact of expanded HIV treatment programmes". In: *PLoS medicine* 9.7, e1001258.
- Diekmann, Odo et al. (1990). "On the definition and the computation of the basic reproduction ratio R_0 in models for infectious diseases in heterogeneous populations". In: *Journal of mathematical biology* 28.4, pp. 365–382.
- Disease Control, Centers for, Prevention (CDC, et al. (2000). "Updated guidelines for the use of rifabutin or rifampin for the treatment and prevention of tuberculosis among HIV-infected patients taking protease inhibitors or nonnucleoside reverse transcriptase inhibitors." In: *MMWR. Morbidity and mortality weekly report* 49.9, p. 185.
- Disease Control, Centers for et al. (2011). "Guidance on community viral load: a family of measures, definitions, and method for calculation". In: *Atlanta (GA): Centers for Disease Control and Prevention (US)*.
- Dodd, Peter J et al. (2010). "Examining the promise of HIV elimination by 'test and treat' in hyper-endemic settings". In: *AIDS (London, England)* 24.5, p. 729.
- Doekes, Hilje M et al. (2017). "Effect of the Latent Reservoir on the Evolution of HIV at the Within-and Between-Host Levels". In: *PLoS computational biology* 13.1, e1005228.
- Donner, Allan and Neil Klar (2000). "Design and analysis of cluster randomization trials in health research". In:
- Dorp, Christiaan H van et al. (2014). "Immuno-epidemiological modeling of HIV-1 predicts high heritability of the set-point virus load, while selection for CTL escape dominates virulence evolution". In: *PLoS computational biology* 10.12, e1003899.
- Dorratoltaj, Nargesalsadat et al. (2017). "Multi-scale immunoepidemiological modeling of within-host and between-host HIV dynamics: systematic review of mathematical models". In: *PeerJ* 5, e3877.

- Driessche, Pauline Van den and James Watmough (2002). "Reproduction numbers and sub-threshold endemic equilibria for compartmental models of disease transmission". In: *Mathematical biosciences* 180.1, pp. 29–48.
- Durmuş, Saliha et al. (2015). "A review on computational systems biology of pathogen–host interactions". In: *Frontiers in microbiology* 6.
- El-Sayed, Badria et al. (2007). "A randomized open-label trial of artesunate-sulfadoxine-pyrimethamine with or without primaquine for elimination of sub-microscopic *P. falciparum* parasitaemia and gametocyte carriage in eastern Sudan". In: *PLoS One* 2.12, e1311.
- Estill, Janne et al. (2012). "Viral load monitoring of antiretroviral therapy, cohort viral load and HIV transmission in Southern Africa: a mathematical modelling analysis". In: *AIDS (London, England)* 26.11, p. 1403.
- Fallahi-Sichani, Mohammad et al. (2011). "Multiscale computational modeling reveals a critical role for TNF- α receptor 1 dynamics in tuberculosis granuloma formation". In: *The Journal of Immunology* 186.6, pp. 3472–3483.
- Fang, Chi-Tai et al. (2004). "Decreased HIV transmission after a policy of providing free access to highly active antiretroviral therapy in Taiwan". In: *Journal of Infectious Diseases* 190.5, pp. 879–885.
- Fedosov, Dmitry A et al. (2011). "Multiscale modeling of red blood cell mechanics and blood flow in malaria". In: *PLoS computational biology* 7.12, e1002270.
- Feng, Zhilan et al. (2012). "A model for coupling within-host and between-host dynamics in an infectious disease". In: *Nonlinear Dynamics* 68.3, pp. 401–411.
- Feng, Zhilan et al. (2013). "A mathematical model for coupling within-host and between-host dynamics in an environmentally-driven infectious disease". In: *Mathematical biosciences* 241.1, pp. 49–55.
- Feng, Zhilan et al. (2015). "Coupled within-host and between-host dynamics and evolution of virulence". In: *Mathematical biosciences* 270, pp. 204–212.
- Fewtrell, Lorna et al. (2005). "Water, sanitation, and hygiene interventions to reduce diarrhoea in less developed countries: a systematic review and meta-analysis". In: *The Lancet infectious diseases* 5.1, pp. 42–52.
- Ford, Kathleen et al. (1996). "Behavioral interventions for reduction of sexually transmitted disease/HIV transmission among female commercial sex workers and clients in Bali, Indonesia." In: *Aids* 10.2, pp. 213–222.
- Fraser, Christophe et al. (2007). "Variation in HIV-1 set-point viral load: epidemiological analysis and an evolutionary hypothesis". In: *Proceedings of the National Academy of Sciences* 104.44, pp. 17441–17446.
- Fung, Isaac Chun-Hai (2014). "Cholera transmission dynamic models for public health practitioners". In: *Emerging themes in epidemiology* 11.1, p. 1.
- Garira, Winston (2017). "A complete categorization of multiscale models of infectious disease systems". In: *Journal of Biological Dynamics* 11.1, pp. 378–435.
- Garira, Winston et al. (2014). "A mathematical modelling framework for linked within-host and between-host dynamics for infections with free-living pathogens in the environment". In: *Mathematical biosciences* 256, pp. 58–78.
- Gerardin, Jaline et al. (2015). "Mass campaigns with antimalarial drugs: a modelling comparison of artemether-lumefantrine and DHA-piperaquine with and without primaquine as tools for malaria control and elimination". In: *BMC infectious diseases* 15.1, p. 144.
- Ghys, Peter D et al. (2002). "Increase in condom use and decline in HIV and sexually transmitted diseases among female sex workers in Abidjan, Cote d'Ivoire, 1991–1998". In: *Aids* 16.2, pp. 251–258.

- Gog, Julia R et al. (2015). "Seven challenges in modeling pathogen dynamics within-host and across scales". In: *Epidemics* 10, pp. 45–48.
- Granich, Reuben M et al. (2009). "Universal voluntary HIV testing with immediate antiretroviral therapy as a strategy for elimination of HIV transmission: a mathematical model". In: *The Lancet* 373.9657, pp. 48–57.
- Gray, Ronald H et al. (2001). "Probability of HIV-1 transmission per coital act in monogamous, heterosexual, HIV-1-discordant couples in Rakai, Uganda". In: *The Lancet* 357.9263, pp. 1149–1153.
- Gray, Ronald H et al. (2007). "Male circumcision for HIV prevention in men in Rakai, Uganda: a randomised trial". In: *The Lancet* 369.9562, pp. 657–666.
- Greenwood, Brian (2006). "Intermittent preventive treatment—a new approach to the prevention of malaria in children in areas with seasonal malaria transmission". In: *Tropical medicine & international health* 11.7, pp. 983–991.
- Griffin, Jamie T et al. (2010). "Reducing Plasmodium falciparum malaria transmission in Africa: a model-based evaluation of intervention strategies". In: *PLoS medicine* 7.8, e1000324.
- Griffith, David E et al. (2007). "An official ATS/IDSA statement: diagnosis, treatment, and prevention of nontuberculous mycobacterial diseases". In: *American journal of respiratory and critical care medicine* 175.4, pp. 367–416.
- Grosskurth, Heiner et al. (1995). "Impact of improved treatment of sexually transmitted diseases on HIV infection in rural Tanzania: randomised controlled trial". In: *The lancet* 346.8974, pp. 530–536.
- Gupta, Geeta Rao et al. (2008). "Structural approaches to HIV prevention". In: *The Lancet* 372.9640, pp. 764–775.
- Gutierrez, Juan B et al. (2015). "From within host dynamics to the epidemiology of infectious disease: scientific overview and challenges". In: *Mathematical biosciences* 270, pp. 143–155.
- Hadjichrysanthou, Christoforos et al. (2016). "Understanding the within-host dynamics of influenza A virus: from theory to clinical implications". In: *Journal of The Royal Society Interface* 13.119, p. 20160289.
- Halsey, Neal A et al. (1998). "Randomised trial of isoniazid versus rifampicin and pyrazinamide for prevention of tuberculosis in HIV-1 infection". In: *The lancet* 351.9105, pp. 786–792.
- Hamby, DM (1994). "A review of techniques for parameter sensitivity analysis of environmental models". In: *Environmental monitoring and assessment* 32.2, pp. 135–154.
- Handel, Andreas and Pejman Rohani (2015). "Crossing the scale from within-host infection dynamics to between-host transmission fitness: a discussion of current assumptions and knowledge". In: *Phil. Trans. R. Soc. B* 370.1675, p. 20140302.
- Handel, Andreas et al. (2013). "A multi-scale analysis of influenza A virus fitness trade-offs due to temperature-dependent virus persistence". In: *PLoS computational biology* 9.3, e1002989.
- Hartley, David M et al. (2005). "Hyperinfectivity: a critical element in the ability of *V. cholerae* to cause epidemics?" In: *PLoS medicine* 3.1, e7.
- Hayes, RJ et al. (2010). "Treatment of sexually transmitted infections for HIV prevention: end of the road or new beginning?" In: *AIDS (London, England)* 24.0 4.
- Heldt, Frank S et al. (2013). "Multiscale modeling of influenza A virus infection supports the development of direct-acting antivirals". In: *PLoS computational biology* 9.11, e1003372.

- Helton, Jon C et al. (1985). "Sensitivity analysis of the asymptotic behavior of a model for the environmental movement of radionuclides". In: *Ecological modelling* 28.4, pp. 243–278.
- Herbeck, Joshua T et al. (2014). "An HIV epidemic model based on viral load dynamics: value in assessing empirical trends in HIV virulence and community viral load". In: *PLoS computational biology* 10.6, e1003673.
- Hosseini, Iraj and Feilim Mac Gabhann (2012). "Multi-scale modeling of HIV infection in vitro and APOBEC3G-based anti-retroviral therapy". In: *PLoS Comput Biol* 8.2, e1002371.
- Ikeda, Hiroki et al. (2014). "Improving the estimation of the death rate of infected cells from time course data during the acute phase of virus infections: application to acute HIV-1 infection in a humanized mouse model". In: *Theoretical Biology and Medical Modelling* 11.1, p. 22.
- Jain, Vivek et al. (2014). "Changes in population HIV RNA levels in Mbarara, Uganda during scale-up of HIV antiretroviral therapy access". In: *Journal of acquired immune deficiency syndromes (1999)* 65.3, p. 327.
- Jeffery, Geoffrey M and Don E Eyles (1955). "Infectivity to Mosquitoes of Plasmodium Falciparum as Related to Gametocyte Density and Duration of Infection¹". In: *The American journal of tropical medicine and hygiene* 4.5, pp. 781–789.
- John, Chandy C (2016). "Primaquine plus artemisinin combination therapy for reduction of malaria transmission: promise and risk". In: *BMC medicine* 14.1, p. 65.
- John M. Last Sander Greenland, Miguel Hernán Isabel dos Santos Silva (2014). *A Dictionary of Epidemiology*. Vol. 6th Edition. Oxford University Press.
- Johnston, Geoffrey L et al. (2014). "Modeling within-host effects of drugs on Plasmodium falciparum transmission and prospects for malaria elimination". In: *PLoS computational biology* 10.1, e1003434.
- Kalichman, Seth C et al. (2011). "Prevalence of sexually transmitted co-infections in people living with HIV/AIDS: systematic review with implications for using HIV treatments for prevention". In: *Sexually transmitted infections* 87.3, pp. 183–190.
- Kaplan, Jonathan E et al. (1996). "Male-to-female transmission of human T-cell lymphotropic virus types I and II: association with viral load". In: *JAIDS Journal of Acquired Immune Deficiency Syndromes* 12.2, pp. 193–201.
- Kato, Masaya et al. (2013). "The potential impact of expanding antiretroviral therapy and combination prevention in Vietnam: towards elimination of HIV transmission". In: *Journal of acquired immune deficiency syndromes (1999)* 63.5, e142.
- Keenan, Jeremy D et al. (2013). "Elimination and eradication of neglected tropical diseases with mass drug administrations: a survey of experts". In: *PLoS neglected tropical diseases* 7.12, e2562.
- Kiszewski, Anthony E (2010). "Blocking Plasmodium falciparum malaria transmission with drugs: the gametocytocidal and sporontocidal properties of current and prospective antimalarials". In: *Pharmaceuticals* 4.1, pp. 44–68.
- Kostova, Tanya (2007). "Persistence of viral infections on the population level explained by an immunoepidemiological model". In: *Mathematical biosciences* 206.2, pp. 309–319.
- Kranzer, Katharina et al. (2013). "Community viral load and CD4 count distribution among people living with HIV in a South African township: implications for treatment as prevention". In: *Journal of acquired immune deficiency syndromes (1999)* 63.4, p. 498.
- Landis, R Clive et al. (2013). "Ten year trends in community HIV viral load in Barbados: implications for treatment as prevention". In: *PloS one* 8.3, e58590.

- Lange, Alexander and Neil M Ferguson (2009). "Antigenic diversity, transmission mechanisms, and the evolution of pathogens". In: *PLoS computational biology* 5.10, e1000536.
- Lawley, Trevor D et al. (2008). "Host transmission of *Salmonella enterica* serovar Typhimurium is controlled by virulence factors and indigenous intestinal microbiota". In: *Infection and immunity* 76.1, pp. 403–416.
- Lawley, Trevor D et al. (2009). "Antibiotic treatment of *Clostridium difficile* carrier mice triggers a supershedder state, spore-mediated transmission, and severe disease in immunocompromised hosts". In: *Infection and immunity* 77.9, pp. 3661–3669.
- Legros, Mathieu and Sebastian Bonhoeffer (2016). "A combined within-host and between-hosts modelling framework for the evolution of resistance to antimalarial drugs". In: *Journal of The Royal Society Interface* 13.117, p. 20160148.
- Li, Hong-Chuan et al. (2004). "Provirus load in breast milk and risk of mother-to-child transmission of human T lymphotropic virus type I". In: *The Journal of infectious diseases* 190.7, pp. 1275–1278.
- Lima, Viviane D et al. (2008). "Expanded access to highly active antiretroviral therapy: a potentially powerful strategy to curb the growth of the HIV epidemic". In: *The Journal of infectious diseases* 198.1, pp. 59–67.
- Lofgren, Eric T et al. (2016). "Patients as Patches: Ecology and Epidemiology in Healthcare Environments". In: *infection control & hospital epidemiology* 37.12, pp. 1507–1512.
- Long, Elisa F et al. (2010). "The cost-effectiveness and population outcomes of expanded HIV screening and antiretroviral treatment in the United States". In: *Annals of internal medicine* 153.12, pp. 778–789.
- Lou, Jie et al. (2015). "The coupled within-and between-host dynamics in the evolution of hiv/aids in china". In: *Journal of Applied Analysis and Computation* 5.4, pp. 731–750.
- Lukens, Sarah et al. (2014). "A large-scale immuno-epidemiological simulation of influenza A epidemics". In: *BMC Public Health* 14.1, p. 1019.
- Lythgoe, Katrina A et al. (2013). "Is HIV short-sighted? Insights from a multistrain nested model". In: *Evolution* 67.10, pp. 2769–2782.
- Magombedze, Gesham et al. (2006). "Mathematical modeling of chemotherapy of human TB infection". In: *Journal of Biological Systems* 14.04, pp. 509–553.
- (2008). "Modelling the immunopathogenesis of HIV-1 infection and the effect of multidrug therapy: the role of fusion inhibitors in HAART". In:
- Martcheva, Maia (2011). "An Immuno-epidemiological Model of Paratuberculosis". In: *AIP Conference Proceedings*. Vol. 1404. 1. AIP, pp. 176–183.
- Martcheva, Maia and Xue-Zhi Li (2013). "Linking immunological and epidemiological dynamics of HIV: the case of super-infection". In: *Journal of biological dynamics* 7.1, pp. 161–182.
- Martcheva, Maia et al. (2015a). "An immuno-epidemiological model for Johne's disease in cattle". In: *Veterinary research* 46.1, p. 69.
- Martcheva, Maia et al. (2015b). "Coupling Within-Host and Between-Host Infectious Diseases Models". In: *BIOMATH* 4.2, p. 1510091.
- Martin, Andrea Blue (2017). "Development and Modeling of Multi-scale Continuous High Gradient Magnetophoretic Separator for Malaria-infected Red Blood Cells". In:
- Matthews, L et al. (2006). "Heterogeneous shedding of *Escherichia coli* O157 in cattle and its implications for control". In: *Proceedings of the National Academy of Sciences of the United States of America* 103.3, pp. 547–552.

- Maude, Richard J et al. (2012). "Optimising strategies for Plasmodium falciparum malaria elimination in Cambodia: primaquine, mass drug administration and artemisinin resistance". In: *PLoS One* 7.5, e37166.
- Mbah, Martial L Ndeffo et al. (2013). "Potential cost-effectiveness of schistosomiasis treatment for reducing HIV transmission in Africa—the case of Zimbabwean women". In: *PLoS neglected tropical diseases* 7.8, e2346.
- McKenzie, F Ellis and William H Bossert (2005). "An integrated model of Plasmodium falciparum dynamics". In: *Journal of theoretical biology* 232.3, pp. 411–426.
- McMorrow, ML et al. (2011). "Malaria rapid diagnostic tests in elimination settings—can they find the last parasite?" In: *Clinical Microbiology and Infection* 17.11, pp. 1624–1631.
- Mellors, John W et al. (1996). "Prognosis in HIV-1 infection predicted by the quantity of virus in plasma". In: *SCIENCE-NEW YORK THEN WASHINGTON-*, pp. 1167–1169.
- Metzger, Vincent T et al. (2011). "Autonomous targeting of infectious superspreaders using engineered transmissible therapies". In: *PLoS Comput Biol* 7.3, e1002015.
- Miller, Ezer et al. (2014). "Quantifying the contribution of hosts with different parasite concentrations to the transmission of visceral leishmaniasis in Ethiopia". In: *PLoS neglected tropical diseases* 8.10, e3288.
- Miller, William C et al. (2013). "Community viral load as a measure for assessment of HIV treatment as prevention". In: *The Lancet infectious diseases* 13.5, pp. 459–464.
- Montaner, Julio SG et al. (2010). "Association of highly active antiretroviral therapy coverage, population viral load, and yearly new HIV diagnoses in British Columbia, Canada: a population-based study". In: *The Lancet* 376.9740, pp. 532–539.
- Moore, John P and Robert W Doms (2003). "The entry of entry inhibitors: a fusion of science and medicine". In: *Proceedings of the National Academy of Sciences* 100.19, pp. 10598–10602.
- Moyle, Graeme (2003). "Stopping HIV fusion with enfuvirtide: the first step to extracellular HAART". In: *Journal of Antimicrobial Chemotherapy* 51.2, pp. 213–217.
- Mukandavire, Z and W Garira (2007a). "Effects of public health educational campaigns and the role of sex workers on the spread of HIV/AIDS among heterosexuals". In: *Theoretical population biology* 72.3, pp. 346–365.
- (2007b). "Sex-structured HIV/AIDS model to analyse the effects of condom use with application to Zimbabwe". In: *Journal of mathematical biology* 54.5, pp. 669–699.
- Mukandavire, Zindoga et al. (2007). "Modelling circumcision and condom use as HIV/AIDS preventive control strategies". In: *Mathematical and Computer Modelling* 46.11, pp. 1353–1372.
- Mukandavire, Zindoga et al. (2016). "Comparing the impact of increasing condom use or HIV pre-exposure prophylaxis (PrEP) use among female sex workers". In: *Epidemics* 14, pp. 62–70.
- Nguyen, Nguyet Minh et al. (2013). "Host and viral features of human dengue cases shape the population of infected and infectious Aedes aegypti mosquitoes". In: *Proceedings of the National Academy of Sciences* 110.22, pp. 9072–9077.
- Nourani, Esmaeil et al. (2015). "Computational approaches for prediction of pathogen-host protein-protein interactions". In: *Frontiers in microbiology* 6.
- Ogunjimi, Benson et al. (2015). "Integrating between-host transmission and within-host immunity to analyze the impact of varicella vaccination on zoster". In: *Elife* 4, e07116.

- Padian, Nancy S et al. (2010). "Weighing the gold in the gold standard: challenges in HIV prevention research". In: *AIDS (London, England)* 24.5, p. 621.
- Palombi, Leonardo et al. (2012). "Predicting trends in HIV-1 sexual transmission in sub-Saharan Africa through the Drug Resource Enhancement Against AIDS and Malnutrition model: antiretrovirals for 5 reduction of population infectivity, incidence and prevalence at the district level". In: *Clinical infectious diseases* 55.2, pp. 268–275.
- Pannell, David J (1997). "Sensitivity analysis of normative economic models: theoretical framework and practical strategies". In: *Agricultural economics* 16.2, pp. 139–152.
- Pesko, Kendra et al. (2009). "Effects of infectious virus dose and bloodmeal delivery method on susceptibility of *Aedes aegypti* and *Aedes albopictus* to chikungunya virus". In: *Journal of medical entomology* 46.2, pp. 395–399.
- Quinn, Thomas C et al. (2000). "Viral load and heterosexual transmission of human immunodeficiency virus type 1". In: *New England journal of medicine* 342.13, pp. 921–929.
- Roberts, Mick et al. (2015). "Nine challenges for deterministic epidemic models". In: *Epidemics* 10, pp. 49–53.
- Rockstroh, JK and S Mauss (2004). "Clinical perspective of fusion inhibitors for treatment of HIV". In: *Journal of Antimicrobial Chemotherapy* 53.5, pp. 700–702.
- Rynkiewicz, Evelyn C et al. (2015). "An ecosystem approach to understanding and managing within-host parasite community dynamics". In: *Trends in parasitology* 31.5, pp. 212–221.
- Saenz, Roberto A and Sebastian Bonhoeffer (2013). "Nested model reveals potential amplification of an HIV epidemic due to drug resistance". In: *Epidemics* 5.1, pp. 34–43.
- Schleicher, Jana et al. (2016). "Facing the challenges of multiscale modelling of bacterial and fungal pathogen–host interactions". In: *Briefings in functional genomics* 16.2, pp. 57–69.
- Schulze, Sylvie et al. (2015). "Computational prediction of molecular pathogen–host interactions based on dual transcriptome data". In: *Frontiers in microbiology* 6.
- Schwartländer, Bernhard et al. (2011). "Towards an improved investment approach for an effective response to HIV / AIDS". In: *The Lancet* 377.9782, pp. 2031–2041.
- Seblova, Veronika et al. (2013). "Phlebotomus orientalis sand flies from two geographically distant Ethiopian localities: biology, genetic analyses and susceptibility to *Leishmania donovani*". In: *PLoS neglected tropical diseases* 7.4, e2187.
- Shen, Mingwang et al. (2015). "Global stability of an infection-age structured HIV-1 model linking within-host and between-host dynamics". In: *Mathematical biosciences* 263, pp. 37–50.
- Sicard, Mathieu et al. (2014). "A host as an ecosystem: Wolbachia coping with environmental constraints". In: *Environmental microbiology* 16.12, pp. 3583–3607.
- Simpson, Lindsay and Abba B Gumel (2017). "Mathematical assessment of the role of pre-exposure prophylaxis on HIV transmission dynamics". In: *Applied Mathematics and Computation* 293, pp. 168–193.
- Sloot, Peter MA and Alfons G Hoekstra (2009). "Multi-scale modelling in computational biomedicine". In: *Briefings in bioinformatics*, bbp038.
- Smith, M Kumi et al. (2012). "HIV treatment as prevention: the utility and limitations of ecological observation". In: *PLoS medicine* 9.7, e1001260.
- Smits, Henk L (2009). "Prospects for the control of neglected tropical diseases by mass drug administration". In: *Expert review of anti-infective therapy* 7.1, pp. 37–56.

- Sun, Xiaodan et al. (2016). "Early HAART initiation may not reduce actual reproduction number and prevalence of MSM infection: Perspectives from coupled within-and between-host modelling studies of Chinese MSM populations". In: *PloS one* 11.3, e0150513.
- Tanner, Marcel et al. (2015). "Malaria eradication and elimination: views on how to translate a vision into reality". In: *BMC medicine* 13.1, p. 167.
- Tseroni, Maria et al. (2015). "Prevention of malaria resurgence in Greece through the association of mass drug administration (MDA) to immigrants from malaria-endemic regions and standard control measures". In: *PLoS neglected tropical diseases* 9.11, e0004215.
- Valdiserri, Ronald O (1997). "HIV counseling and testing: its evolving role in HIV prevention." In: *AIDS education and prevention: official publication of the International Society for AIDS Education* 9.3 Suppl, pp. 2–13.
- Van Damme, Pierre and Koen Van Herck (2007). "A review of the long-term protection after hepatitis A and B vaccination". In: *Travel medicine and infectious disease* 5.2, pp. 79–84.
- Vegvari, Carolin et al. (2016). "How Can Viral Dynamics Models Inform Endpoint Measures in Clinical Trials of Therapies for Acute Viral Infections?" In: *PloS one* 11.7, e0158237.
- Velasco-Hernandez, JX et al. (2002). "Could widespread use of combination antiretroviral therapy eradicate HIV epidemics?" In: *The Lancet infectious diseases* 2.8, pp. 487–493.
- Vermund, Sten H and Richard J Hayes (2013). "Combination prevention: new hope for stopping the epidemic". In: *Current Hiv/aids Reports* 10.2, pp. 169–186.
- Vernazza, P et al. (2008). "HIV-infected patients under HAART without any other sexually transmitted infection do not transmit HIV by sexual intercourse". In: *Bull Med Suisse* 89, pp. 165–169.
- Vickers, David M and Nathaniel D Osgood (2007). "A unified framework of immunological and epidemiological dynamics for the spread of viral infections in a simple network-based population". In: *Theoretical Biology and Medical Modelling* 4.1, p. 1.
- (2014). "The arrested immunity hypothesis in an immunoepidemiological model of Chlamydia transmission". In: *Theoretical population biology* 93, pp. 52–62.
- Wang, Xia et al. (2016). "Dynamics of an HIV model with multiple infection stages and treatment with different drug classes". In: *Bulletin of mathematical biology* 78.2, pp. 322–349.
- Wang, Xueying and Jin Wang (2017). "Disease dynamics in a coupled cholera model linking within-host and between-host interactions". In: *Journal of biological dynamics* 11.sup1, pp. 238–262.
- Webster, Joanne P et al. (2014). "The contribution of mass drug administration to global health: past, present and future". In: *Phil. Trans. R. Soc. B* 369.1645, p. 20130434.
- Wen, Wan-Hsin et al. (2013). "Mother-to-infant transmission of hepatitis B virus infection: significance of maternal viral load and strategies for intervention". In: *Journal of hepatology* 59.1, pp. 24–30.
- WHO (2005). *The World Health Report 2005: Make every mother and child count*. World Health Organization.
- WHO et al. (2004). "The World health report: 2004: changing history". In:
- Wilson, David P (2012). "HIV treatment as prevention: natural experiments highlight limits of antiretroviral treatment as HIV prevention". In: *PLoS medicine* 9.7, e1001231.

- Xu, Xiaxia et al. (2013). "Modeling sexual transmission of HIV/AIDS in Jiangsu province, China". In: *Mathematical Methods in the Applied Sciences* 36.2, pp. 234–248.
- Yamshchikov, Alexandra et al. (2009). "Vitamin D for treatment and prevention of infectious diseases: a systematic review of randomized controlled trials". In: *Endocrine Practice* 15.5, pp. 438–449.
- Yang, Hyun M (2000). "Malaria transmission model for different levels of acquired immunity and temperature-dependent parameters (vector)". In: *Revista de saude publica* 34.3, pp. 223–231.
- Yeghiazarian, Lilit et al. (2013). "A stochastic multi-scale model of HIV-1 transmission for decision-making: application to a MSM population". In: *PloS one* 8.11, e70578.
- Zhang, Changwang et al. (2015). "Hybrid spreading mechanisms and T cell activation shape the dynamics of HIV-1 infection". In: *PLoS Comput Biol* 11.4, e1004179.